OPTIMAL SUSPENSION DAMPING AND AXLE VIBRATION ABSORBER FOR REDUCTION OF DYNAMIC TIRE LOADS

Venu Muluka

A Thesis

in

The Department

of

Mechanical Engineering

Presented in Partial Fulfillment of the Requirements
for the Degree of Master of Applied Science
Concordia University
Montreal, Quebec, Canada

May 1998

ABSTRACT

OPTIMAL SUSPENSION DAMPING AND AXLE VIBRATION ABSORBER FOR REDUCTION OF DYNAMIC TIRE LOADS

Venu Muluka

Variations in the dynamic tire forces of commercial freight vehicles, known to accelerate the road damage, are strongly related to vibration modes of the vehicle associated with vertical and pitch motions of the sprung and unsprung masses. The high levels of tire induced road damage caused by heavy vehicles has prompted a growing demand for the design of road-friendly vehicles. In this study, the enhancement of road friendliness of heavy vehicles is investigated using two methods to control the resonant forces: (i) Determination of optimal asymmetric force velocity characteristics of the suspension dampers to control the tire forces corresponding to the resonant modes; (ii) Optimal design of an axle vibration absorber to control the tire forces corresponding to the unsprung mass resonant modes. An analogy between the dynamic wheel loads and the ride quality performance characteristics of heavy vehicles is established through analysis of a linear quarter-vehicle model to illustrate the potential benefits of optimal damping. Since the vehicle ride quality and dynamic wheel loads are both related to vehicle vibration modes, the suspension damping considered adequate for improved ride quality can lead to enhanced road friendliness of the vehicle. Assuming negligible contributions due to roll dynamics, an in-plane analytical model of a three axle truck is formulated with linear and non linear suspension springs. The validity of the analytical models of nonlinear suspension components is asserted with the experimental data. A weighted

optimization function comprising the dynamic load coefficient (DLC) and the overall rms vertical acceleration at the driver's location is formulated to determine the design parameters of the damper and axle absorbers for a range of vehicle speeds and road roughnesses. It is concluded that the implementation of tuned axle absorbers can lead to reductions in the DLC ranging from 11.5% to 21%, and the optimal asymmetric damping can provide considerable reduction in both the overall rms acceleration and the DLC due to tire forces.

ACKNOWLEDGMENT

The author is sincerely grateful to his supervisors, Dr. S. Rakheja and Dr. Eliza Haseganu for their guidance and encouragement throughout the course of this research. The author also wishes to thank members of the faculty and staff of CONCAVE Research Centre for their time and assistance during the progression of this work.

Financial support provided by Concordia University FRDP (Faculty Research and Development Program) and NSERC (National Sciences of Engineering and Research Council) is gratefully acknowledged.

TABLE OF CONTENTS

CHAPTER 3

ENHANCEMENT OF ROAD FRIENDLINESS OF A HEAVY VEHICLE USING DYNAMIC VIBRATION ABSORBER

CHAPTER 4

ENHANCEMENT OF DRIVER AND ROAD FRIENDLINESS THROUGH OPTIMAL SUSPENSION DAMPING

CHAPTER 5

CONCLUSIONS AND RECOMMENDATIONS FOR FUTURE WORK

LIST OF FIGURES

LIST OF TABLES

NOMENCLATURE

Symbol	
P	Static tire load
m_S	Sprung mass of the vehicle model.
I	Pitch mass moment of inertia of the sprung weight about its centroid.
m_F, m_R	Unsprung mass of the front and rear axle.
z_1	Displacement of the sprung mass.
z_2	Displacement of the front unsprung mass.
z_3	Displacement of the rear unspurng mass.
θ	Pitch angle of the sprung mass.
z_{0F}	Road excitation to the front tire.
z_{0R}	Road excitation to the rear tire.
F_{SF}, F_{SR}	Front and rear axle suspension force.
F_{TF}, F_{TR}	Force developed by the front and composite rear axle tires.
g	Acceleration Due to gravity.
C_S	Front axle suspension damping.
C_{SR}	Rear axle suspension damping.
K_{SF}, K_{SR}	Linear or equivalent spring rates due to front and rear suspension.
F_{DF}, F_{DR}	Damping force of the front and rear suspension.
δ_{Si}	Static deflection of the suspension (i= F, R).
δ_{Ti}	Static deflection of the tire (i= F, R).
$\ddot{z}_1$	Sprung mass acceleration relative to the ride quality.
m_{AF}, m_{AR}	Masses due to the dynamic vibration absorbers (front and rear axles)

ω_{AF}, ω_{AR}	Uncoupled natural frequencies of front and rear axle absorbers.
ς_{AF}, ς_{AR}	Uncoupled damping ratios of front and rear axle absorbers.
x_4, x_5	Relative deflection of front and rear axle absorber masses with respect to the axle masses they are attached.
K_{Ai}, C_{Ai}	Linear stiffness and damping coefficient due to the front and rear axle absorbers (i= F, R).
F_i	Suspension force developed due to deflection x_i at instant t_I of leaf suspension.
F_{i-1}	Suspension force corresponding to deflection x_{i-1} at previous instant t_{i-1} of leaf suspension.
$F_{Env\,i}$	Limiting values of forces corresponding to the upper and lower curves of the measured characteristics corresponding to deflection x_i of leaf suspension.
β	Parameter used to describe the rate at which the leaf suspension force within a hystersis loop approaches the envelope.
$P(x, t)$	Instantaneous air pressure of air suspension as a function of deflection x.
P_0, V_0	Charge pressure and volume of air bag.
A_E	The effective piston area of air bag.
F_{AR}	The spring force developed by the air bag.
φ	Pitch motion of the trailing arm of air suspension.
I_B	Pitch mass moment of inertia of arm.
μ_{Ai}	Mass ratio of the axle absorber.
Ω_{Ai}	Frequency ratio of the axle absorebr.
ξ_{Ai}	Damping ratio of the axle absorber.
M, C, K	(nxn) Mass, Damping and Stiffness matrices, respectively
C_O, K_O	(nx2) Forcing damping and Stiffness matrices

q, q_O	(nx1) and (2x1) vectors of response and excitation coordinates.
λ	Eigen values.
Φ	Modal or eigen vectors.
T	Transformation matrix.
β_i	The normalized dynamic force due to tires on axle i.
ω_{Ai}	Uncoupled absorber natural frequency of the absorber i.
ω_{Ui}	Uncoupled resonant frequency of the unsprung mass i.
â:	Overall rms at acceleration at driver's seat.
$\overline{F}_T$	Mean tire force.
ξ_F, ξ_R	The linear suspension damping in terms of uncoupled vertical mode damping ratios.

CHAPTER 1

INTRODUCTION AND REVIEW OF LITERATURE

1.1 INTRODUCTION

Commercial freight vehicles transmit high magnitudes of dynamic wheel loads to the pavement and bridges leading to their rapid fatigue and premature failure. The gross vehicle weight and axle loads of commercial vehicles have been considerably relaxed during the past few decades in an attempt to enhance the freight transportation economy. Various studies conducted by transportation research organizations and regulatory bodies have established that the directional stability and control, ride vibration environment, and dynamic tire forces of heavy vehicles are strongly affected by the increased size and weight in an adverse manner [2]. The dynamic wheel loads (DWL), arising from the dynamics of the vehicle and the tire-road interactions are believed to be an important cause of the premature pavement damage. They are known to cause high magnitudes of bending and shear stresses in the pavement structure, leading to reduced pavement life. The dynamic wheel loads due to heavy vehicles can increase pavement wear by 50 to 400% at the most severely loaded locations [3]. Both the dynamic wheel loads and the ride quality are directly related to the vibration modes associated with vertical, pitch and roll motion of the vehicle.

Heavy vehicles with high axle loads and high tire inflation pressure transmit high magnitudes of dynamic forces to the pavement through tires. The high magnitudes of

dynamic tire forces are known to accelerate pavement fatigue and rut formation [13]. The total annual cost of highway infrastructure maintenance by the federal and provincial governments in Canada has been estimated at $8 billion. While part of this cost is due to environmental factors, at least 40% of this cost has been directly attributed to the heavy vehicle tire loads [3]. In recent years, OECD (Organization for Economic Cooperation and Development) has reported that the cost of highway infrastructure maintenance in the OECD countries can be considerably reduced through enhancement of road friendliness of the vehicles by decreasing the magnitudes of dynamic wheel loads [17].

The vehicular vibration and the resulting dynamic wheel loads are influenced by various design and operating parameters in a highly complex manner. Among the various design and operating parameters, vehicle suspension properties, road roughness, and speed are known to affect the road and driver friendliness of the vehicle in a very significant manner, where the driver friendliness relates the ride quality environment of the vehicle. The handling, directional control and stability, ride quality, and suspension rattle space performance characteristics of the vehicle, however, pose conflicting design requirements for suspension design. While soft suspension springs are highly desirable to enhance the ride quality and wheel load performance, the realization of adequate directional control and rattle space performance necessitates relatively hard suspension springs. The suspension springs are thus selected to achieve a compromise among these conflicting requirements, with relatively larger weighting placed on the rattle space and directional control performance. Since both the dynamic wheel loads and the ride quality are related to vehicular vibration modes, the suspension design with optimal multi-stage asymmetric damping offers significant potential to enhance the DWL and ride quality

performance without affecting the rattle space and directional control requirements. A dynamic vibration absorber tuned to the unsprung mass resonant frequency can be further employed to reduce the dynamic wheel loads in the vicinity of wheel-hop frequencies. This dissertation research is therefore directed towards the optimal design of asymmetric suspension damping and axle vibration absorber to enhance road and driver friendliness of the vehicle.

1.2 LITERATURE REVIEW

A review of previous investigations relevant to the study of dynamic wheel loads such as, failure mechanism of the pavement tire loads and influencing factors, dynamic vibration absorbers, suspension damping and vehicle models, is presented in the following subsections.

1.2.1 Failure Mechanisms of the Pavement

From a structural point of view, modern road surfaces (or pavements) may be classified as flexible, composite or rigid surface [4]. A flexible pavement consists of one or more layers of asphalt supported by a granular sub grade. Composite pavements consist of a flexible surface layer supported by a stiff Portland cement concrete (PCC) base; and rigid road surfaces consist of a layer of PCC on a granular foundation. Rigid pavements can be further classified according to their arrangement of steel reinforcement and joints. The pavements are also classified by the volume of traffic by high, intermediate or *low type*. *High type* pavement structures are used for principal roads and truck route with heavy traffic. Such pavements comprise of strong surface layer of asphalt or Portland cement concrete, of a thickness of 150 mm or more, built on one or more

layers of compacted granular material. *Intermediate* and *low type* pavements are used for moderate traffic local routes and unsealed rural roads.

The main structural difference between rigid and flexible pavements is that the rigid pavements have considerable higher bending stiffness than the flexible pavements, and thus can be used on relatively weak natural soils [Baladi.G 1989]. Bituminous materials are very sensitive to temperature: some mixes can rut easily at high temperatures, and they become brittle at low temperatures [84, 85, 86]. Both flexible and rigid pavements can crack at low temperatures because of thermal contraction, but rigid pavements are usually reinforced or provided with joints that minimize this problem. It has been reported that, the working life of rigid pavements can be increased significantly by a modest increase in the concrete thickness, and such pavements in general are designed for a service life of 40 years [83]. Conversely, the Flexible pavements are considered to be more economical for a relatively shorter service life, and can be easily overlaid to extend the service life [13]. It is also important to note that the curing period of new concrete is approximately 28 days, while the asphalt surfaces can be trafficked almost immediately after construction or maintenance. This can be an important consideration in minimizing the traffic disruptions. The cost associated with local initial construction and subsequent maintenance, local soil and drainage properties are known to form the most important considerations in selecting the types of pavement.

Pavement damage refers to degradation of the structural integrity or surface profile of a road. Since roads are designed for a finite service life and are expected to deteriorate in time, it may alternatively be defined as wear. The primary modes of failure described by Rauhut et al. [5] and Pell [6] are:

(i) Fatigue cracking for all types of pavements,

(ii) Rutting and reduced skid-resistance for flexible and composite pavements,

(iii) Reflection cracking for composite pavements,

(iv) Low temperate cracking for flexible and reinforced rigid pavements,

(v) Spalling for rigid pavements,

(vi) Faulting for jointed rigid pavements,

(vii) Punchouts and steel rupture for continuous reinforced rigid pavements.

Although a precise physical mechanism by which road surface cracking and permanent deformation damage occur has not yet been reported, the studies have shown that each failure mode is affected by many factors, such as the roadway design, construction methods, the material properties of each constituent layer, the traffic loading and the environmental conditions throughout the service life. While the fatigue damage of the pavement has been related to the static loads of the individual axles, the rut damage of the pavement has been related to the gross weight of the vehicles [7].

1.2.2 Tire Loads

Static Loads

The vehicle induced road damage has been investigated using the static tire loads as a first approximation, while neglecting the dynamics of the vehicle. The most important result of the AASHO (American Association of State Highway Officials) road test was the 'fourth power law' which has had a profound influence on pavement design and operating practice throughout the world ever since [13]. The results of the study revealed that the decrease in 'pavement serviceability' [18] caused by a heavy vehicle axle could be related to the fourth power of its static load [68]. A fourth power law was

thus proposed, which has been extensively used to express the loads due to different vehicles into a number of *Equivalent Standard Axle Loads* (ESALs) [88]. The number of ESALs N is attributed to static load *P* is given by:

$$N = (P / P_0)^n, \tag{1.1}$$

where n = 4, and P_0 is generally taken to be 80 kN.

This equation provided enormous simplifications in pavement design and a simple tool for evaluating the road damaging potential of vehicles. Many concerns, however, have been raised on the validity of the 'fourth power law' since the current axle loads, and axle group configurations, tire sizes and inflation pressures; road construction; and traffic volumes are significantly different from the conditions of AASHO road tests [38, 89, 90]. More recent studies have reported that the damage exponent n in equation (1.1) may take a wide range of values, ranging from 2 to 6 for flexible pavements [89, 91], and 8 to 33 for composite and rigid pavements [92, 93, 94].

Gillespie et al [7] performed an extensive theoretical study of vehicle-road interaction and concluded, that the gross vehicle weight is the dominating factor in rutting damage, whereas the individual static axle loads are responsible for the fatigue damage. Most tandem and tri-axle truck suspension systems are designed to equalize the static loads carried by the individual axles in a group. In practice, the effectiveness of load equalization on moving vehicles varies significantly among different suspension design [18]. Uneven static load sharing increases fatigue damage, since the power-law damage relationships accentuate the effects of more heavily loaded axles [18]. Sweatman [20] introduced the 'Load Sharing Coefficient' (LSC), defined as the ratio of mean measured

wheel load to nominal static load to study the influence of load sharing on the road damage. The nominal static load was defined as the mean load acting on a single wheel in the group. The LSC is theoretically 1.0 for perfect load sharing. For a tri-axle group with leaf spring suspension, the lightest axle revealed loads, which were typically 60-70% of the most heavily loaded axle. The study reported that air suspensions, with load variation being in the vicinity of 10%, offer enhanced load equalization. Although tandem-axle suspensions generally equalize better than the tri-axle suspension groups, the walking-beam tandem suspension was observed to yield poor load sharing properties [19], which was attributed to inappropriate installation practice and incorrect torque rod location. The study further concluded that $\pm 5\%$ variations in the LSC yield only insignificant fatigue damage, while the fatigue damage increases by 40-50% when LSC approaches 1.2, depending on the axle spacing, and the type and strength of the pavement [7].

Dynamic Loads

Dynamic interactions between the tire and road surface cause considerable fluctuations in the tire loads. Such fluctuations about the static load are referred to as the dynamic wheel loads (DWL) or dynamic tire forces. For continuous flexible or rigid pavements, the dynamic tire forces generated by the vehicles are generally observed to be broad-band, and close to Gaussian distribution [32, 33]. A number of analytical and experimental studies have been carried out to assess the dynamic tire forces, their road damage potential, and to derive reliable pavement damage assessment tools. These studies have established that the magnitude of the dynamic tire loads is directly influenced by the vehicular vibration modes associated with the vertical and pitch motion of the sprung and unsprung masses [17], vehicle and axle configurations, inertial and

geometric properties of the vehicle, speed, road roughness, and restoring and dissipative properties of suspension and tire [54, 60, 70]. The DWL's generated by heavy vehicles predominate in two distinct frequency ranges:

- 1.5-4 Hz, corresponding to bounce, pitch and roll mode resonant frequencies of the sprung masses, and
- 8-15 Hz, corresponding to bounce and roll mode frequencies of the unsprung masses, and 'load-sharing' pitch modes of the suspensions.

The above frequency bands associated with sprung and unsprung mass resonances corresponding to roughness irregularities with wave lengths ranging from 6.9 m to 18.5 m and from 1.9 m to 3.5 m, respectively at a speed of 100 km/h. Various experimental and theoretical studies have shown that the lower frequency sprung mass modes usually dominate the dynamic tire forces on highways, except for vehicles equipped with axle group suspension with poorly damped bogie pitch modes [16]. The natural frequencies of heavy vehicles equipped with nonlinear suspension may depend upon the amplitude of vibration and thus the roughness of the road surface. The leaf-spring suspensions with considerable interleaf friction result in lower natural frequencies under high levels of excitations. Low level excitations arising from smooth roads can result in lockup of suspension with high interleaf friction. The vehicle thus exhibits lightly damped resonant oscillations in the 3-4 Hz frequency range due to compliance of the tires. The walking beam suspensions, due to their poor pitch mode damping, and air suspensions, due to their reduced spring rate in rebound, yield high dynamic loads in the higher frequency range (8-15 Hz) associated with the resonance of the unsprung masses [17].

The dynamic wheel loads of vehicles employing multiple-axle suspensions are strongly influenced by the suspension design, and load sharing mechanism. Tandem air-spring suspensions behave largely like two independent air suspensions due to slow reaction time of the pneumatic load equalization system [13]. Although walking-beam tandem suspension yield superior load equalization during bump encounters at high speeds, their performance is deteriorated by high interleaf friction. While the walking beam suspension provides good at static load equalization, it is prone to "tandem-hop" vibration at high speeds, resulting in relatively high dynamic loads [13]. The influence of axle spacing on the pavement wear depends on the degree to which the response under one axle is affected by the response induced by a nearby axle. Rigid pavements distribute loads over distances that are of the same order as the common axle spacing. The axle spacing is thus a factor in determining rigid pavement fatigue. The influence of axle spacing on the potential damage of flexible pavements, however, is insignificant since the, stresses are more localized in the wear course of a flexible pavement. It has been established that axle spacing has only insignificant influence on the rutting [36].

The response characteristics of the road materials and structures are sensitive to vehicle speed, and thus to the roughness profile of the road interacting with the tires. Recent studies have shown that spatial repeatable dynamic loads result in rapid wear of spatially the most severely loaded locations of pavements [37, 38]. Higher speeds reduce the time duration of the application of the wheel load on a given pavement location. The decrease exposure time can reduce fatigue and rutting of the viscoelastic material in flexible pavements [7]. As the speed increases, the peak strain under a constant moving load diminishes in amplitude and occurs behind the point of application of the load [39,

40]. The dominant frequencies of dynamic tire forces, however, may vary significantly with vehicle speed due to the phenomenon known as 'wheel-base filtering' [41, 42, 43, 44]. Although the excitations caused by the road surface roughness comprise various frequency components, the geometric effects can result in relative attenuation or amplification of certain frequency components [42]. These geometric effects depend on the spacing between axles and the vehicle speed.

The vibration of heavy trucks, transmitted through the tires to the pavement, is a major cause of pavement damage. In the recent years, cross-ply tires have largely been replaced by radial-ply tires, and average inflation pressures have increased from 550 kPa to 690-760 kPa [21]. Furthermore, wide-base single tires with enhanced load capacities are replacing the dual tires, particularly for the triaxle group suspensions. The engineering community has expressed serious concern that such changes in tires and inflation pressure may cause increased pavement damage, particularly the rutting [22]. The wide-base single tires have the potential to do more damage to the pavement due to a relatively smaller contact area. On the basis of asphalt strain measurements, Huhtala [24] reported that wide-base single tires are likely to cause 3.5 to 7 times more damage than the dual tires. Bonaquist [28] reported that wide single tires generate pavement strains approximately twice as large as those of the dual tires under identical loads. They also generate twice the rutting damage, and four times the fatigue damage. Furthermore, wide single tires are likely to cause up to 10 times more damage than dual tires on relatively thin asphalt pavements that fail by fatigue cracking. For thicker pavements, where permanent deformation is the main mode of failure, wide single tires are likely to cause

1.5 to 2 times more damage than dual tires. For rigid pavements, wide single tires are likely to cause a relatively small increase in fatigue damage [29].

An increase in tire inflation pressure tends to increase the road damage considerably. The tire-road contact conditions, such as the contact area and the pressure distribution over the contact patch, affect the stresses and strains the surface of the pavement, whereas the corresponding response of the lower layers depends mainly on the overall load [21, 26, 27]. From the strain measurements performed on asphalt pavement strain measurements, it was reported that a 40% increase in tire pressure can increase fatigue damage by 26%.

The magnitudes of the dynamic tire forces strongly depend on the road surface roughness and speed of the vehicle as well as on the suspension and tire properties, vehicle configuration, geometry and mass distribution of the vehicle. The road-damaging effects of dynamic tire forces has been primarily estimated using two methods. The first approach is based upon the assumption that the loading at each point along the road is essentially random and the localized zones incur statistically similar forces leading to uniformly distributed damage along the road. The studies based upon this assumption have estimated that the dynamic loads increase the road damage by approximately by 20-30% [10, 11]. The second approach assess the road damage through spatial repeatability of the tire forces on the basis that the peak forces applied by the heavy vehicle fleet are concentrated at specific locations along the road [12]. The heavily loaded locations along the road may thus be expected to incur up to four times more damage than that due to static loads [13].

A parameter often used to characterize the magnitude of dynamic tire forces is the dynamic load coefficient (DLC), defined as the ratio of root mean square (rms) tire force to the mean tire force [15]. Here the rms tire force is estimated from the standard deviation of the random tire force, while the mean value of the dynamic tire force is referred to as the static tire load. Under normal operating conditions, heavy vehicles typically yield DLC ranging from 0.05 to 0.3. Many studies have reported that the DLC increases with the increasing road roughness, speed, tire inflation pressure and suspension stiffness [70], while the influence of roll mass moment of inertia of sprung and unsprung masses, roll centre height, auxiliary roll stiffness, lateral suspension spread, track width, and cornering and longitudinal stiffness of tires on the DLC is found to be relatively insignificant [71].

From the truck manufacture's view point, suspensions and tires are identified as the most important elements in the design process, when pavement life is to be taken into account [65]. Many experimental studies have established that the properties of heavy vehicle suspensions strongly affect the magnitude of the dynamic loads transmitted to the road surfaces [66]. A reliable methodology to assess the pavement failure, however, does not yet exist due to the complex dynamics associated with the wheel-road interactions and the pavement structure. Although considerable efforts have been made to derive effective assessment tools, the agreement between theory and experiment is often unsatisfactory [67]. Concerns on the validity of the fourth power law, variations in the vehicle configurations, and climatic effects are some of the complicating factors that can result in underestimating pavement fatigue by a factor of 100 [67-69]. The damage caused by dynamic wheel loads is thus considered to be an area of high uncertainty [70].

It has thus been proposed, that various vehicle configurations should be classified based on the magnitudes of tire forces, represented by the dynamic load coefficients in order to assess their road damage potentials.

1.2.3 Suspension Damping

Dynamic wheel loads are known to be responsible for a significant component of the road damage. Since implementation of softer spring suspensions may be considered impractical, due to constraints posed by rattle space, handling and control requirements, effective suspension damping is vital for the reduction of the dynamic tire loads. The suspension dampers, in general, exhibit high damping at low relative velocities due to bleed flows, and low damping at higher velocities due to flow through blow-off valves. Since both the vehicle ride quality and dynamic tire loads are related to vehicular vibration modes, the suspension damping is expected to affect both in a very similar manner. Thus the suspension design considered adequate for improving the ride quality may lead to enhanced road friendliness of the vehicle [60]. The service life of damper and their ability to dissipate energy over various road roughness conditions is important to the overall acceptability of "road friendliness" of heavy truck suspensions.

Many studies have established important influence of vehicle weight and axle configurations; inertial and geometric properties of the vehicle, speed; road roughness, and restoring properties of suspension on the dynamic tire load variations [49,50]. The effect of dissipative properties of suspensions and tire on the dynamic wheel loads has been analyzed in a limited number of studies [51, 52]. Extensive studies on ride dynamics of road vehicles, however, have concluded that suspension damping affects the vehicle vibration behavior in a significant manner [53, 54]. A relationship between the dynamic

wheel loads and ride dynamics can be demonstrated through examination of measured dynamic wheel loads and the ride vibration data, reported in the literature. Studies performed by Sweatman [55] have concluded that a walking-beam tandem suspension yields the highest DLC, which may be attributed to very light pitch-mode damping of this suspension. Similar conclusions have been established in a study on the vehicle ride quality [56]. The poor performance dynamic wheel load of leaf spring suspensions, in terms of high dynamic loads, has been primarily attributed to their high vertical spring stiffness and dry friction (Coulomb damping) [57, 58]. The adverse influence of high magnitude of dry friction on the DLC has also been supported by studies on ride quality [56, 61]. Studies performed with softer and low friction leaf spring suspension in conjunction with a hydraulic damper, revealed considerable reduction in dynamic tire forces [59]. The study reported a 31% reduction in the rms values of the dynamic tire loads and 13% lower the road damage.

The influence of linear symmetric and asymmetric suspension damping on the dynamic wheel loads and sprung mass rms acceleration response was recently investigated through the analysis of a quarter-truck model [60]. The study concluded that an increase in damping from low to moderate levels can reduce the DLC. A further increase in the damping, however, did not result in a significant reduction in DLC. The study also reported that air suspensions with light linear damping of 10% yield significant improvement in the road friendliness of the vehicle with slight deterioration in the ride quality. It was also reported that asymmetric damping with ratio of rebound to compression damping near 5 offers considerable reduction in the DLC without deteriorating the ride quality. Heath and Good [72] reported normalized leading drive

axle load standard deviation, a measure of the DLC, equipped with undamped, lightly damped and strongly damped drive axle suspension. While the quantitative values of damping coefficients are not reported, the study concluded that the DLC can be considerably reduced by implementing auxiliary dampers. Hedrick [50] investigated the dynamic road stress factors due to articulated freight vehicles, buses and trucks. The study concluded that a soft and damped bus suspension yields a considerably lower dynamic road stress factor than that caused by a truck with stiff and lightly damped suspension. Pavement rutting has been related to the number and magnitude of load repetitions transmitted to the pavement. The implementation of adequate damping within the suspension may contribute to reduction in pavement rutting by decreasing the magnitudes of repetitive loads. Recognizing the potential benefits of soft and adequately damped suspension designs, as demonstrated in a few reported studies, the Council of European Communities has elaborated a directive describing the desired characteristics of road friendly suspension and the test procedures. The directive 92/7/EEC [62] is a suspension protocol that applies to all driven axles and defines road-friendliness with the following component and performance requirements:

- The axle must have dual tires.
- The suspension must use hydraulic dampers and the sprung mass natural frequency of the vehicle must not exceed 2 Hz;
- Damping ratio of the sprung mass must be more than 20% of the critical damping (with dampers fitted);
- The sprung mass must have a damping ratio no more than 50% of the above damping ratio when all dampers are removed.

The EEC test procedures involve the identification of a single resonant frequency and damping ratio, associated with the vertical vibration mode of the sprung mass, from

the measured suspension deflection of the tractor drive axle. Following test methods are recommended.

- Traverse a specified 80 mm step at 5 km/h and analyze the suspension frequency and damping from the transient response time history occurring after the ramp.
- Pull down the vehicle chassis such that the drive axle load approaches 1.5 times its maximum static load and release the vehicle, and analyze the subsequent oscillations to determine the natural frequency and damping ratio.
- Pull up the chassis to lift the sprung mass by 80 mm above the drive axle and release, and analyze the subsequent oscillations.

It is recommended to derive the resonant frequency from the oscillation period of the first two compression peaks, while the damping ratio may be calculated from the ratio of amplitudes of the same two peaks. The EC proposal, however, does not specify how the payload mass should be applied to the tractor. The EC pull down test is also questionable, since high damping may be measured when the first test event is associated with suspension rebound. The results derived from recent drop experiments also confirmed that dampers play a crucial role in the road-friendly performance of the suspensions [63]. Only one air suspension was found to meet the EC directive on the suspension performance. It was also concluded that frequency was a strong indicator of road-friendliness, and the sprung natural frequency ranging from 1.5 to 2 Hz with damping ratio of at least 10% were considered appropriate.

1.2.4 Dynamic Vibration Absorbers

The dynamic wheel forces generated by the heavy vehicles predominate in two distinct frequency ranges: (i) 1.5-4 Hz corresponding to bounce, pitch and roll resonant frequencies of the sprung masses; and (ii) 8-15 Hz corresponding to the bounce and roll

resonant frequencies of the unsprung masses, and the suspension pitch modes associated with load-sharing. Most vehicle suspensions yield significant dynamic loads in the low frequency range, which is associated with resonances of the sprung masses. The walking-beam suspensions, due to their poor pitch mode damping, and air suspensions, due to their reduced spring rate in rebound, yield high dynamic loads in the higher frequency range (8-15 Hz), which is associated with the resonances of the unsprung masses [78]. Reduction of dynamic wheel loads or enhancement of road friendliness of heavy vehicles necessitates control of resonant wheel forces near the sprung and unsprung mass resonant frequencies. Tuned dynamic vibration absorbers have been extensively used to suppress the resonant oscillations of machines and structures [59, 80]. An absorber attached to the axle and tuned to the wheel-hop frequency, may lead to considerable reduction in dynamic tire loads near the usnprung mass resonant frequencies. An absorber tuned to the sprung mass resonant frequency, however, is considered to be impractical due to requirement of large absorber mass. Further more, a dynamic vibration absorber does not affect the vehicle ride quality in the frequency range of 3-8 Hz, where the human body is most sensitive to whole-body vibrations [54, 56].

1.2.5 Analytical Vehicle Models

The study of pavement vehicle interaction and ride quality of the heavy vehicle involves the development of a representative dynamic model that closely describes the vehicle behavior. Many vehicle models ranging from linear quarter vehicle models with two degrees-of-freedom (DOF) to complex three-dimensional models with as many as 19 DOF have been reported in the literature. While the majority of the models consider the sprung and unsprung masses as rigid bodies, few models have incorporated the flexibility

of the trailer structure to study the contributions due to frame bending modes [46, 47, 48]. Simple one and two DOF of linear vehicle models have been used by several investigators to study the dynamic interaction of the heavy vehicle with the pavement [60, 61, 64]. Such models permit the analysis of different suspension concepts under uncoupled vertical motions in a highly convenient manner. These models, however, cannot be used to analyze the total dynamic interactions of the heavy vehicles with the roads, which comprise various vibration modes associated with vertical, roll and pitch motions of axles and sprung masses, nonlinarties due to friction, and influence of coupled suspensions systems.

Many analytical and experimental studies on pavement damage and dynamic wheel loads are reported in the literature. The primary objective of these studies include the analysis of the influence of various design and operating parameters of the vehicle on the dynamic wheel loads and thus on the pavement damage. Since the simple one-dimensional vehicle models cannot be used to predict the complex dynamics associated with heavy vehicles, a number of comprehensive two and three-dimensional vehicle models have been developed to study the tire forces and the ride quality of the vehicle. Analytical models with limited number of DOF, but realistic enough to provide reasonable accurate estimate of the tire force characteristics and ride quality are desirable for design and optimization studies [73, 74]. The majority of the studies, related to dynamic pavement vehicle interactions and ride quality, have concluded that the contributions of the roll-plane dynamics of highway vehicles are relatively insignificant [75]. Many research studies have demonstrated that a four DOF in plane model of a

single unit can be effectively used to determine vehicle behavior pertaining to dynamic tire loads and ride quality [55, 61].

Bending vibration of the frame, that are known to exhibit bending modes in the 6 to 9 Hz frequency range, have been included in some of the reported models of heavy vehicles in order to study the contribution due to frame bending [46]. The motion imposed on the axles by frame bending is relatively small when compared to the motion induced by the resonances of the sprung and unsprung masses. Thus, the majority of the studies have concluded that the contributions of the frame bending modes to the overall dynamic behavior are insignificant [46, 47, 48]. These studies have established that the development of an analytical vehicle model for the analysis of dynamic tire forces and ride quality primarily involves the characterization of the suspension and tires. Vehicle suspension systems often exhibit nonlinearites associated with Coulomb friction of leaf spring and progressive hardening nature of the air springs, and variable force-velocity properties of the dampers due to bleed and blow-off hydraulic flows. Majority of the analytical investigations, however, were based on the assumption of linear suspension damping, while the influence of nonlinear and asymmetric suspension damping, on the dynamic behavior of the vehicle has been addressed only in few studies [95].

The tire-terrain interactions have been characterized by different types of linear and nonlinear tire models. The tire models, reported in the literature, can be grouped in four categories based upon the characterization of the tire-road contact: point contact; rigid tread band; fixed foot print; and adaptive foot print models [81, 82]. In view of the high inflation pressure used in the commercial vehicle tires, a point-contact model is often considered appropriate for analysis of the dynamic tire forces. Majority of the

analytical studies have thus employed either linear or nonlinear tire models based upon the point contact.

1.3 SCOPE OF THE THESIS

The overall objective of this dissertation research is to contribute towards enhancement of road friendliness and driver friendliness of freight vehicles. The specific objective of the dissertation research is to analyze the effectiveness of suspension damping and dynamic vibration absorbers in reducing the dynamic wheel loads transmitted to the pavement. An analogy between the dynamic wheel loads and ride quality performance characteristics of heavy vehicles is established in order to illustrate the potential benefit of optimal damping in conjunction with different suspension springs used in heavy vehicles. The detailed objectives of this study are:

1. To establish an analogy between the dynamic wheel loads and ride quality performance characteristics of heavy vehicle through analysis of an in-plane vehicle model.

2. To analyze the effectiveness of a dynamic axle vibration absorber and study the influence of its tuning parameters on the dynamic wheel loads under excitations arising from interaction with the roads of different roughness.

3. To determine the optimal tuning parameters of the dynamic vibration absorbers, while limiting the absorber mass to minimal.

4. To formulate a performance criterion comprising dynamic load coefficient due to tires on different axles and overall rms acceleration transmitted to the driver station.

5. To study the influence of nonlinear and asymmetric suspension damping on the performance criterion for freight vehicles employing linear, leaf and air suspension springs to perform multi-parameter optimization to identify optimal force-velocity characteristics of the suspension dampers in conjunction with typical linear, leaf and air suspension springs.

6. To evaluate the role of combined optimal dynamic vibration absorber and suspension damping on the road-and driver-friendliness of the vehicle under varying operating condition.

1.4 LAYOUT OF THE THESIS

In Chapter 2, an in-plane model of a three axle truck is formulated with an objective to assess interactions with the road in terms of vertical tire loads transmitted to the road, and vertical acceleration transmitted to the driver station. Nonlinear leaf and air suspension springs are analytically modeled and validated against the available experimental data. The suspension damping is characterized by multi-stage and asymmetric force velocity characteristics identified from the laboratory tests conducted at CONCAVE.

In Chapter 3, the enhancement of road friendliness of heavy vehicles is analytical investigated using a concept of dynamic vibration absorber, tuned to the resonant frequencies of the unsprung masses of the vehicle model. A parametric study is performed to analyze the influence of frequency ratio, damping ratio and mass ratio of the absorber on the tire loads and the acceleration response for deterministic and stochastic excitations at the tire-road interface. Optimal absorber parameters were determined using a weighted multi parameter objective function for a wide range of vehicle speeds and road roughness.

In Chapter 4, An analogy between the dynamic wheel loads and ride quality performance characteristics of heavy vehicles is established through analysis of linear quarter-vehicle model in order to illustrate the potential benefits of optimal damping. A performance criterion comprising dynamic load coefficient due to tires on different axles and overall rms acceleration transmitted to the driver station is formulated. A multi-parameter optimization problem is formulated and solved to identify optimal force-velocity characteristics of the suspension dampers in conjunction with linear, leaf and air suspension springs. The effect of optimal suspension damping on the DLC and the ride quality are illustrated through analysis of a straight truck model with linear and non linear suspension stiffness. The influence of optimal suspension damping and optimal axle absorber on the dynamic loads and ride is further investigated for the linear, leaf-leaf and leaf-air suspensions of a truck under varying operating condition.

Finally, major contributions of the study are outlined together with the major conclusions in Chapter 5.

CHAPTER 2

DEVELOPMENT OF VEHICLE MODELS

2.1 INTRODUCTION

The dynamic wheel loads of heavy vehicles transmitted to the pavements are strongly related to tire-road interactions, road roughness, vehicle weights and dimensions, axle loads and configurations, suspension and tire compliance, and operating speed. A study of dynamic wheel loads primarily arising from the vehicle-pavement interactions necessitates the development of a dynamic vehicle model that closely describes the vehicle and components behavior. Since the dynamic wheel loads and the ride quality are related to vehicle vibration modes, the vehicle model considered to study the tire-road interactions can also be used to study the ride dynamics of the vehicle. Various studies performed on heavy vehicles have established significant influence of suspension and tire properties on both the dynamic wheel loads and ride quality performance [18]. Although vehicle suspensions exhibit strongly nonlinear force-deflection and asymmetric force-velocity characteristics, majority of these studies considers only linear viscous suspension damping. Other studies have established insignificant contributions due to roll dynamics of the vehicle [13]. An in-plane vehicle model describing the vehicle-road interactions associated with vertical and pitch modes of vibration is thus considered appropriate to study the driver-and road-friendliness of the vehicle. It is, however, vital to identify and

incorporate the important nonlinear properties of the suspension and tires, to enhance the effectiveness of the model.

2.2 ANALYTICAL MODEL OF A THREE-AXLE TRUCK

An in-plane model of a three axle truck is formulated to study its interactions with the road in terms of vertical tire loads transmitted to the road, and vertical acceleration transmitted to the driver station, assuming negligible contributions due to roll dynamics of the vehicle. Two closely spaced rear axles are grouped together and represented by a single composite axle, as shown in Figure 2.1. The vehicle body, chassis and cargo are characterized by a rigid sprung mass m_S with two-degrees-of-freedom (DOF): vertical and pitch. The front and composite rear wheel and axle assemblies are represented by rigid masses, referred to as unsprung masses, with only vertical DOF. Each unsprung mass is coupled to the sprung mass through the respective suspension components, modeled as parallel combinations of energy restoring and dissipative elements. The front and rear axle tires are modeled as damped elastic elements, assuming point contact with the road. The contributions of the frame bending modes to the vibration behavior of the vehicle are considered to be insignificant due to relatively small deflections of the frame, and location of the suspensions near the nodes. The equations of motion of the four-DOF in-plane vehicle model shown in Figure 2.1, can be expressed as:

$$
\begin{aligned}
&m_S\ddot{z}_1 + F_{SF}(z_1, z_2, \theta) + F_{SR}(z_1, z_3, \theta) + m_S g = 0,\\
&I\ddot{\theta} + \ell_R F_{SR}(z_1, z_3, \theta) - \ell_F F_{SF}(z_1, z_2, \theta) = 0,\\
&m_F\ddot{z}_2 - F_{SF}(z_1, z_2, \theta) + F_{TF}(z_2, z_{OF}) + m_F g = 0,\\
&m_R\ddot{z}_3 - F_{SR}(z_1, z_3, \theta) + F_{TR}(z_2, z_{OR}) + m_R g = 0.
\end{aligned}
\tag{2.1}
$$

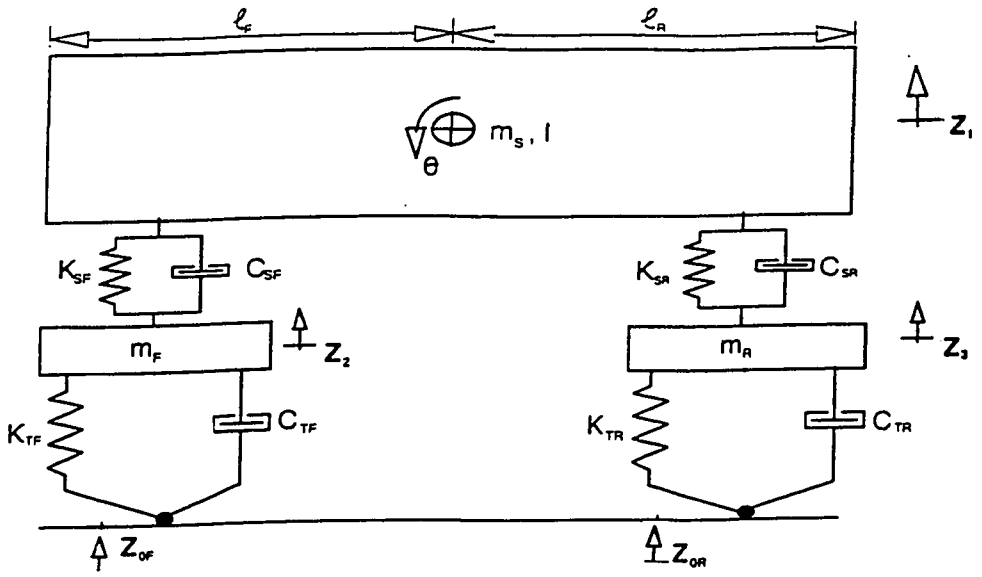

Figure 2.1 In plane model representation of a straight truck.

Where F_{SF} and F_{SR} are suspension forces developed by the front and rear suspension respectively. The suspension forces depend upon the type of suspension employed in the vehicle. Heavy vehicles employ leaf spring or air suspension. While the suspension forces due to such suspensions are presented in the later section, the suspension forces due to linear springs may be expressed as:

$$F_{SF}(z_1, z_2, \theta) = K_{SF}(z_1 - \ell_F\theta - z_2 - \delta_{SF}) + F_{DF}$$
$$F_{SR}(z_1, z_2, \theta) = K_{SR}(z_1 + \ell_R\theta - z_3 - \delta_{SR}) + F_{DR} \qquad (2.2)$$

where K_{SF} and K_{SR} are the linear or equivalent linear spring rates due to front and rear suspension, and F_{DF} and F_{DR} are the respective damping forces. The damping forces, in general, are non-linear and asymmetric functions of the velocity, which are derived in the later section. δ_{Si} is the static deflection of the suspension i (i=F, R). The tire is modeled as a parallel combination of a nonlinear asymmetric spring and a linear damper, assuming point contact with the road. F_{TF} and F_{TR} are the forces developed by the front and composite rear axle tires.

$$F_{TF}(z_2, z_{OF}) = K_{TF}(z_2 - z_{OF} - \delta_{TF}) + C_{TF}(\dot{z}_2 - \dot{z}_{OF}); \qquad \text{for } (z_2 - z_{OF} - \delta_{TF}) \le 0;$$
$$F_{TR}(z_3, z_{OR}) = K_{TR}(z_3 - z_{OR} - \delta_{TR}) + C_{TR}(\dot{z}_3 - \dot{z}_{OR}); \qquad \text{for } (z_3 - z_{OR} - \delta_{TR}) \le 0;$$
$$F_{TF}(z_2, z_{OF}) = 0; \qquad \text{for} (z_2 - z_{OF} - \delta_{TF}) \ge 0,$$
$$F_{TR}(z_3, z_{OR}) = 0; \qquad \text{for} (z_3 - z_{OR} - \delta_{TR}) \ge 0. \qquad (2\,3)$$

where K_{Ti} and C_{Ti} (i=F,R) are the vertical spring rate and viscous damping coefficient of the tire i respectively and δ_{Ti} is its static deflection. z_{0F} and z_{0R} are the displacement excitations encountered at the front and rear tire load interface, respectively. m_S, m_F and m_R are the masses due to sprung weight of the vehicle, and front and rear axles. I is the pitch mass moment of inertia of the sprung weight about its centroid. Equations (2.1) to (2.3) describe the vertical and pitch dynamics of the three-axle truck, where the sprung mass acceleration $\ddot{z}_1$ relative to the ride quality, and the tire forces F_{TF} and F_{TR} describe the dynamic tire forces transmitted to the pavements.

2.2.1 Dynamic Axle Vibration Absorber

The dynamic tire forces transmitted to the road are frequently evaluated in terms of the Dynamic Load Coefficient (DLC), defined as the standard deviation of the dynamic wheel force normalized by its mean force [5]. The DLC is used to determine the relative pavement loads and road-friendliness characteristics of the vehicles. Many studies have reported that the DLC increases with the increasing road roughness, speed, tire inflation pressure and suspension stiffness [6, 7].

The dynamic wheel forces generated by the heavy vehicles predominate in the two distinct frequency ranges:

- 1.3-4.0 Hz corresponding to bounce, pitch and roll resonant frequencies of the sprung masses.
- 8-15 Hz corresponding to the bounce and roll resonant frequencies of the unsprung masses, and the suspension pitch modes associated with load sharing.

Most vehicle suspensions yield significant dynamic loads in the low frequency range, associated with resonance of the sprung masses. The walking-beam suspensions,

due to their poor pitch mode damping, and air suspension, due to their reduced spring rate in rebound, yield high dynamic loads in the higher frequency range (9-15 Hz) associated with the resonances of the unsprung masses [8]. Reduction of dynamic wheel loads or enhancement of road-friendliness of heavy vehicles thus necessitates control of resonant wheel forces near the sprung and unsprung mass resonant frequencies. Dynamic vibration absorber tuned to the unsprung mass resonant frequency can be employed to reduce the dynamic wheel loads in the vicinity of wheel-hop frequencies. Tuned dynamic vibration absorbers have been extensively used to suppress the resonant oscillations of machines and structures [9, 10]. The primary design constraints associated with the implementation of a dynamic vibration absorber are:

- The absorber mass should be minimal such that payload capacity of the vehicle is not significantly affected.
- The absorber deflection relative to the primary structure, to which it is attached, should be small.

An absorber tuned to the sprung mass resonant frequency may be considered impractical due to requirement of large absorber mass, the absorber attached to the axle and tuned to the wheel-hop frequency, can lead to considerable reduction in dynamic tire loads near the unspurng mass resonant frequencies. Furthermore, an effective axle vibration absorber can be realized with relatively small mass. In this study, the concept of dynamic vibration absorber is explained to reduce the contribution of axle vibrations to the DLC. The axle absorber, constrained to move along the vertical coordinates, may be conveniently attached to the axles, as illustrated in the roll-plane schematic in Figure 2.2. The front and rear axle absorbers in the pitch-plane vehicle model are represented by

absorber masses attached to the front and rear axles through a damper and a spring, as shown in Figure 2.3.

Equations of Motion

The differential equations, describing the vertical and pitch dynamic motions of the vehicle model comprising the axle vibration absorbers are derived, assuming small motions. The coupled differential equations of motion arising from the vehicle-road interactions are expressed as:

$$m_S\ddot{z}_1 + F_{SF}(z_1,z_2,\theta) + F_{SR}(z_1,z_3,\theta) + m_S g = 0\,,$$

$$I\ddot{\theta} + \ell_R F_{SR}(z_1,z_3,\theta) - \ell_F F_{SF}(z_1,z_2,\theta) = 0\,,$$

$$m_F\ddot{z}_2 - F_{SF}(z_1,z_2,\theta) + F_{TF}(z_2,z_{OF}) + m_F g + m_{AF}\left[\omega^2{}_{AF}x_4 + 2\varsigma_{AF}\omega_{AF}\dot{x}_4\right] = 0\,,$$

$$m_R\ddot{z}_3 - F_{SR}(z_1,z_3,\theta) + F_{TR}(z_2,z_{OR}) + m_R g + m_{AR}\left[\omega^2{}_{AR}x_5 + 2\varsigma_{AF}\omega_{AF}\dot{x}_5\right] = 0\,,$$

$$m_{AF}\ddot{z}_4 - \left[\omega^2{}_{AF}x_4 + 2\varsigma_{AF}\omega_{AF}\dot{x}_4\right] + m_{AF}g = 0\,,$$

$$m_{AR}\ddot{z}_5 - \left[\omega^2{}_{AR} + 2\varsigma_{AR}\omega_{AR}\dot{x}_5\right] + m_{AR}g = 0. \qquad (2.4)$$

Where m_{AF} and m_{AR} are the masses due to the dynamic vibration absorbers attached to the front and rear axles, respectively. ω_{AF} and ω_{AR} are the uncoupled natural frequencies of the front and rear axle absorbers, and ς_{AF} and ς_{AR} are the respective uncoupled damping ratios, expressed as:

$$\omega_{Ai}{}^2 = \frac{k_{Ai}}{m_{Ai}};\ \varsigma_{Ai} = \frac{C_{Ai}}{2m_{Ai}\omega_{Ai}};\ i = F,R\,, \qquad (2.5)$$

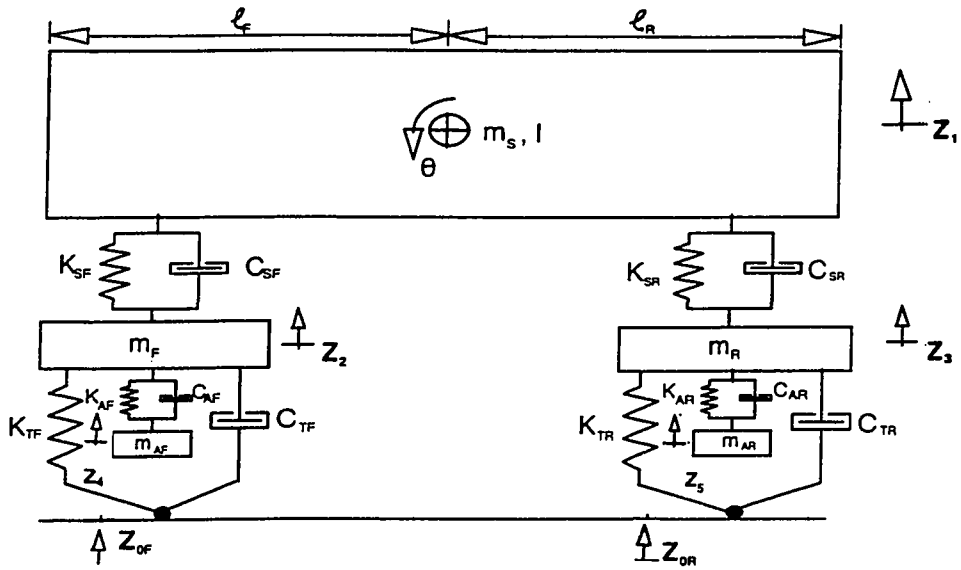

Figure 2.3 In-Plane model representation of a straight truck with dynamic Axle vibration Absorbers.

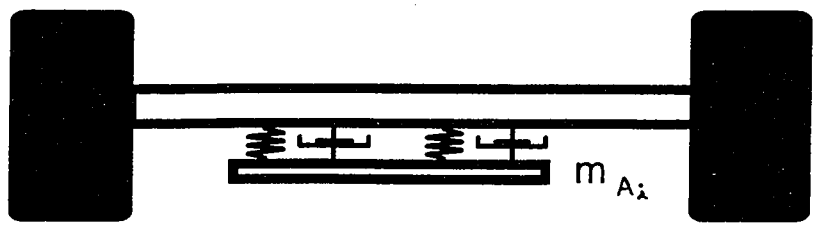

Figure 2.2 Schematic of damped vibration absorber attached to an axle.

where K_{Ai} and C_{Ai} (i= F, R) are the linear stiffness and damping coefficient due to the front and rear axle absorbers. x_4 and x_5 are the relative deflection of front and rear axle absorber masses with respect to the axle masses they are attached.

The tire is a visco-elastic element that supports the unsprung mass on the road surface. Tire is modeled as parallel combination of a nonlinear asymmetric spring and a linear damper assuming point contact with the road. Since the ground can not pull back the tire, tire forces are set to zero, in case of wheel hop.

2.3 ANALYTICAL MODELING OF NON LINEAR SUSPENSIONS

Heavy vehicle suspensions frequently employ leaf and air springs, which exhibit strongly nonlinear force-deflection characteristics. The force-deflection properties of the springs are thus characterized and incorporated into the vehicle model to develop effective models. Leaf spring suspensions exhibit strongly hysteretic behaviour due to high magnitudes of inter-leaf friction. The restoring force developed by an air spring is directly related to the instantaneous pressure, volume and the effective cross-sectional area of the air bag, which are highly nonlinear functions of the suspension deflection.

2.3.1 Leaf spring suspension

Leaf spring suspensions employed in trucks are complex force-generating mechanisms, which may exhibit varying levels of effective spring rate and hysteresis, depending upon the loading of the spring and the amplitude of the oscillation. Fancher [58] proposed a semi-empirical model to characterize the force deflection properties of a hysteretic leaf spring suspension, that may be applied over a wide range of loads and

deflection amplitudes. The proposed model is based upon the equivalent stiffness and a hysteretic force expressed as a function of the deflection and the velocity. Figure 2.4 illustrates the measured force-deflection properties of a typical leaf spring employed in front suspension. The suspension force, F_i as a function of the relative deflection x, may be expressed as:

$$F_i = F_{Env\,i} + (F_{i-1} - F_{Env\,i})\, e^{-\frac{|x_i - x_{i-1}|}{\beta}} \qquad (2.6)$$

where F_i is the suspension force developed due to deflection x_i at instant t_i, and F_{i-1} is the suspension force corresponding to deflection x_{i-1} at previous instant t_{i-1}.

$F_{Env\,i}$ represents the limiting values of forces corresponding to the upper and lower curves of the measured characteristics corresponding to deflection x_i. β is an input parameter used to describe the rate at which the suspension force within a hystersis loop approaches the envelope, F_{Env}. The envelope force curves and the β values, derived using curve-fitting techniques, for the front and multi-leaf suspension considered in this study, are expressed as:

$$F_{Env} = 227.6535\,x + 1.3344 \text{ kN};\ \beta = 0.0019304 \text{ m}, \quad \text{for } (x_i - x_{i-1}) > 0,$$

$$F_{Env} = (192.62992)\,x - 0.4488 \text{ kN};\ \beta = 0.002032 \text{ m}, \quad \text{for } (x_i - x_{i-1}) < 0. \qquad (2.7)$$

The force-deflection properties of front multi-leaf suspension, derived from Equations (2.6) and (2.7) under harmonic deflection, are illustrated in Figure 2.4. The results show that the hystersis tends to increase with the magnitude of suspension deflection and the suspension load. Relatively small amplitude deflection of the suspension yields high stiffness and low effective damping. The validity of the semi-

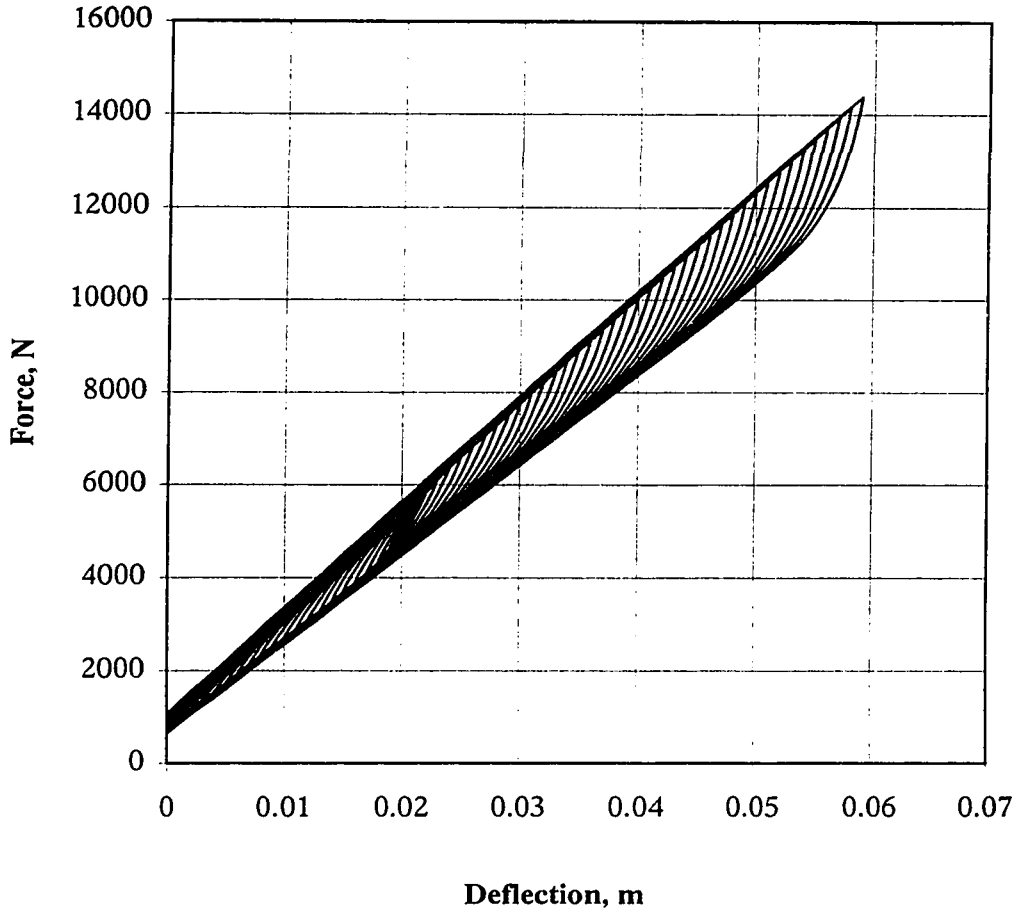

Figure 2.4 Force-deflection characteristics of front leaf spring suspension

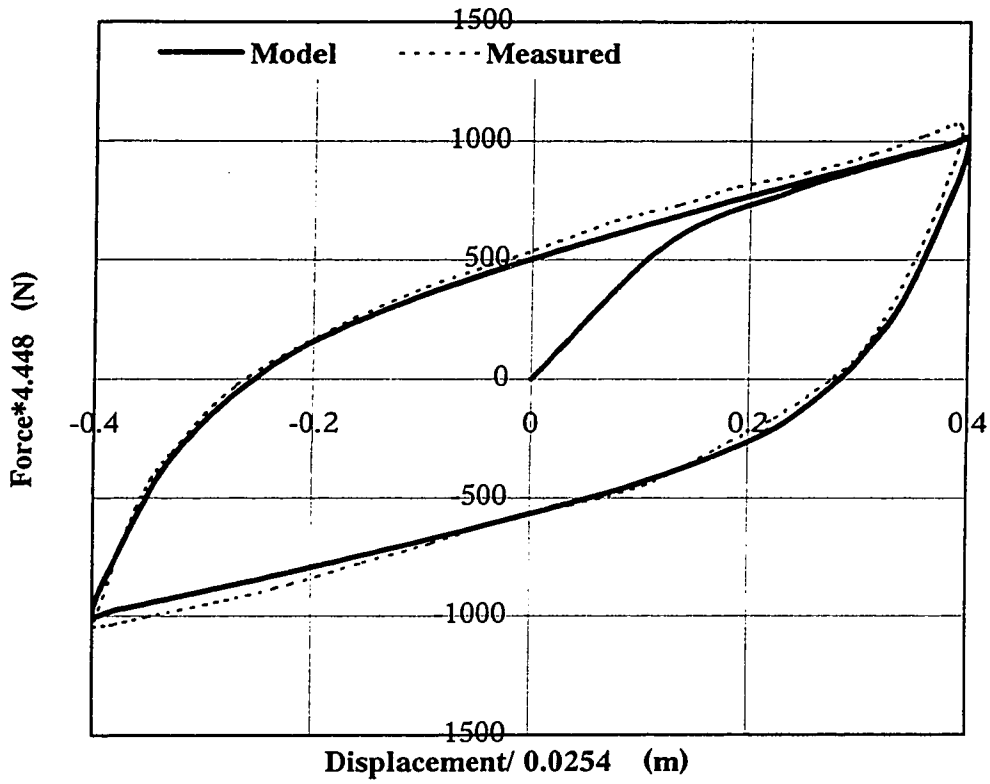

Figure 2.5 Comparison of model & measured force-deflection characteristics of front Leaf spring

empirical model is further examined by comparing the estimated force-deflection characteristics with the measured data reported in [58]. Figure 2.5 illustrates the comparison under 0.01m amplitude harmonic deflection and 26.688 KN static load. The results clearly reveal that the semi-empirical model can provide reasonably accurate description of the force-deflection characteristics of the front leaf-spring suspension, with only small errors near the extremities.

The force-deflection properties of multi-leaf rear suspension considered in this study are also derived using the measured data reported in [58]. The envelope forces and β values are expressed as:

$$F_{Env} = 0.310 + (279.359)x + (3058.530)\,x^2 \text{ kN};\ \beta = 9.494\,e^{-4} - (0.0062)x \text{ m, for } (x_i - x_{i-1}) > 0$$

$$F_{Env} = 0.093 + (186.336)\,x + (3463.608)\,x^2 \text{ kN};\ \beta = 5.08\,e^{-4} \text{ m; for } (x_i - x_{i-1}) < 0 \qquad (2.8)$$

The force-deflection characteristics of the multi-leaf rear suspension, derived from equations (2.6) and (2.8) as a function of the static load and deflection are illustrated in Figure 2.6. The effectiveness of the semi-empirical formulation is further illustrated by comparing the estimated force-deflection behaviour with the measured data [58] under 0.005 m harmonic deflection, as shown in Figure 2.7. The static load dynamic deflection, used in the simulation of front and rear suspension models is summarized in Table 2.1. The results are further analyzed to estimate the equivalent linear spring rates and the average coulomb damping forces due to both suspension, which are also summarized in Table 2.1.

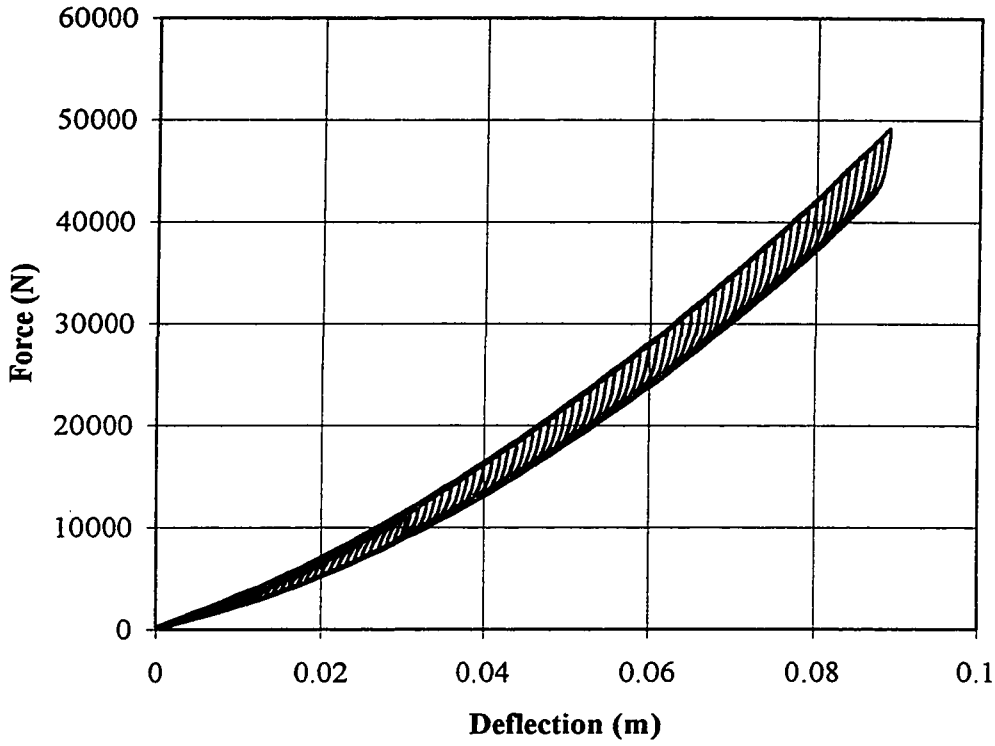

Figure 2.6 Force-deflection characteristics of the rear leaf spring suspension.

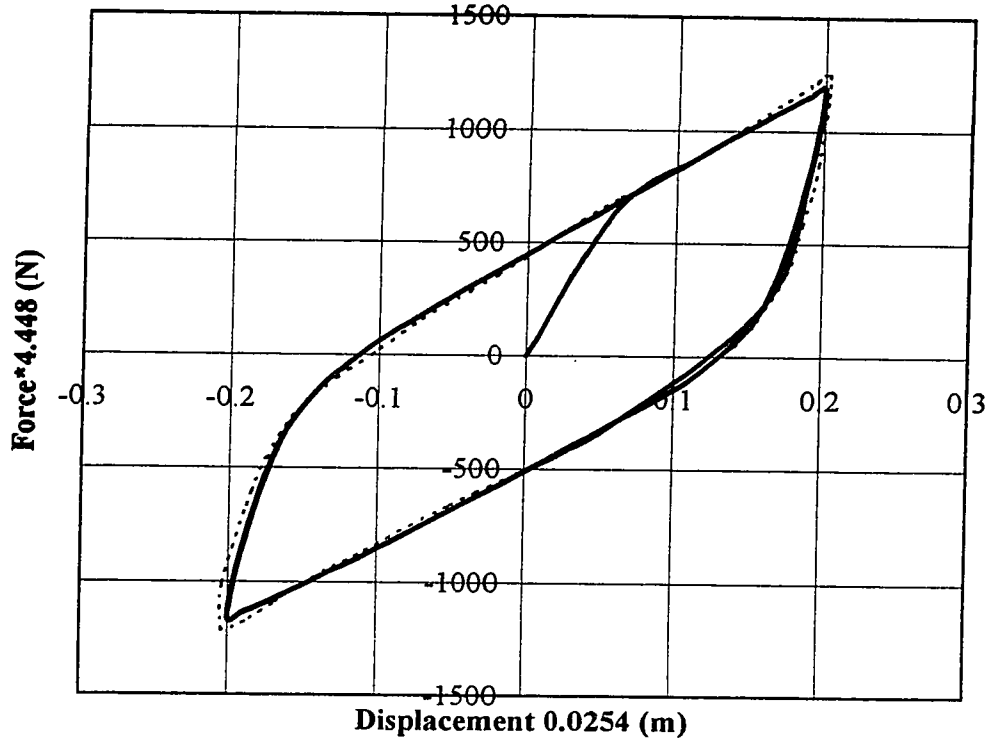

Figure 2.7 Comparison of estimated and measured force-deflection characteristics of the rear leaf spring suspension.

Table 2.1 Summary of the simulation and test conditions employed for the front and rear leaf suspensions.

	Front Leaf Spring	Rear Leaf spring
Nominal Load	26688.0 N	26688.0 N
Static deflection	0.1222 m	0.06102 m
Amplitude of deflection	0.01016	0.00508 m
Effective mean stiffness	218360.33 N/m	437795.27 N/m
Average Coulomb Damping (c_f)	2224.0 N	2001.6 N

Equations of Motion

The equations of motion of the four-DOF vehicle model equipped with front and rear multi-leaf suspension are identical to those expressed in equation (2.1). The suspension forces, F_{SF} and F_{SR}, comprise the forces due to multi-leaf springs, given in Equations (2.6) and (2.8). The leaf spring suspension, however, may or may not employ external dampers. The damping forces, F_{DF} and F_{DR} , are considered negligible when external dampers are not used.

2.3.2 Air spring suspensions

Air springs are widely used in heavy vehicle suspension and they are unique in that the loads are supported by pressure in the air bags. The pneumatic spring has been able to supplement, and in many cases replace, more conventional steel suspensions by virtue of unique characteristics:

(i) Variable spring rate over a wide load range,

(ii) Nearly frictionless action,

(iii) Outstanding noise and vibration isolation,

(iv) Wide range of load-carrying ability constant leveling, or leveling on demand,

(v) Simplicity of height control,

(vi) Engineered control of spring rate,

(vii) Low maintenance operation,

(viii) Durability.

A typical air suspension comprises a flexible air bag mounted between the chassis and a trailing arm link, as shown in Figure 2.8. The restoring force is developed by the air medium, which is a complex function of the air pressure, effective piston area, air volume, and the deflection. The piston area varies considerably with the deflection due to flexibility of the bag, which together with the pressure-volume relationship, contributes to the non-linear restoring properties of an air spring. The force-deflection properties of the air spring are characterized in the laboratory as a function of the charge pressure [95]. Figure 2.9 illustrates the measured pressure-deflection properties of the spring for different charge pressures (689 Kpa, 551 Kpa, 413 Kpa), over the spring travel ranging from -7.5 cm to 12.5 cm. The measured characteristics clearly reveal nonlinear progressively hardening characteristics, which are attributed to the pressure-volume relationship of the gas and the variation in the effective piston area. The results also exhibit small hystersis attributed to the hysteretic properties of the flexible air bag and the rubber piston.

An analytical model of the air spring is derived to determine its pressure-deflection characteristics, assuming negligible hystersis and constant temperature

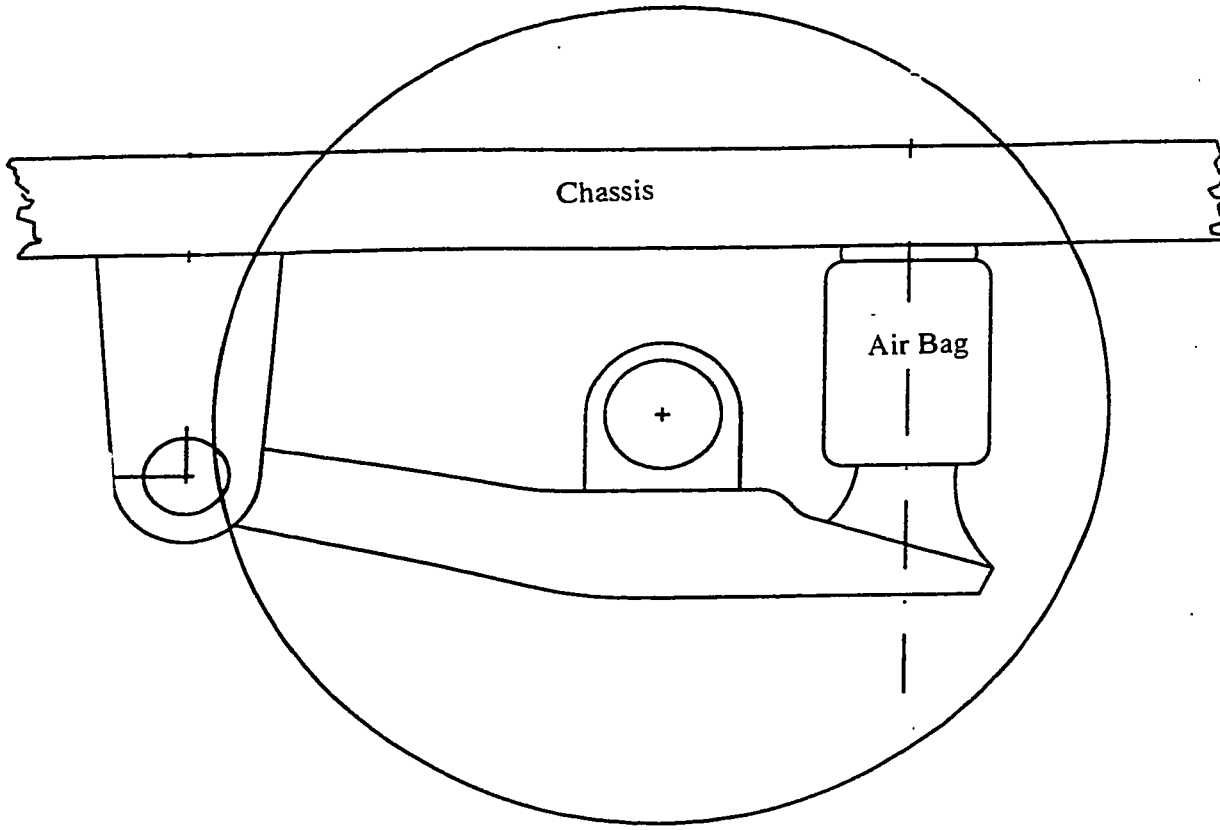

Figure 2.8 Schematic of a trailing-arm air suspension.

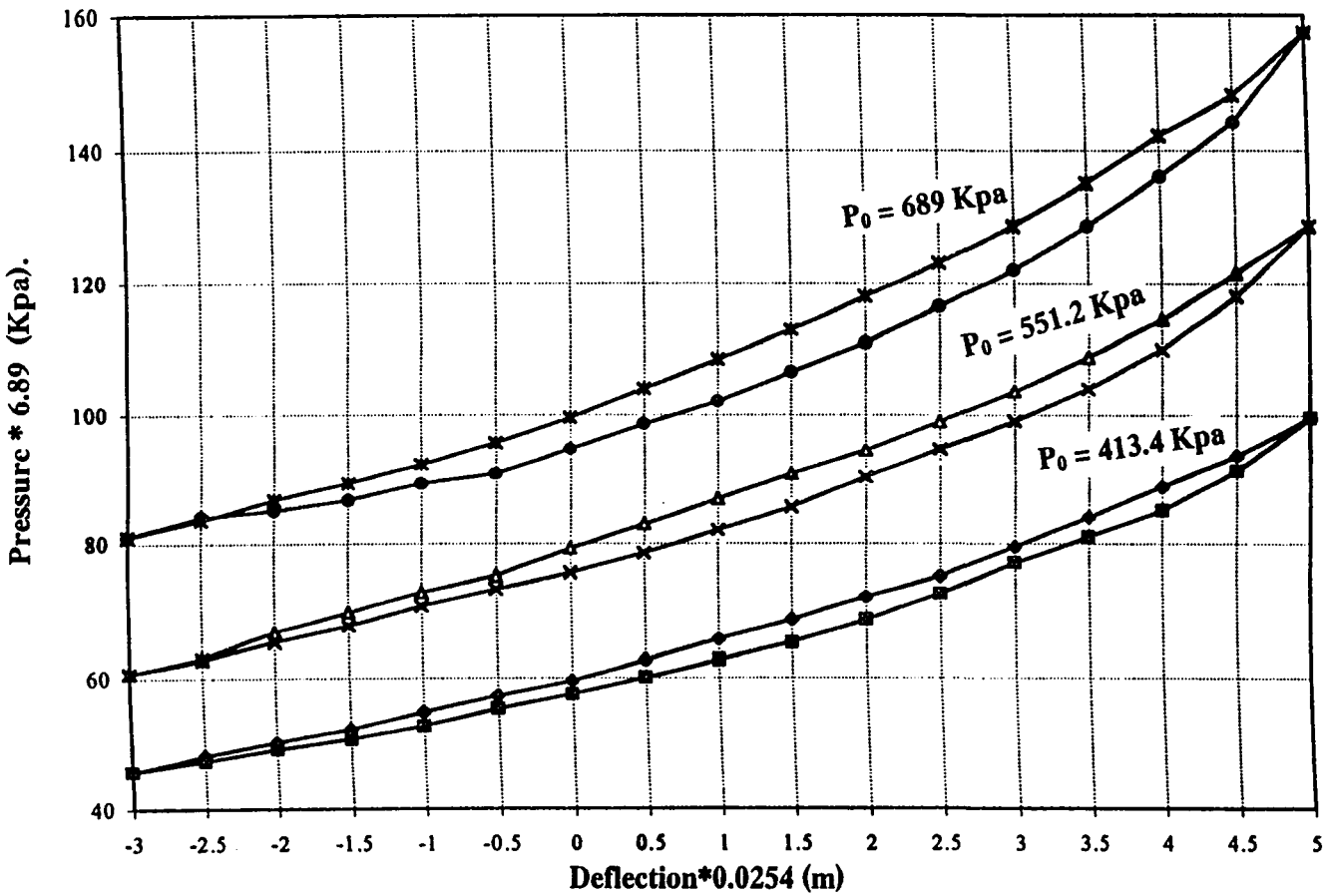

Figure 2.9 Measured Pressure-deflection properties of the air bag

compression and expansion of the air. The instantaneous air pressure as a function of the deflection can be expressed as:

$$P(x, t) = \left[\frac{P_0 V_0}{(V_0 - A_E(x)x(t))}\right], \tag{2.9}$$

where P(x, t) is the instantaneous air pressure as a function of deflection x. P_0 and V_0 are the charge pressure and volume, respectively. A_E is the effective piston area. The spring force developed by the air bag, F_{AR}, is given by:

$$F_{AR} = [P(x,t) - P_A]A_E(x) \tag{2.10}$$

where P_A is the atmospheric pressure. The effective area, A_E, is known to be strongly dependent upon the spring deflection and considerably less dependent upon the air pressure. The effective area is further dependent upon the geometry of the piston. In this dissertation, the volume-deflection data supplied by the manufacturer [95] is studied to derive the effective area as a function of the deflection. A regression analysis is then performed to derive a polynomial function relating the effective area to the corresponding deflection in the following manner:

$$A_E(x) = a_0 + x(a_1) - x^2(a_2) + x^3 a_3 \quad m^2 \tag{2.11}$$

For the air bag considered in this study, the coefficients a_0 to a_3 are obtained as: a_0= 0.0450; a_1= 0.000748; a_2= 0.0003; a_3= 0.0000437. The effective area estimated form

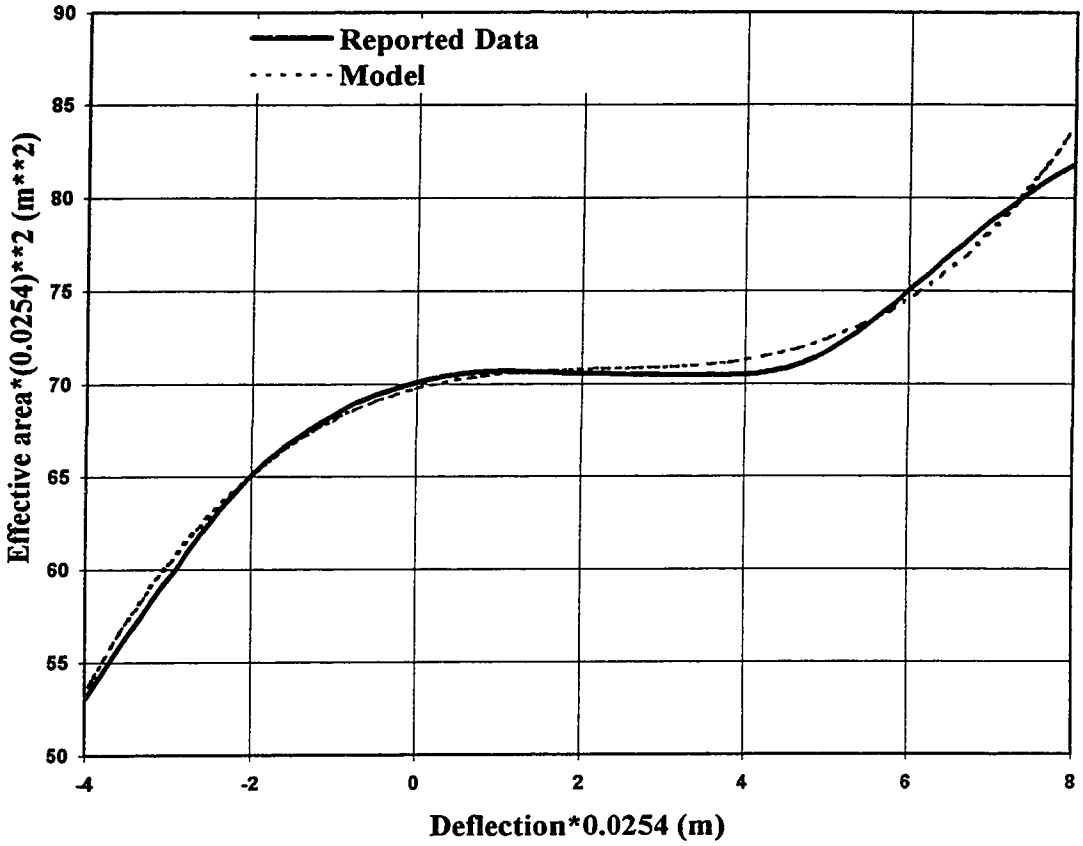

Figure 2.10 Comparison of estimated effective area with the reported data by the manufacture [95]

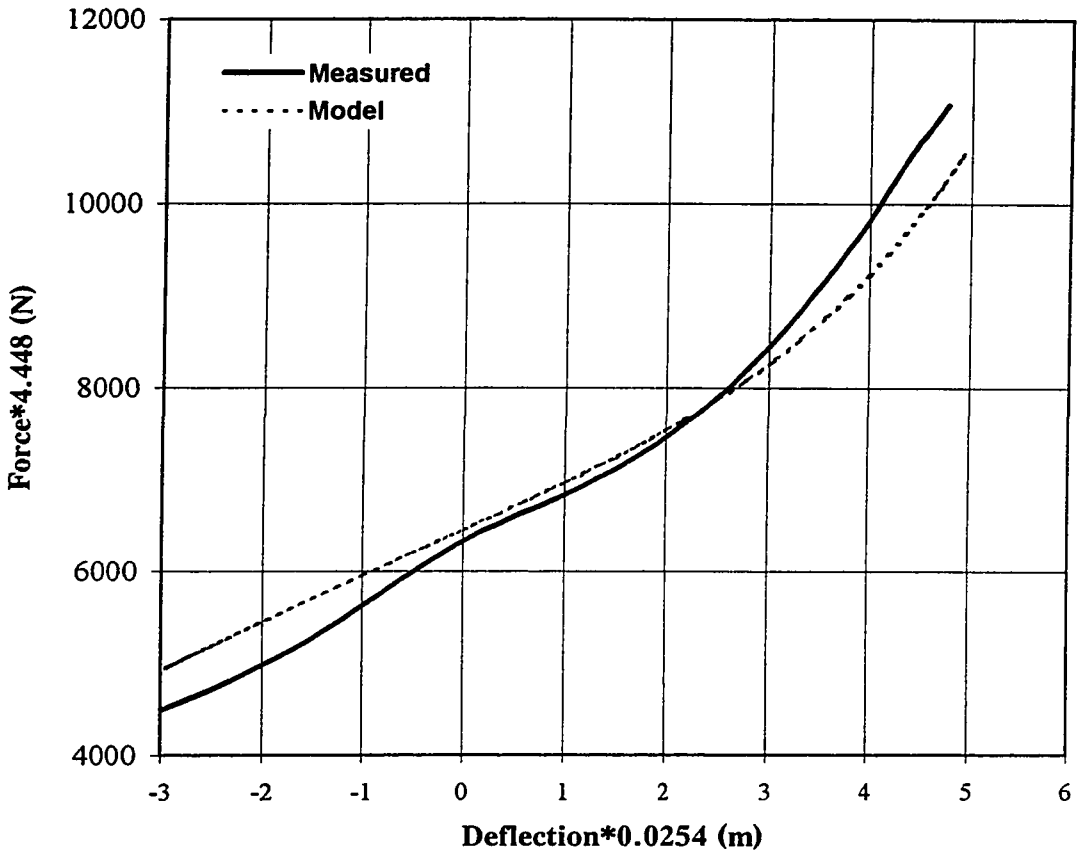

Figure 2.11 Comparison of model & measured force-deflection characteristics of an airride spring.

Equation (2.11) is compared with the data reported by the manufacturer, as shown in Figure 2.10. While the results show good correlation between the estimated and reported data, a strong dependence on the deflection is observed. The effective area tends to remain nearly constant for small deflection in the vicinity of the static equilibrium, and increases rapidly under high magnitude compressive deflection. The effective area also decreases rapidly during the rebound stroke. Such variations in the effective area yield increasingly hardening and softening forces during compression and rebound, respectively. Equations (2.9) and (2.10) are solved for a charge pressure P_0= 689 Kpa, and charge volume, V_0 = 0.02 m^3. The resulting force-deflection characteristics are compared with those derived from the laboratory tests, as shown in Figure 2.11. The restoring force derived from the analytical model tends to be lower than the measured force, when deflection amplitude exceeds 7 cm. The measured force, however, is smaller than the estimated force during rebound stroke. The discrepancy between the measured and analytical response is attributed to the assumption of the isothermal process. It has been reported that the use of polytropic process with polytropic exponent, ranging 1.1 to 1.4, can provide better estimation of the air spring force [100]. The analytical model used in this study, however, yields peak error below 5%, and thus considered to provide reasonably accurate estimate of the spring force.

Equation of motion

Analytical model of the vehicle employing rear axle air suspension, and either leaf or linear suspension within the front-axle, is illustrated in Figure 2.12. The air suspension is represented by an air spring and an inclined damper mounted between the sprung mass

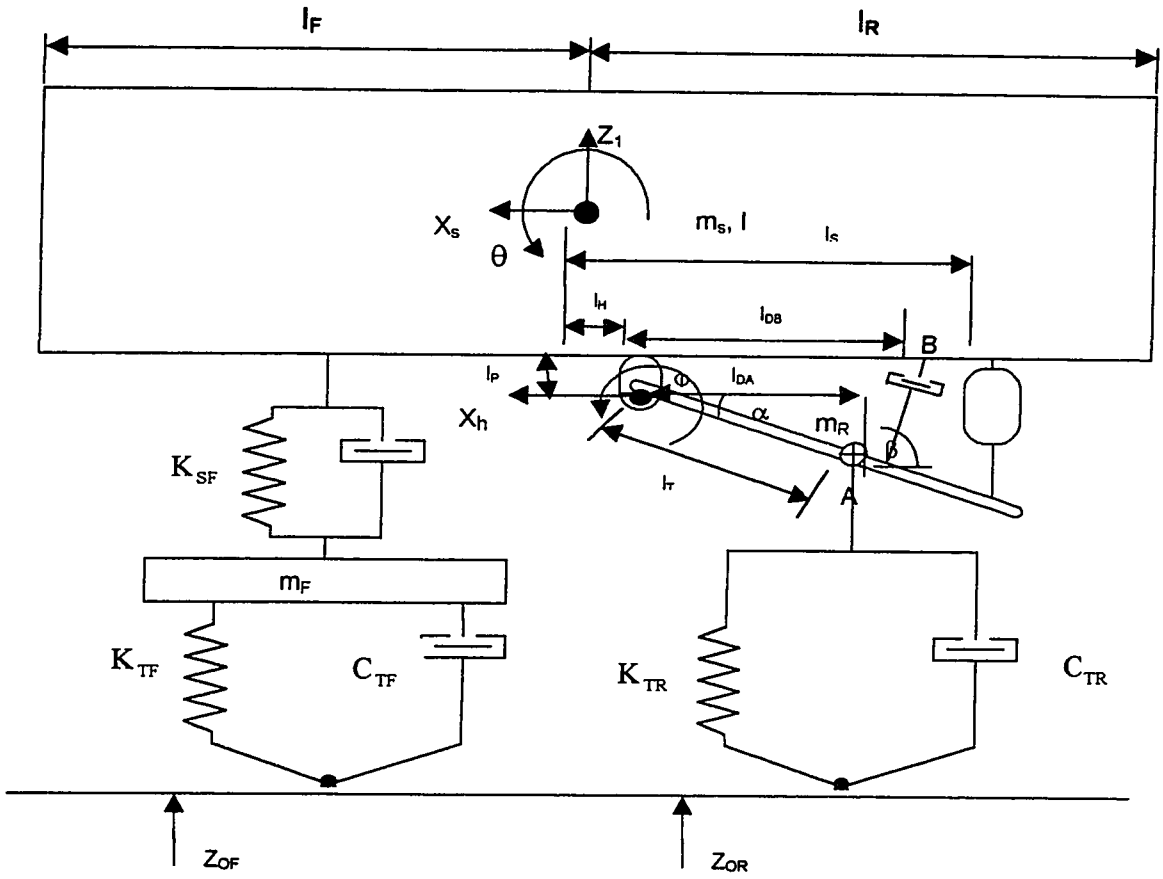

Figure 2.12 In plane model of truck of rear air suspension with the linkage.

and the trailing arm link. The degrees-of-freedom for the model are selected as: vertical (z_1) and pitch (θ) motion of the spring mass m_S , vertical motion (z_2) of the front axle unsprung mass m_F, and pitch motion (φ) of the trailing arm. The equations of motion of the four-DOF vehicle model, incorporating the trailing arm suspensions, are derivedassuming small oscillation, and expressed as:

$$
\begin{aligned}
&m_S\ddot{z}_1 + m_R(\ddot{z}_1 + \ell_S\ddot{\theta} + \ell_T\cos\alpha\ddot{\varphi}) + F_{SF} + m_R g + F_{TR} + m_S g = 0,\\
&I\ddot{\theta} + \ell_H m_R(\ddot{z}_1 + \ell_H\ddot{\theta} + \ell_T\cos\alpha\ddot{\varphi}) - \ell_A F_{SF} + (\ell_S - \ell_H)F_{AR} + \ell_H(F_{TR} + m_R g) + F_D = 0,\\
&m_F\ddot{z}_2 + F_{TF} - F_{SF} + m_F g = 0,\\
&I_B\ddot{\varphi} + \ell_T\cos\alpha m_R(\ddot{z}_1 + \ell_H\ddot{\theta} + \ell_T\cos\alpha\ddot{\varphi}) + \ell_T\cos\alpha(F_{TR} + m_R g) - L\cos\alpha F_{SR} + F_D = 0,
\end{aligned}
\tag{2.12}
$$

where F_{SF} is the force due to front suspension, is derived from Equation 2.2 for linear spring, and Equation (2.6) for the leaf spring. F_{AR} is the restoring force developed by the air spring, which is derived from equation (2.10), as a function of the relative deflection, δ_A, given by:

$$\delta_A = \left[(\ell_S - \ell_H)\theta - L\cos\alpha - \delta_{SR}\right]. \tag{2.13}$$

The force due to air spring is thus expressed as:

$$F_{AR} = \left[\frac{P_0 V_0}{(V_0 - A_E(\delta_A) * \delta_A} - P_A\right] A_E(\delta_A) \tag{2.14}$$

I_B is the pitch mass moment of inertia of the trailing link, and α is its inclination with respect to the horizontal axis. ℓ_H, ℓ_T, and ℓ_S describe the geometric coordinates of arm hinge, rear axle mass, and air spring, respectively, and L is the trailing arm length. The

damping force developed by the suspension damper is related to the relative velocity across the damper and geometry of the damper link as shown in Figure 2.12 a, the relative velocity, $\dot{\delta}$ across the damper, along its axis, may be expressed as:

$$\dot{z}_A = \dot{z}_1 + \ell_H\dot{\theta} + (\ell_{DA}\dot{\varphi}\cos\alpha), \qquad \dot{x}_A = \dot{x}_S - (h_1 + \ell_P)\dot{\theta} - (\ell_{DA}\dot{\varphi}\sin\alpha),$$

$$\dot{z}_B = \dot{z}_1 + (\ell_H + \ell_{DB})\dot{\theta}, \qquad \dot{x}_B = \dot{x}_S + h_1\dot{\theta},$$

$$V_A = \dot{z}_A\sin\beta - \dot{x}_A\cos\beta, \qquad V_B = \dot{z}_B\sin\beta - \dot{x}_B\cos\beta,$$

$$\dot{\delta} = V_B\text{-}V_A,$$

$$\dot{\delta} = \left[\ell_{DB}\dot{\theta}_S - \ell_{DA}\dot{\theta}\cos\alpha\right]\sin\beta - \left[\ell_P\dot{\theta}_S + \ell_{DA}\dot{\theta}\sin\alpha\right]\cos\beta. \qquad (2.15)$$

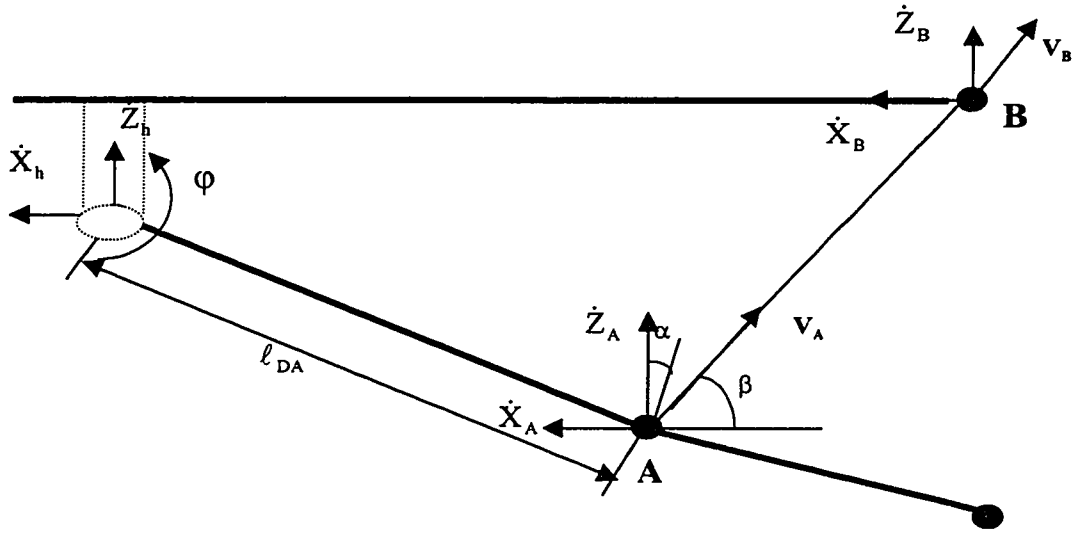

Figure 2.12a: Velocity components of air suspension damper inclined to the linkage.

where ℓ_{DB} and ℓ_{DA} are the distance from the hinge to the chassis of the damper and distance from hinge to the point where the damper is attached on the link respectively. β is the inclined angle of the damper with the horizontal axis.

Assuming viscous damping, the damping force F_D developed along the axis of the damper is expressed as:

$$F_D = C_{Eq}\,\dot{\delta} \tag{2.16}$$

where C_{Eq} is the equivalent viscous coefficient of the air suspension damper.

While the dynamic force due to front axle tires is derived from Equation (2.3), the force developed by the rear axle tire is related to the kinematic behaviour of the trailing axis. Assuming liner stiffness (K_{TR}) and damping (C_{TR}) properties and point contact with the road, the tire force F_{TR} is derived as:

$$F_{TR} = K_{TR}x_T + C_{TR}\dot{x}_T; \qquad \text{for } x_T \le 0.$$

$$F_{TR} = 0; \qquad \text{for } x_T \ge 0. \tag{2.17}$$

where x_T is the relative vertical deflection of the tire, given as:

$$x_T = z_1 + \ell_S\theta + \ell_T\cos\alpha\varphi - z_{0R} - \delta_{TR}\,. \tag{2.18}$$

Equation (2.12) to (2.18), together with (2.2), (2.3) and (2.6), describe the pitch plane dynamics of the three-axle truck equipped with trailing arm rear axle suspension and subject to road excitations, z_{0F} and z_{0R}, at the front and rear tire-road contacts.

2.3.3 Characterization Of Suspension Damping

The vehicle suspensions, in general, yield high dynamic wheel loads in the low frequency range associated with resonances of the sprung masses. The control of vehicle vibration in these frequency bands is thus necessary for both the road friendliness and ride quality of the vehicle. The suspension springs are often selected to achieve a

compromise among improved ride quality offered by the soft springs, and improved handling performance offered by medium hard springs. While the influence of restoring properties of heavy vehicle suspension and axle configurations on the dynamic wheel loads has been reported in many analytical and experimental studies [49], the influence of dissipative properties of the suspension has been addressed only in a limited number of studies [51, 60]. The influence of suspension damping on ride dynamics of vehicles, however, has been extensively investigated [53]. Since the vehicle ride quality and dynamic wheel loads are both related to vehicle vibration modes, the suspension damping considered adequate for improved ride quality can lead to enhanced road friendliness of the vehicle.

Suspension dampers play an important role in reducing the transient loads transmitted to the chassis and the pavement, thereby improving the ride quality of the vehicle. The vehicle vibration modes, and thus the dynamic chassis and pavement loads, and vehicle ride quality are strongly related to the damping properties of the suspension. The importance of suspension dampers increases for the air suspension, as it does not provide any inherent damping (coulomb damping) unlike the leaf spring suspension. The suspension dampers, in general, are designed to yield high damping at low relative velocity, due to the bleed flows, and low damping at higher velocities, due to flows through blow-off valves. The transition from high to low damping occurs in the vicinity of a transition velocity. Furthermore, typical suspension dampers yield asymmetric damping in compression and rebound, as shown in Figure 2.13. The force velocity characteristics reveal low damping coefficient in compression and two-stage damping properties in the rebound stroke attributed to bleed and blow-off flows. The transition

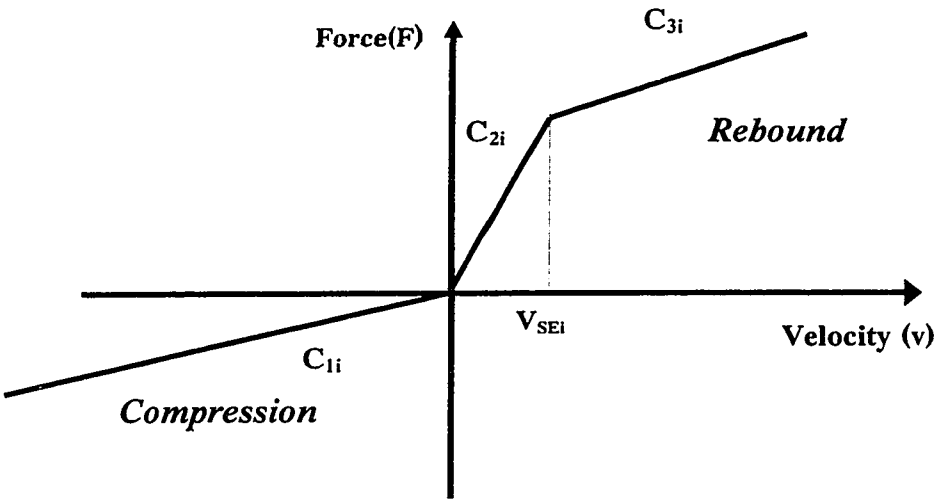

Figure 2.13 Force-Velocity characteristics of a typical hydraulic damper

from bleed to blow-off flow occurs at predetermined velocity, V_{SE} the low speed-damping coefficient in the rebound stroke is considerably larger than that in the compression stroke. The damping force developed by such asymmetric and nonlinear damper can be expressed as:

$$F_{Di} = C_{1i}\dot{\delta}_i; \quad \text{for} \quad \dot{\delta}_i < 0,$$

$$F_{Di} = C_{2i}\dot{\delta}_i; \quad \text{for} \quad v_{SE} > \dot{\delta}_i \geq 0,$$

$$F_{Di} = C_{2i}v_{SE} + C_{3i}(\dot{\delta}_i - v_{SE}); \quad \text{for} \quad \dot{\delta}_i \geq v_{SE}, \tag{2.19}$$

where F_{Di} is the damping force developed by suspension damper i (i=F,R), C_{1i} and C_{2i} are the compression and rebound damping coefficient corresponding to low velocities. C_{3i} is the damping coefficient corresponding to higher velocities. The damping coefficients and the transition velocity of a hydraulic shock absorber employed in air suspension are identified through measurement of the force-velocity characteristics
in the laboratory [96]. The measured force-velocity characteristics of the damper subject to harmonic relative deflections are shown in Figure 2.14. The measured data reveals considerably lower damping in compression than in rebound, and two-stage damping in the rebound stroke. The measured data is analyzed to derive the mean force-velocity curve and the corresponding damping coefficient, which are summarized below:

C_{1i}= 1625 Ns/m; C_{2I}= 15,257 Ns/m;

C_{3i}= 8023 Ns/m; and V_{SE}= 0.144m/s.

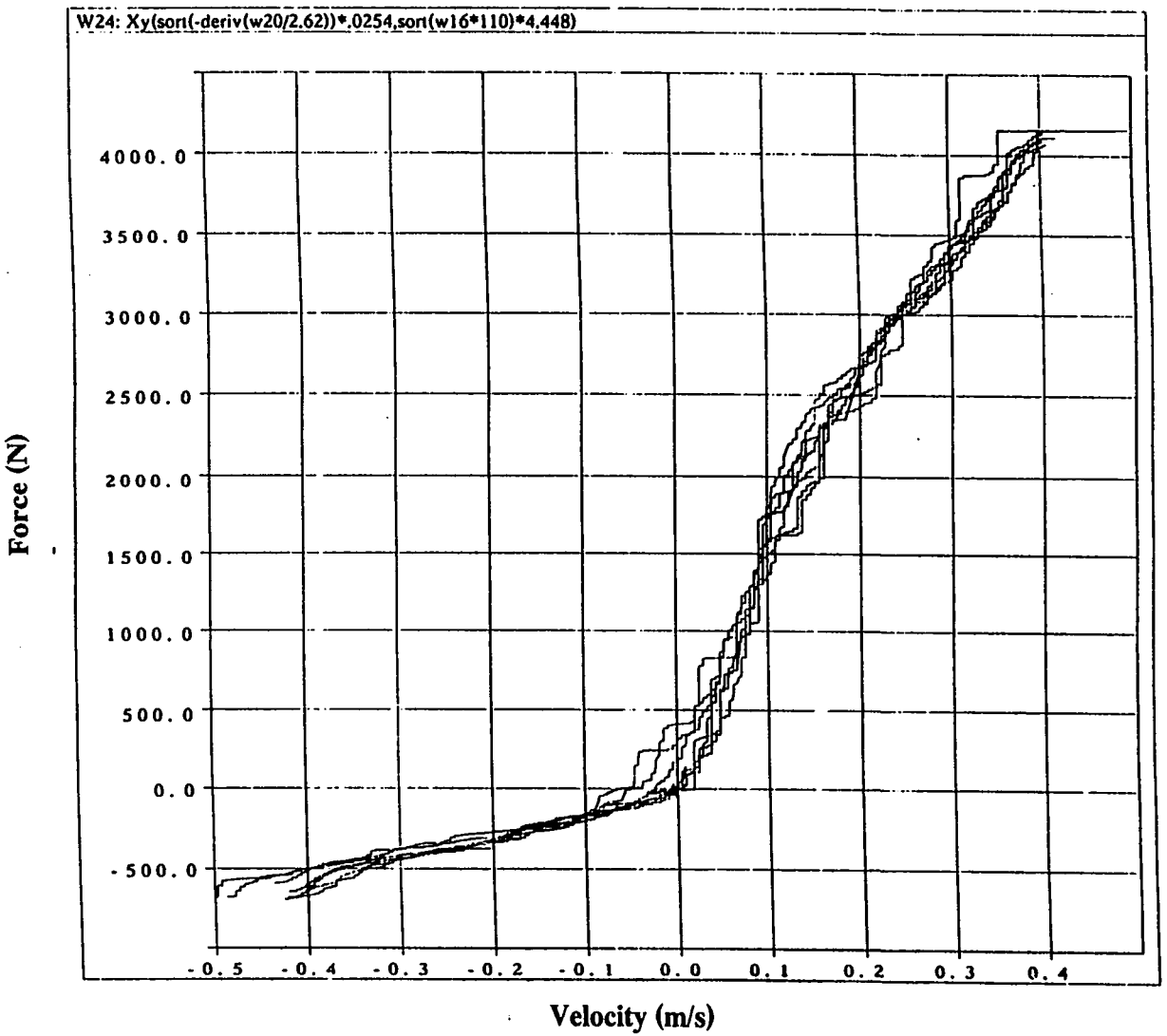

Figure 2.14 Measured force-velocity characteristics of an air suspension damper

2.4 CHARACTERIZATION OF ROAD PROFILE

The dynamic characteristics of the road vehicle, and thus the dynamic wheel loads and the ride quality are strongly related to the road profile. The roads are known to exhibit randomly distributed roughness. A number of studies have established that road roughness closely follows a Gaussian distribution, and proposed spatial spectral density functions to characterize the mean roughness profiles of various roads. Alternatively, the roughness characteristics of various roads in Ontario, reported by Damien [97], can be considered for the study of driver-and road-friendliness of the heavy vehicle. Damien [97] reported the roughness profiles of various roads, ranging from extremely smooth to very rough roads. In this dissertation, the vehicle models are analyzed for the two different roads, referred to as smooth road. The power spectral density (PSD) of the roughness of the selected roads is illustrated in Figure 2.15.

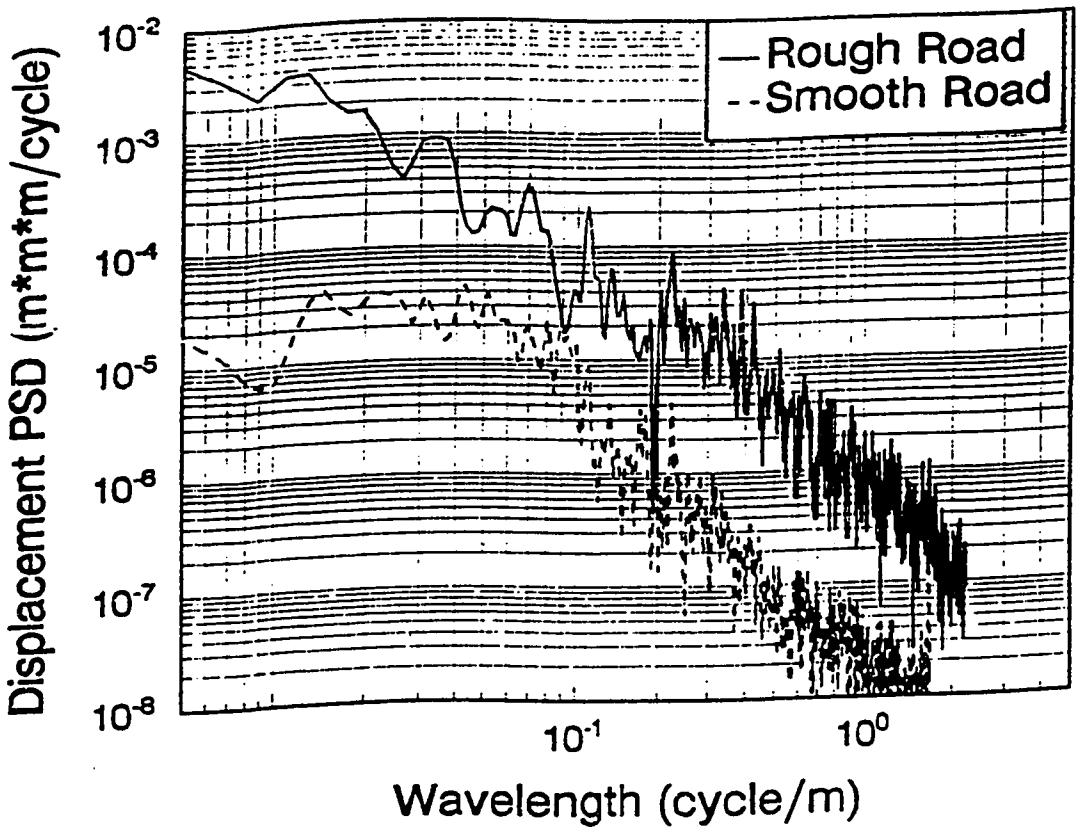

Figure 2.15 Displacement spectral density due to road excitations.

2.5 VEHICLE PARAMETERS

The weights and dimension parameters of the three-axle truck are identified from the data reported by Road Transport Association of Canada [70]. The equivalent spring rates of the suspension and tires are also identified form the reported data. The simulation parameters for the vehicle model are thus compiled and summarized in Table 2.2.

Table 2.2 List of simulation parameters for the three-axle truck models.

Description of the parameters	Parameter values
Mass of the truck (m_S)	7200.0 kg
Truck Pitch moment of inertia (I)	100000.0 kgm^2
Front tire and axle assembly mass (m_{uf})	353.0 kg
Rear tire and axle assembly mass (m_{ur})	653.0 kg
Front axle suspension stiffness (K_{sf})	295.3 KN/m
Rear axle suspension stiffness(K_{sR})	797.3 KN/m
Front axle suspension damping coefficient(C_{Sf})	2.9 KNs/m
Rear axle suspension damping coefficient (C_{Sr})	5.9 KNs/m
Front tire suspension stiffness (K_{Tf})	1100.0 KN/m
Rear tire suspension stiffness(K_{Tr})	2200.0 KN/m
Front tire suspension damping coefficient (C_{Tf})	0.4 KNs/m
Rear tire suspension damping coefficient(C_{Tr})	0.8 KNs/m
Distance from front axle to CG (l_f)	3.757 m
Distance from rear axle to CG (l_r)	2.441 m

2.6 SUMMARY

The suspension components are characterized using the experimental data and corresponding analytical models are derived. The analytical models of a three-axle truck comprising either linear, leaf or air suspension are formulated. The road roughness of two different roads characterized in terms displacement PSD, is described to perform the dynamic analysis of the vehicle models. The vehicle models are analyzed in the following

chapters to determine optimal properties of suspension damping and dynamic vibration absorber.

CHAPTER 3

ENHANCEMENT OF ROAD FRIENDLINESS OF A HEAVY VEHICLE USING DYNAMIC VIBRATION ABSORBER

3.1 INTRODUCTION

Dynamic wheel loads tend to predominate in the vicinity of bounce mode resonant frequencies of the sprung and unsprung masses. To achieve attenuation of dominant resonant vibrations an absorber tuned to the vertical mode resonant frequencies of the vehicle may be implemented. A dynamic vibration absorber is known to be most effective in a narrow frequency band around its natural frequency [11]. The effectiveness of a vibration absorber is further dependent upon its mass and damping properties [12, 13]. A vibration absorber thus need to be tuned to achieve its natural frequency close to the disturbance frequencies, which need to be attenuated, with practically applicable absorber mass. An absorber tuned to the low sprung mass bounce resonant frequency is considered impractical, since it requires a large absorber mass. The vibration absorbers, tuned to the unsprung mass resonant frequencies, however, can be realized with relatively small mass. The vehicular vibration and the dynamic loads in the vicinity of wheel hop frequencies can thus be attenuated. The performance of the absorber is strongly influenced by its non-dimensional tuning parameters such as the mass ratio (μ_{Ai}), the frequency ratio (Ω_{Ai}) and the damping ratio (ξ_{Ai}). In this analysis, a parametric study of absorber characteristics and the methodologies to select their optimal values for an effective tuning are presented.

3.2 TUNING OF THE AXLE ABSORBER

In order to tune the front and rear axle absorbers, the resonant frequencies of the conventional vehicle model without the absorber are identified through an eigenvalue analysis. Neglecting the wheel hop, the linear system of equation corresponding to static equilibrium, is expressed in the matrix form:

$$M\ddot{q} + C\dot{q} + Kq = C_o\dot{q}_o + K_o q_o , \tag{3.1}$$

where M, C and K are (nxn) mass, damping and stiffness matrices, respectively. C_o and K_o are (nx2) forcing damping and stiffness matrices, respectively. q and q_o are (nx1) and (2x1) vectors of response and excitation coordinates. n is the number of degrees-of-freedom of the truck model, and is equal to 4 and 6, respectively, for the models without and with the axle absorbers. Since the current designs of truck suspensions offer very light damping, the resonant frequencies may be conveniently estimated from the eigenvalue analysis of the undamped vehicle model without the absorber:

$$K\varphi = \lambda M\varphi , \tag{3.2}$$

where λ are the eigenvalues and φ are the modal or eigenvectors. Eigenvalues and corresponding resonant frequencies of the sprung and unsprung masses are summarized in Table 3.1.

Table 3.1 Eigenvalues and Resonant Frequencies of the vehicle model.

Dominant Deflection Mode	Eigenvalue (λ)	Resonant Frequency (Hz)
Sprung Mass (Vertical mode)	120.0	1.74
Sprung Mass (Pitch mode)	60.0	1.233
Unpsrung Mass (Front vertical mode)	3970.0	10.03
Unsprung Mass (Rear vertical mode)	4633.00	10.838

3.3 PARAMETRIC STUDY OF THE TUNING PARAMETERS

The performance characteristics of axle absorbers and its tuning parameters are investigated for both deterministic and stochastic road excitations. A performance criterion comprising the tire loads in terms of DLC and the rms acceleration response at the driver seat of the vehicle model is formulated to study the influence of tuning parameters. Since the dynamic wheel loads are primarily attributed to the vertical dynamics of the vehicle, the model is initially analyzed for constant amplitude harmonic displacement excitations, to investigate the influence of axle absorbers on the dynamic tire loads. Fourier transform of equation (3.1) yields the frequency response function matrix:

$$H(j\omega) = \left[K - \omega^2 M + j\omega C\right]^{-1} \left[K_0 + j\omega^2 C_0\right] . \qquad (3.3)$$

The dynamic tire forces are related to the relative tire deflections and restoring and dissipative properties of the tires. The relative deflections of the front, $X_F = Z_2 - Z_{0F}$, and rear, $X_R = Z_3 - Z_{oR}$, tires can be derived from the following transformation:

$$X = \mathbf{T}H(j\omega)Q_0 - Q_0 \qquad (3.4)$$

where T is a (2xn) transformation matrix and X is a (2x1) vector of relative deflections across the tires. The normalized dynamic tire forces, ratio of dynamic tire force to the static load, under harmonic excitations, are then computed from:

$$\beta_i = \left| \frac{(K_{Ti} + j\omega C_{Ti})}{K_T z_{0i}} X_i(j\omega) \right|, \qquad \text{for i= F, R} \qquad (3.5)$$

where β_i is the normalized dynamic force due to tires on axle i.

The coupled differential equations of motion for the vehicle model, incorporating wheel hop, and linear suspension characteristics, derived in section 2.2, are solved for excitations arising from the selected road roughness profiles. Displacement excitations at the front and rear axle tire-road interface are derived from the measured profile, $Z_0(t)$, the vehicle speed V, and wheelbase effect, L/V. The dynamic wheel loads are analyzed in terms of the Dynamic Load Coefficient (DLC), defined as the ratio of rms dynamic force to the static tire load. The response characteristics of the vehicle model under stochastic excitation are further expressed in terms of their power spectral densities (PSD).

3.3.1 Harmonic Excitations

The frequency response characteristics of the vehicle acceleration and tire loads are investigated for various absorber parameters. The frequency response characteristics are presented in terms of the normalized tire loads (ratio of magnitude of steady state dynamic tire force to the static tire force), and acceleration transmissibility (ratio of magnitude of response acceleration to that of the excitation acceleration). Frequency response characteristics are derived for identical harmonic excitations at the front and rear

tire-road interface, and the results are discussed to highlight the influence of absorber parameters.

Influence of frequency ratio:

The influence of uncoupled natural frequency of the absorber on the dynamic tire load is investigated by varying the non-dimensional absorber frequency ratio, Ω_i, defined as:

$$\Omega_i = \frac{\omega_{Ai}}{\omega_{Ui}}, \qquad i= F, R, \tag{3.6}$$

where

ω_{Ai} = Uncoupled absorber natural frequency of the absorber i.

ω_{Ui} = Uncoupled resonant frequency of the unsprung mass i (K_{Ti}/m_i)

Figures 3.1 and 3.2 illustrate the influence of absorber frequency ratio on the unsprung mass acceleration transmissibility and normalized tire load characteristics, respectively. The response characteristics of the vehicle model with the axle absorbers are compared with those of the conventional vehicle without the absorbers. The absorber damping ratios, ξ_{AF} and ξ_{AR} are selected as 0.10. The absorber mass ratios, μ_{AF} and μ_{AR}, the ratio of absorber mass to the unsprung mass to which it is attached, are selected as 0.10. The frequency response characteristics of the vehicle without the absorber reveal dominance of tire loads in the vicinity of bounce and pitch resonant frequencies of the sprung mass (1.74 and 1.23 Hz), and resonate frequencies of the front and rear unsprung masses.

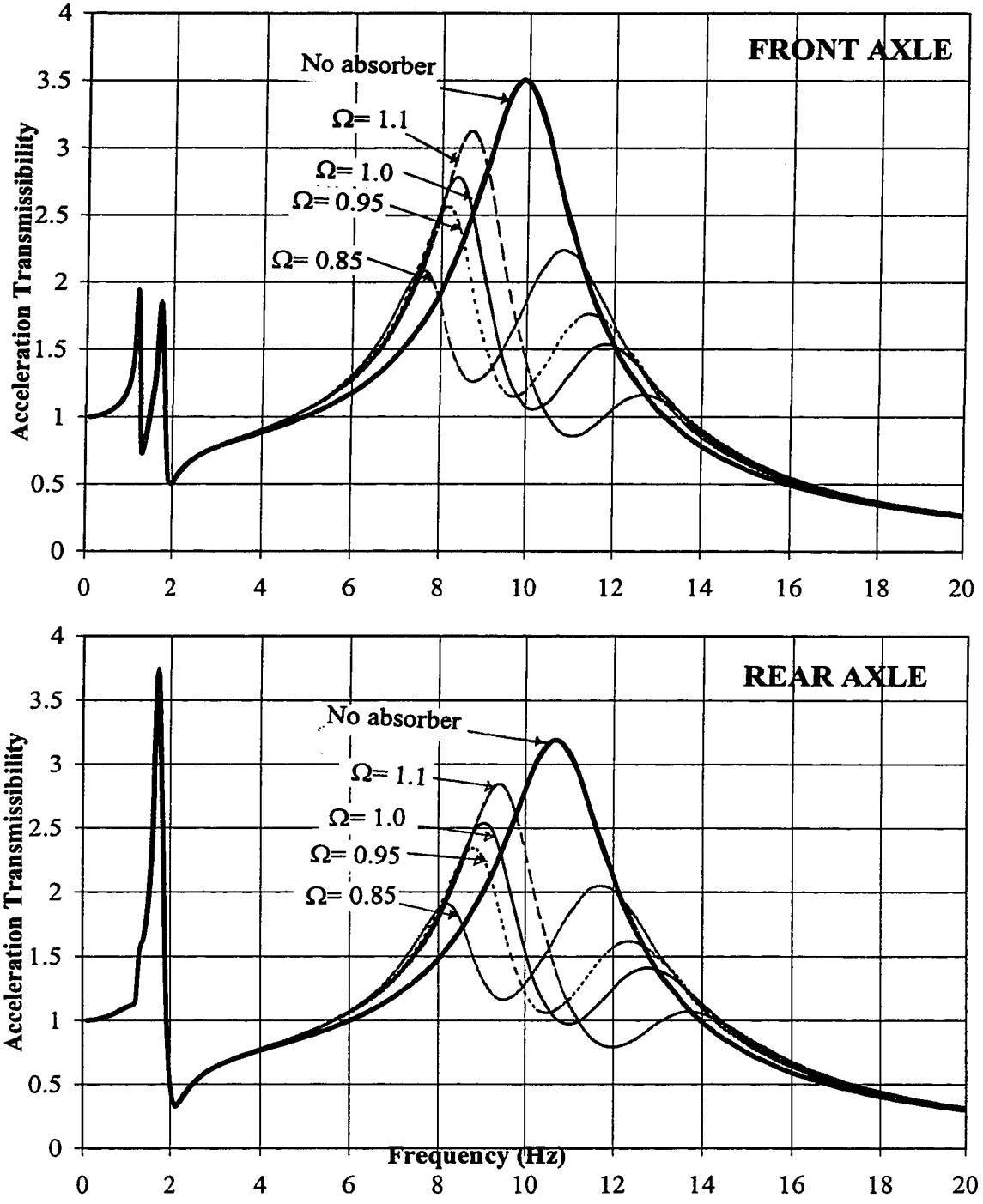

Figure 3.1 Influence of axle absorber frequency ratio on the acceleration Transmissibility of the front and rear unsprung mass

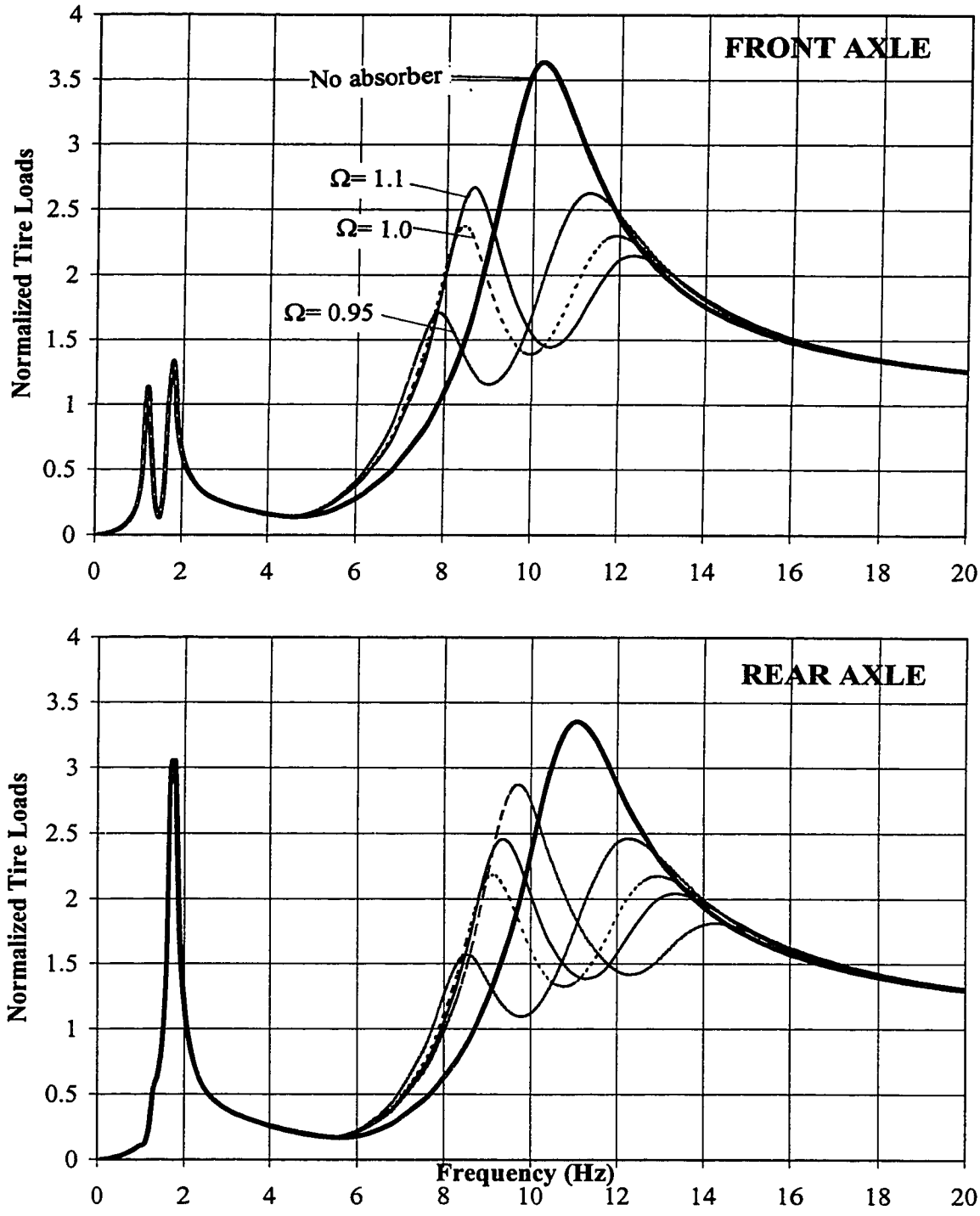

Figure 3.2 Influence of axle absorber frequency ratio on the normalized tire loads

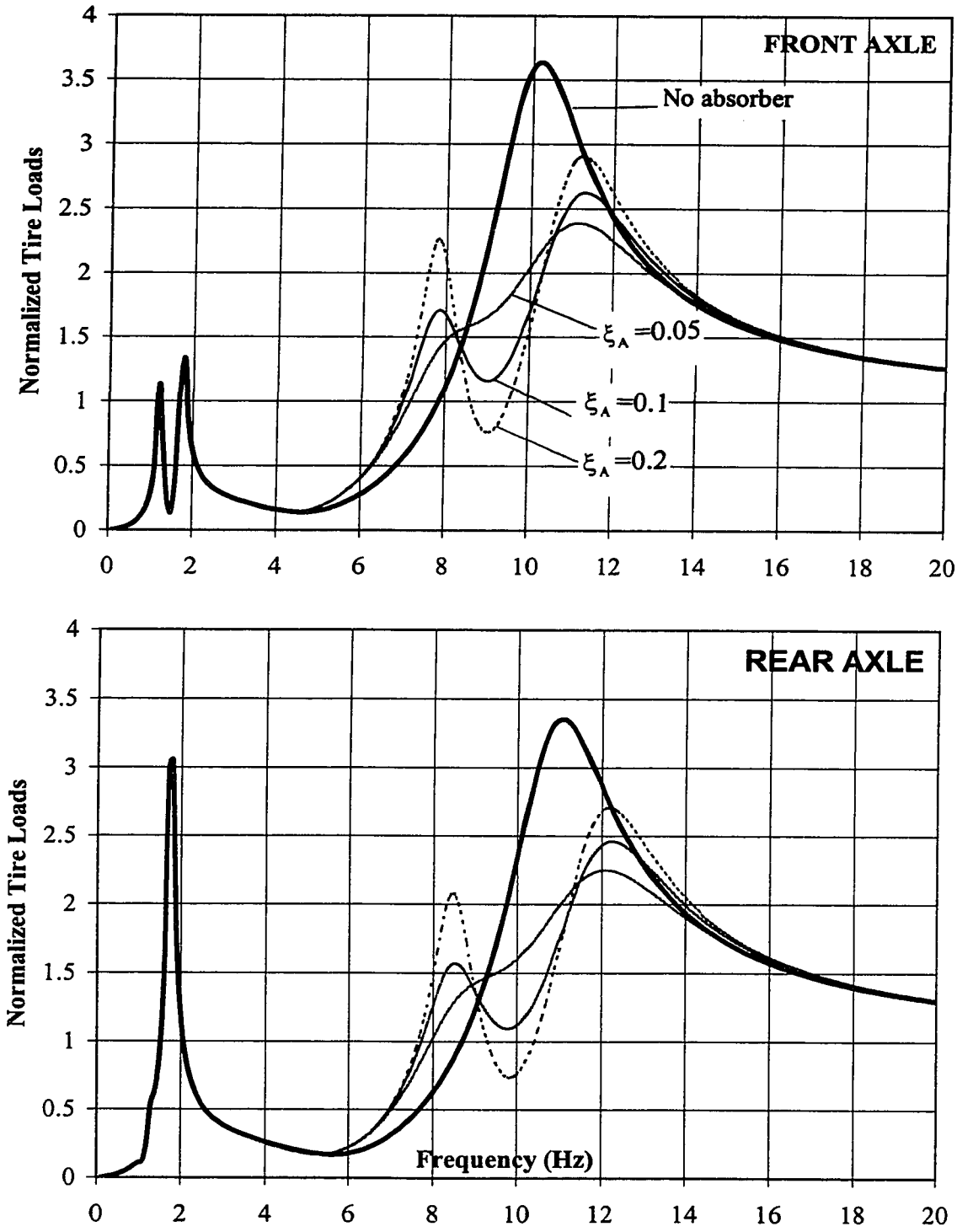

Figure 3.3 Influence of axle absorber damping ratio on the normalized tire loads

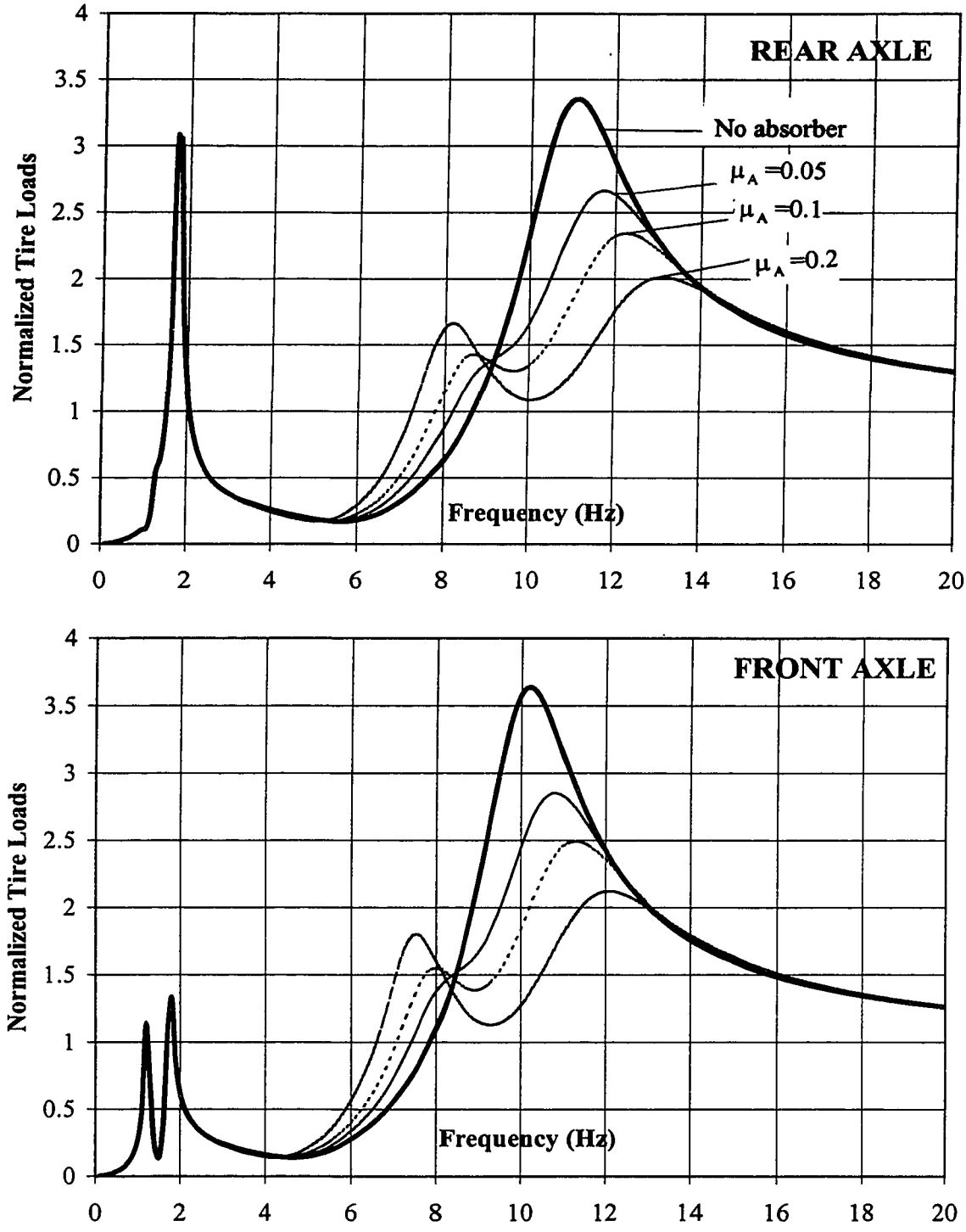

Figure 3.4 Influence of axle absorbers mass ratio on the normalized tire loads.

The axle absorbers tuned to the unsprung mass resonant frequencies, Ω_i=1., reduce the magnitudes of normalized tire loads and the acceleration transmissibility corresponding to the axle resonant frequencies. The peak tire loads as well as the unsprung mass acceleration response near the sprung mass resonant frequencies remain insensitive to the axle absorbers. The axle absorbers, however, yield two resonant peaks on either side of the resonant frequency of each unsprung mass, as shown in the Figures 3.1 and 3.2. These side-band peaks of the rear axle absorber occur around 8 and 12 Hz. The corresponding side band frequencies of the front axle absorber occur around 7.5 and 11 Hz. The magnitudes of these resonant peaks are considerably lower than those due to the vehicle without the absorbers. The magnitudes of the side-band peaks are strongly related to the absorber frequency ratio, Ω_i. An absorber frequency ratio near 0.85 yields nearly similar magnitudes of peak tire loads around the resonant frequencies of unpsrung
Mass of both the front and rear axles.

Influence of Damping Ratio:

The effectiveness of the axle absorbers in reducing the tire loads near the wheel hop frequencies is strongly dependent upon the absorber damping ratio. Figure 3.3 illustrates the influence of the absorber damping ratio on the normalized tire load, for Ω_i=0.85 and μ_{Ai}=0.10. Although a lightly damped absorber (ξ_{Ai}=0.05) significantly reduces the tire load near the unsprung mass frequency, the magnitudes of resulting side-bands resonant peaks are quite large. While an increase in absorber damping tends to suppress the magnitudes of the two resonant peaks, the effectiveness of the absorber at the tuned frequency diminishes, as shown in the Figure 3.3. The results reveal that a damping ratio above 0.20 is not particularly beneficial to reduce the normalized tire loads

in the vicinity of the wheel hop frequencies. The vehicle response near the sprung mass resonances remains insensitive to the damping ratio of the axle absorbers.

Influence of Mass Ratio:

Figure 3.4 illustrates the influence of absorber mass ratio on the normalized tire load response characteristics of the vehicle. Compact and lightweight axle absorbers are desirable for their ease of installation and minimal influence on the payload capacity of the vehicle. The axle absorbers with low mass, however, do not effectively attenuate the resonant peak near the wheel hop frequencies. While an increase in the absorber mass tends to suppress the tire load and unsprung mass acceleration at the tuned frequency, the magnitudes of peaks near 8.1 Hz (rear axle) and 7.6 Hz (front axle) increase. The peak magnitudes corresponding to the wheel hop frequencies of the conventional vehicle, however, decrease with the increase in the absorber mass. The axle absorbers with relatively large weight may thus considered to be detrimental to both the payload capacity of the vehicle and normalized tire loads transmitted to the pavements.

3.3.2 Stochastic Road Excitations

The equations of motion are solved for stochastic road excitations arising from randomly rough roads using numerical integration techniques. The vehicle model incorporating wheel hop and linear suspension properties is analyzed under excitation arising from three different roads. The roughness characteristics of the selected roads have been described in section 2.4. The vehicle response characteristics are analyzed and expressed in terms of *Power Spectral Densities* (PSD) of the sprung, and unsprung mass accelerations, and the tires loads. The dynamic tire loads are also expressed in terms of

the *Dynamic Load Coefficients* (DLC), as a function of the absorber tuning parameters, Ω_i, μ_{Ai} and ξ_{Ai}. The response characteristics of the vehicle model with axle absorbers are also compared to those of the conventional vehicle to demonstrate the effectiveness of the absorbers.

Influence of Frequency Ratio:

Figures 3.5 and 3.6 present the PSD of dynamic tire loads and unsprung mass acceleration response as a function of the absorber frequency ratio, Ω_i, when the vehicle model is subject to excitations arising from the rough road. The axle absorbers tend to suppress the resonant response corresponding to wheel hop frequencies, as illustrated in the case of harmonic excitations. The influence of frequency ratio is investigated for constant values of μ_{Ai}=0.1 and ξ_{Ai}=0.1.

The magnitudes of the peak tire force and acceleration response of the vehicle with the absorbers at frequencies, below the unsprung mass resonant frequency, are considerably larger than those of the conventional vehicle. This is attributed to the existence of the side band frequency around 7.5 and 8 Hz for front and rear axles, respectively. The magnitudes tire load and the acceleration at frequencies (in the vicinity of the side band frequency) higher than the unsprung mass resonant frequency, however, are either lower or similar to those of the conventional vehicle, irrespective of the absorber frequency ratio. The peak response in the 7-8 Hz range tends to decrease with lower absorber frequency ratio. The peak response at higher resonant frequencies in the 11-12 Hz range, however, increases with decrease in the frequency ratio. The results show that the peak tire loads in the vicinity of wheel hop frequencies may be reduced

with absorber frequency ratio ranging from 0.85 to 0.95. The axle absorbers do not influence the dynamic tire loads as well as the acceleration response at frequencies below 5 Hz. Figure 3.7 illustrates a comparison of PSD of vertical and pitch accelerations derived at the driver seat coordinates of the vehicle with and without the axle absorbers. Addition of axle absorbers does not affect the vehicle ride quality at frequencies below 6 Hz, and yields only slight deterioration the vehicle ride quality in the vicinity of 8 Hz. The axle absorbers, however, suppress the vertical and pitch ride vibration considerably in the vicinity of wheel-hop frequencies.

Influence of Damping Ratio:

The influence of absorber damping ratio on the sprung mass acceleration and dynamic tire load characteristics is investigated by varying the damping ratio from 0.1 to 0.2, while Ω_i=0.85 and μ_{Ai}=0.1. Since the addition of axle absorbers does not affect the sprung mass acceleration in the range of important ride frequencies (below 6 Hz), the dynamic tire load characteristics alone are presented. The influence of absorber damping ratio on the PSD of dynamic tire loads is illustrated in Figure 3.8. The undamped axle absorbers (ξ_{Ai}=0) suppress the peaks, corresponding to the respective unsprung mass frequencies, almost entirely. The undamped absorbers, however, yield excessive peak magnitudes corresponding to the side band frequencies, as shown in Figure 3.8. An increase in absorber damping ratio tends to reduce the peak magnitudes of side band frequencies, while diminishing the effectiveness of the absorber at its tuned frequency. The results suggest that the dynamic tire loads corresponding to the unsprung mass resonances can be considerably reduced using axle absorbers with $0.10<\xi_{Ai}<0.20$.

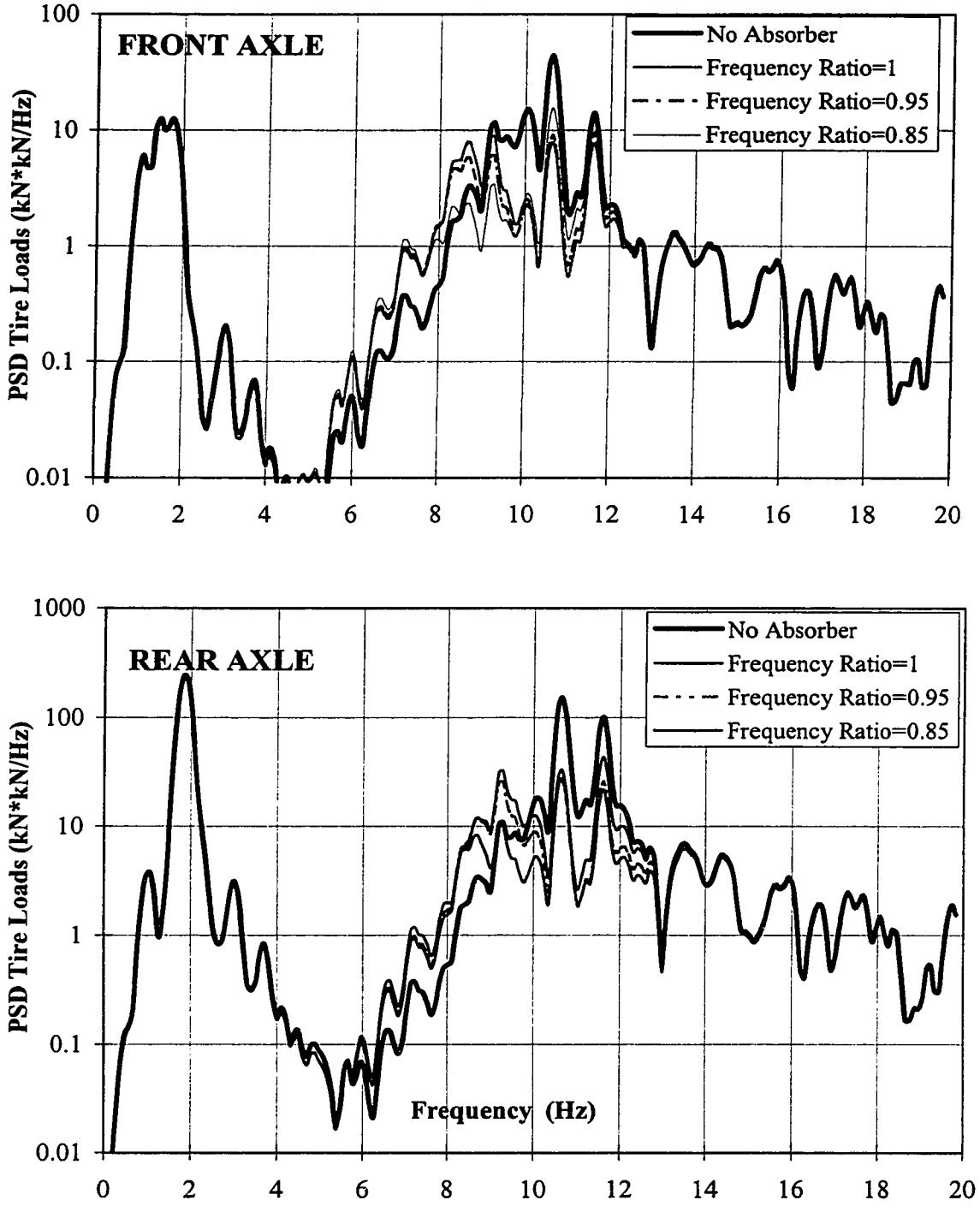

Figure 3.5 Influence of axle absorber frequency ratio on the PSD of Dyanmic Tire Loads.

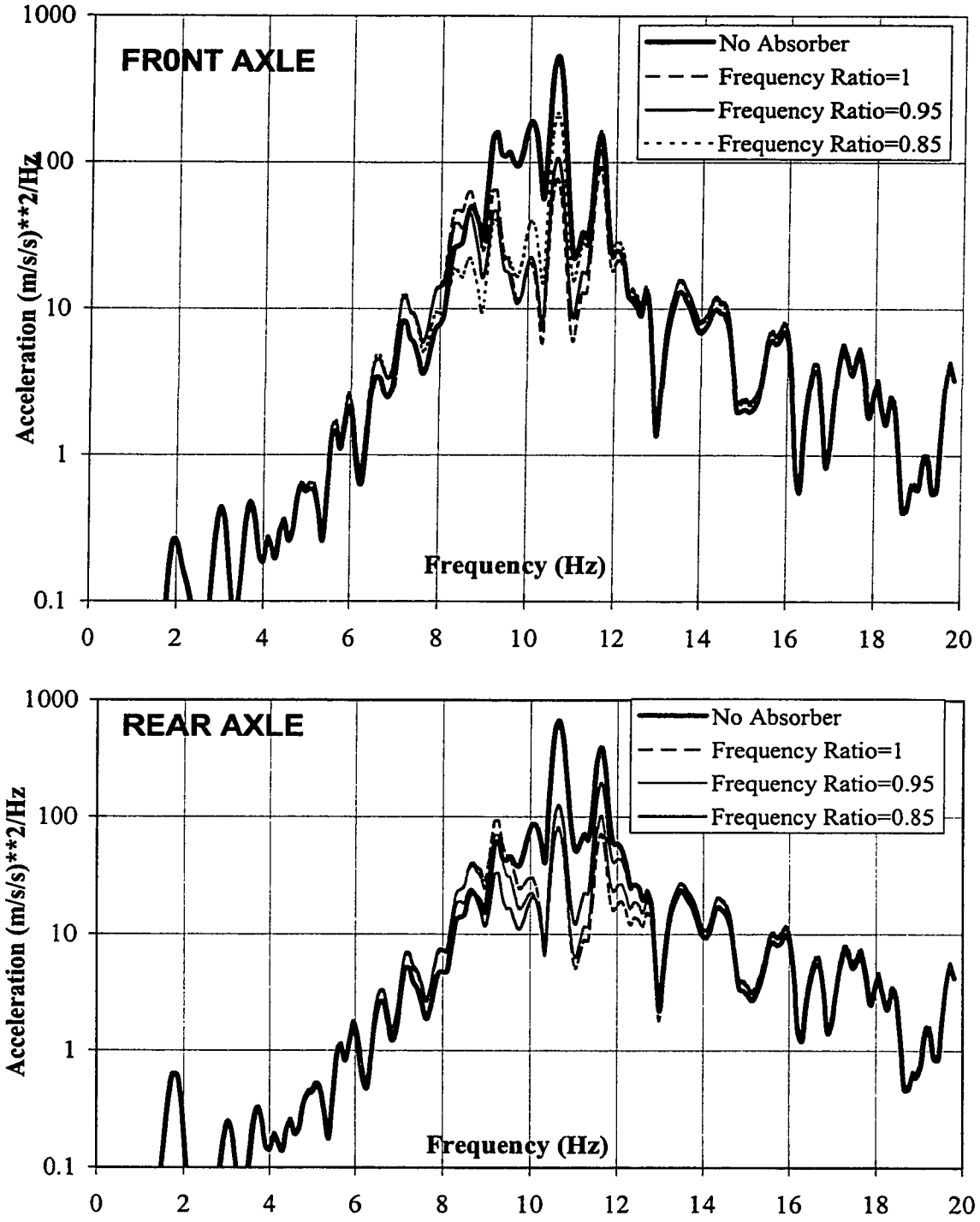

Figure 3.6 Influence of axle absorber frequency ratio on the PSD of vertical

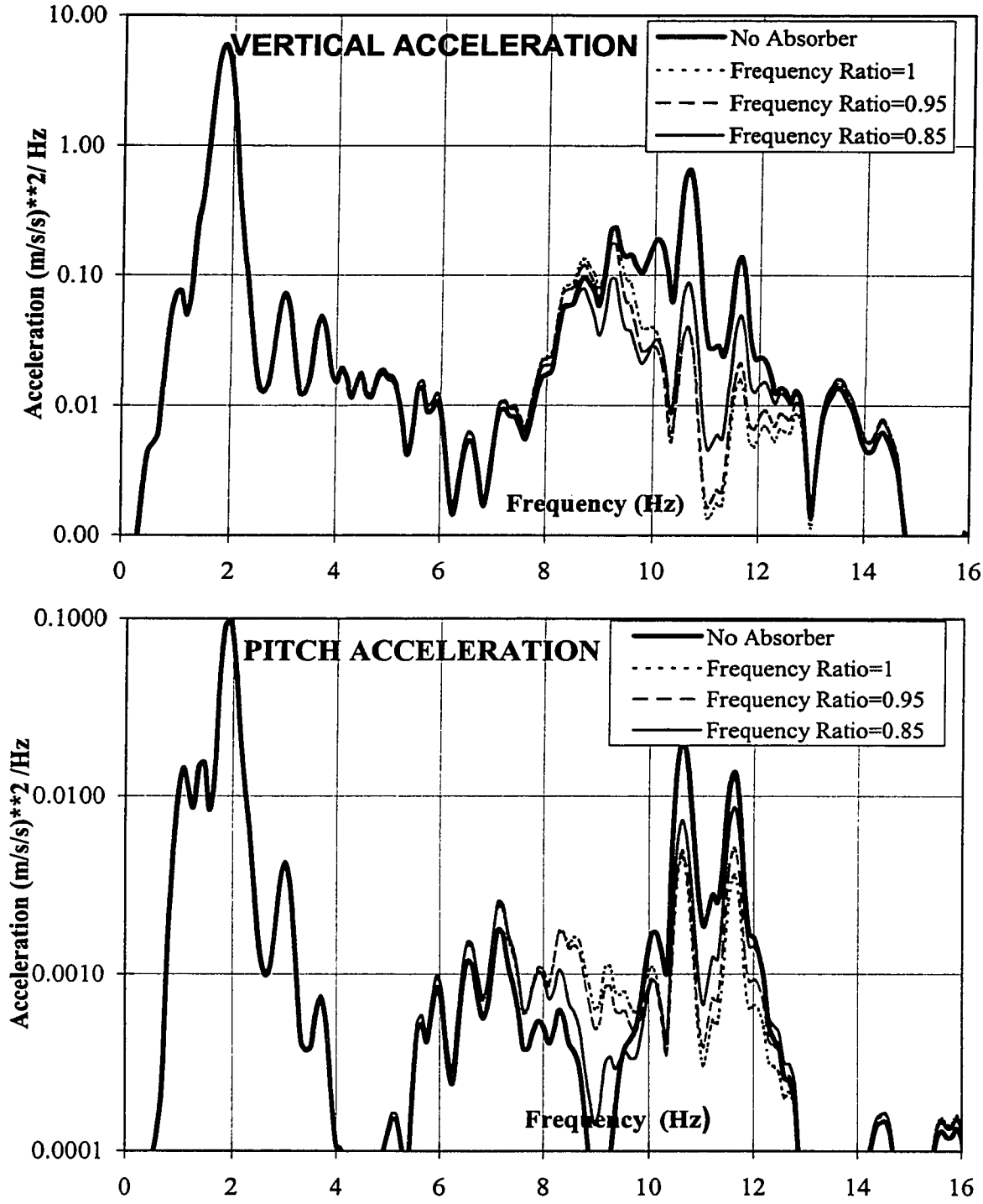

Figure 3.7 Influence of axle absorber frequency ratio on the PSD of vertical

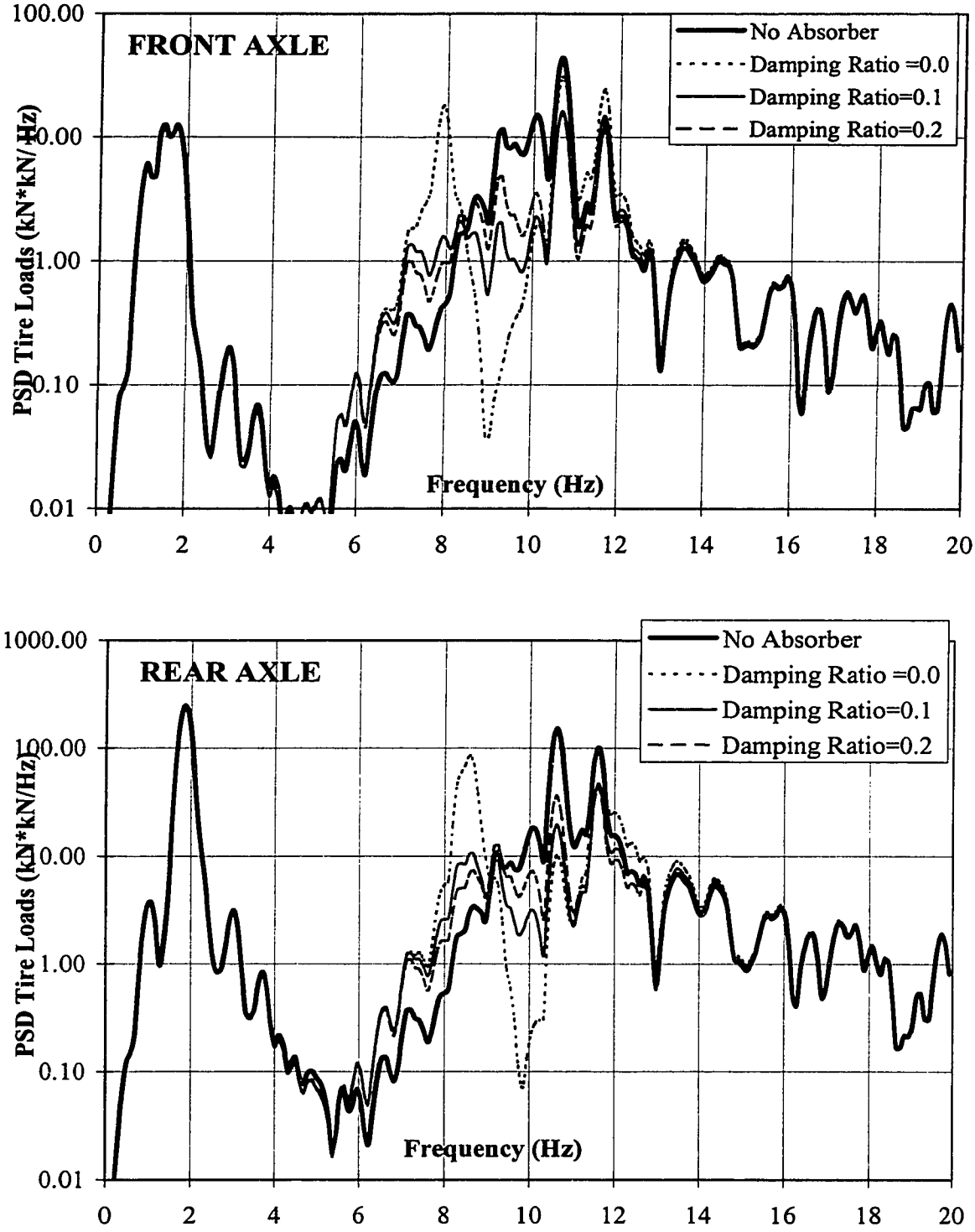

Figure 3.8 Influence of axle absorber damping ratio on the Psd of Dynamic Tire Loads.

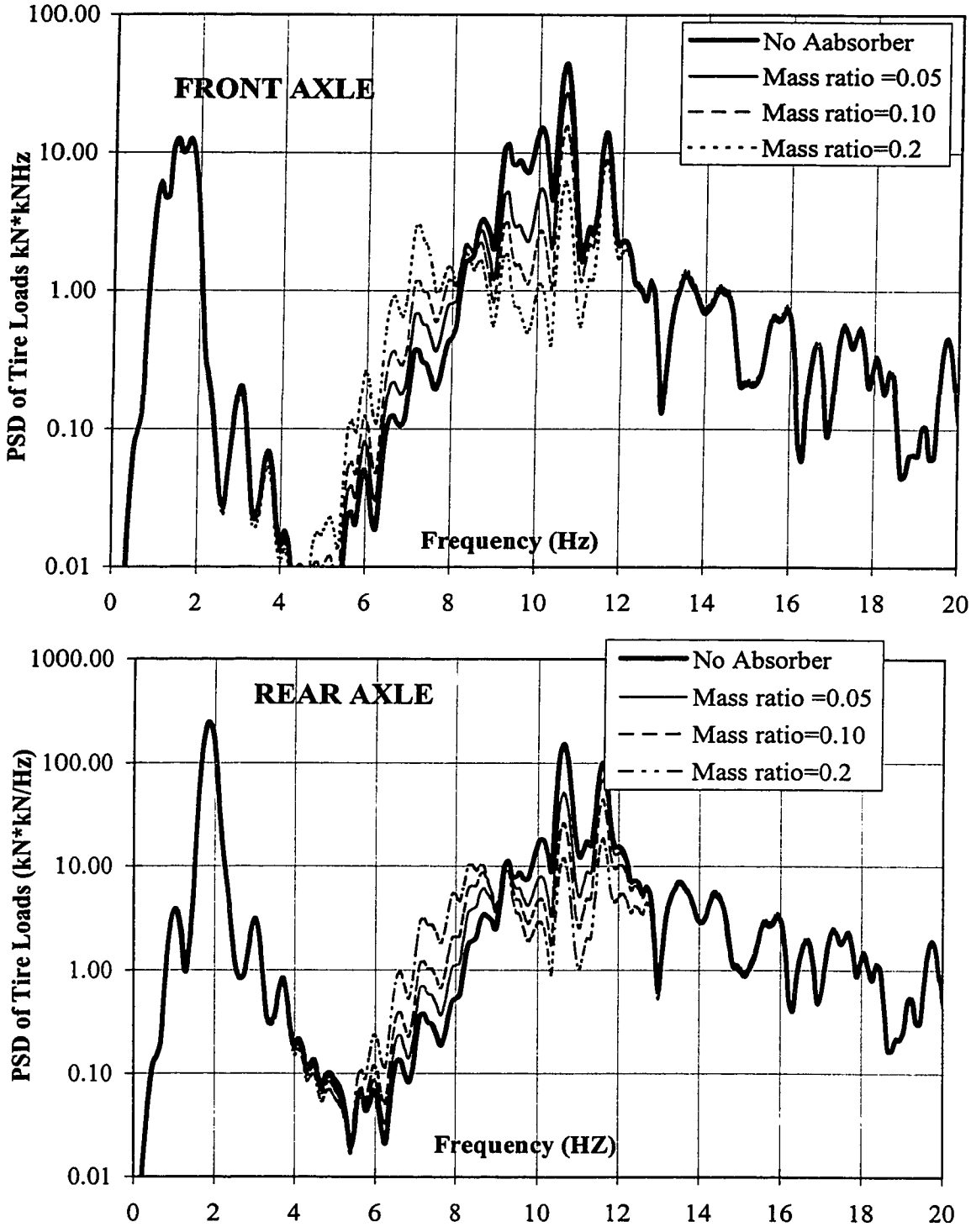

Figure 3.9 Influence of axle absorbers mass ratio on the PSD of Dynamic Tire Loads.

Influence of Mass Ratio:

The influence of absorber mass ratio on the dynamic tire loads is investigated by varying μ_{Ai} from 0.05 to 0.2, while the values of frequency and damping ratios are held constant (Ω_i=0.85, ξ_{Ai}=0.1). Figure 3.9 illustrates the PSD of dynamic tire loads on the front and rear axles as a function of the absorber mass ratio, μ_{Ai}. Lower values of μ_{Ai} reduce the effectiveness of the axle absorber at its tuned frequency, with considerably lower peak value at the side band frequencies in the 7-8 Hz range. An increase in the value of μ_{Ai} tends to improve the effectiveness of the absorbers in the vicinity of their tuned frequencies with excessive peak response at the lower side band frequencies (7-8Hz). A heavier absorber, however, tends to reduce the payload capacity of the vehicle.

3.3.2 Dynamic Load Coefficient

The severity of dynamic tire forces transmitted to the pavement is often assessed in terms of DLC. The DLC of tire forces, however, is strongly dependent upon the road roughness and the vehicle speed. The influence of absorber parameters on the DLC tire forces is thus further investigated as a function of the vehicle speed and the road roughness. The dynamic tire forces of tire vehicle model employing axle absorbers are analyzed for excitations arising from different roads (Smooth, medium rough, and rough) at speeds of 100 km/h and 120 km/h. The tire forces are then analyzed to derive the DLC of front and rear tire forces.

Influence of Damping Ratio:

Figure 3.10 illustrates the influence of absorber damping ratio on the DLC of the tire loads for two different vehicle speeds, 100 and 120 km/h and rough road excitations.

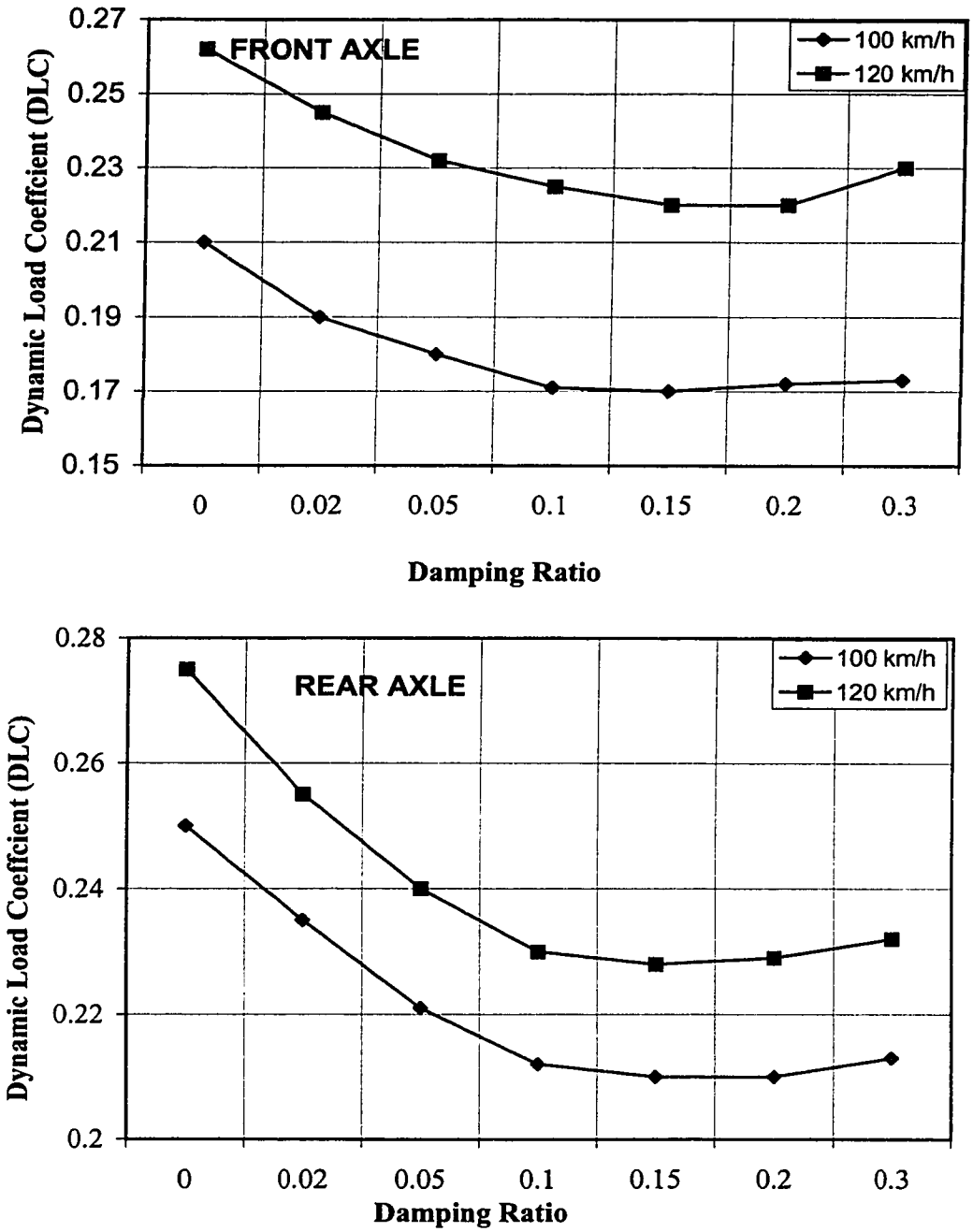

Figure 3.10 Influence of absorber damping ratio on the DLC of the front and rear axle tires at different vehicle speeds.

Table 3.2 Influence of the absorber parameters on the dynamic load coefficients (Vehicle speed= 120 km/h).

	FRONT AXLE TIRES		REAR AXLE TIRES	
Absorber Parameters	**DLC**	**% Reduction**	**DLC**	**%Reduction**
Frequency ratio				
0.85	0.2186	15.04	0.2280	19.83
0.90	0.2190	14.89	0.2272	20.11
0.95	0.2198	14.57	0.2283	19.73
1.0	0.2220	13.72	0.2307	18.88
1.10	0.2274	11.62	0.2376	16.46
Damping ratio				
0.02	0.2455	04.59	0.2551	10.30
0.05	0.2324	09.68	0.2405	15.44
0.10	0.2229	13.37	0.2307	18.88
0.15	0.2198	14.57	0.2283	19.73
0.20	0.2193	14.77	0.2290	19.48
Mass ratio				
0.05	0.2317	09.95	0.2454	13.71
0.10	0.2231	13.29	0.2333	17.97
0.15	0.2198	14.57	0.2283	19..73
0.20	0.2189	14.92	0.2262	20.46
No Absorber	0.2573		0.2844	

The frequency and mass ratios are held constant at 0.95 and 0.15, respectively. The DLC of front and rear axle tire forces of the conventional vehicle at a speed of 120 km/h are obtained as 0.2573 and 0.2844, respectively. An undamped axle absorber tends to increase the DLC of the front axle tire loads, specifically at a speed of 120 km/h, and yields only slight reduction of DLC of the rear axle tires. A slight increase in ξ_{Ai} tends to reduce the DLC considerably, irrespective of the vehicle speed. An increase in damping ratio beyond 0.10 yields insignificant variations in the DLC. A further increase in the absorber damping ratio above 0.20 yields only a slight increase in the DLC. Results show that the axle absorbers with ξ_{Ai}=0.15, can reduce the DLC of front and rear axle tire by 14.5% and 19.75%, respectively. The DLC and the percentage reduction in DLC of the front and rear axle tires caused by various absorber parameters are further summarized in Table 3.2. The results further reveal the existence of optimal damping ratio of vibration absorber.

Influence of Frequency Ratio:

The influence of absorber frequency ratio, Ω_i on the DLC of front and rear axle tires at two different speeds is illustrated in Figure 3.11.The damping and mass ratios are held at 0.10 and 0.1, respectively. While an absorber frequency ratio of 0.83 appears to be optimum for both the front and rear axle absorbers, it is also evident that the DLC is relatively insensitive to the range of frequency ratios considered in this study (0.85-1.0). Results tabulated in Table 3.2 further reveal that the percent reduction in DLC varies by approximately 3.5 over the range of Ω_i values considered. The results also suggest that the axle absorber tuned to the resonant frequencies of the unsprung masses of the nominal

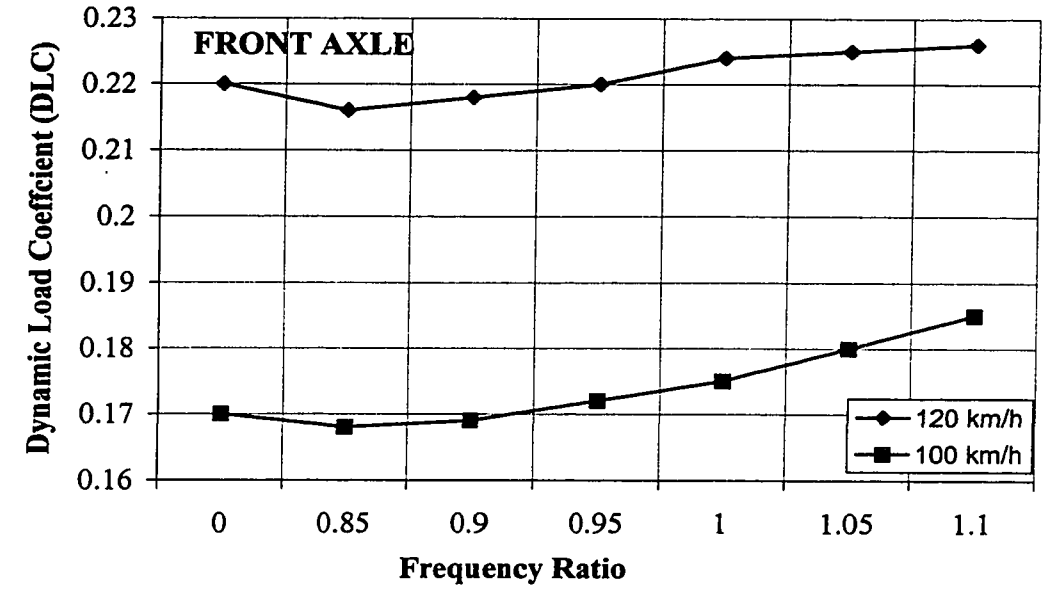

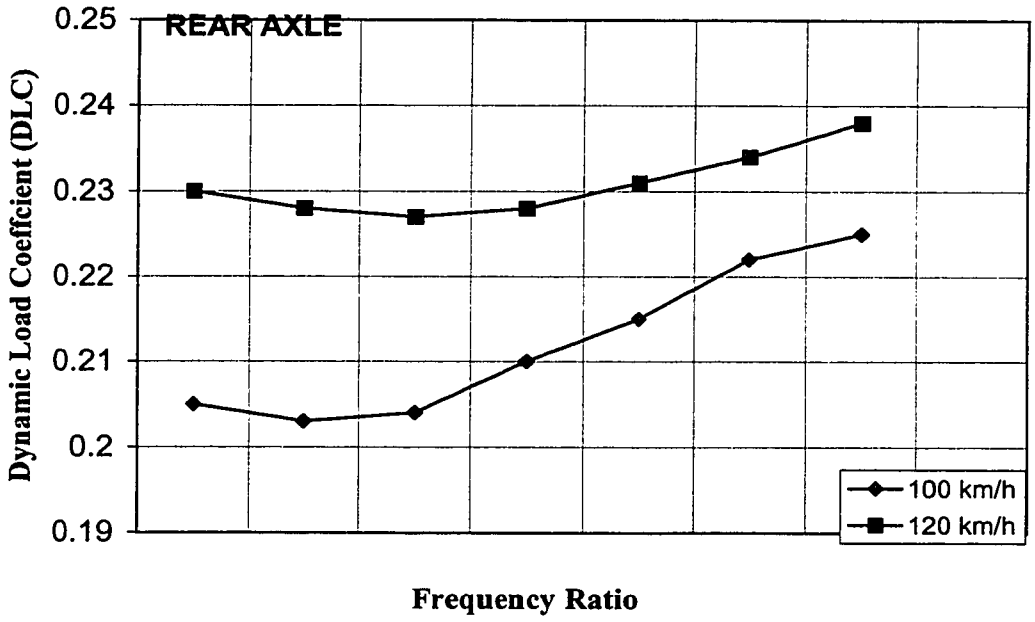

Figue 3.11 Influence of absorber frequency ratio on the DLC of the front and rear axle tires at different vehicle speeds.

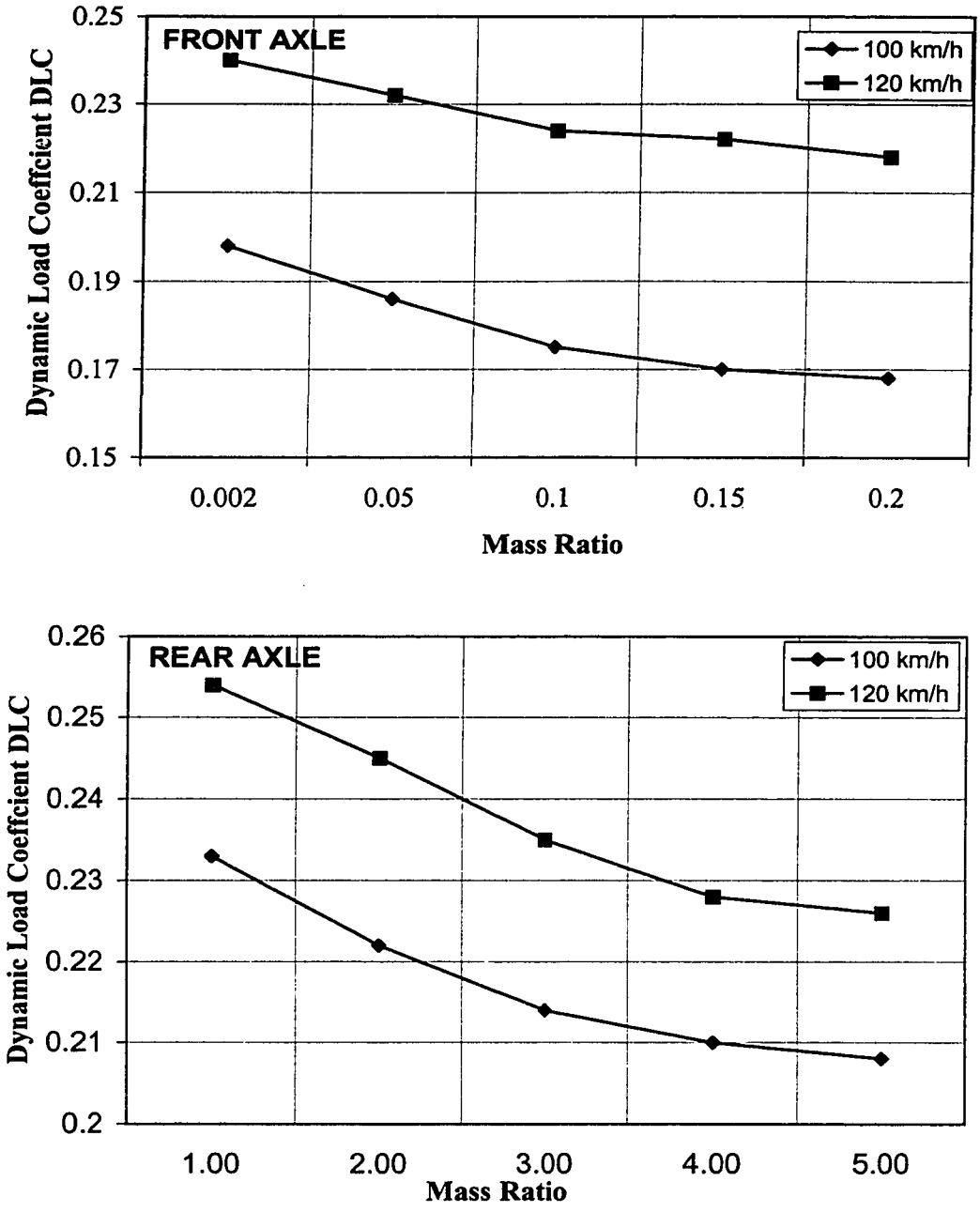

Figue 3.12 Influence of absorber mass ratio on the DLC of the front and rear axle tires at different vehicle speeds.

vehicle will provide effective reductions of the DLC for a range of variations in wheel hop frequencies, caused by changes in the design or operating conditions.

Influence of Mass Ratio:

Figure 3.12 illustrates the influence of the absorber mass ratio, on the DLC of front and rear axle tires at two different speeds. While the light weight axle absorbers ($\mu_{Ai} \leq 0.05$) reduce the overall DLC, the reduction is limited to 9.95% and 13.71% for the front and rear axle tires, respectively. An increase in the absorber mass ratio to 0.10 yields relatively larger reduction in DLC (13.29% and 17.97% for front and rear axle tires, respectively), irrespective of the vehicle speed. A further increase in the absorber mass ratio beyond 0.10 yields only marginal additional reduction in DLC, as illustrated in Figure 3.12 and Table 3.2. It appears from the results that an absorber mass ratio in the range $0.05 < \mu_{Ai} \leq 0.10$, can provide in considerable reduction in DLC, with relatively small effect on the payload capacity of the vehicle.

3.4 OPTIMIZATION OF ABSORBER PARAMETERS

The results discussed in section 3.3 revealed that the dynamic tire loads in the vicinity of wheel-hop frequencies can be reduced through axle absorbers tuned near the unsprung mass resonant frequencies. However the axle absorbers tend to yield peaks at two side band frequencies. Since the peak loads corresponding to these side band frequencies can be suppressed by selecting appropriate absorber damping, frequency and mass ratios, a constrained multi parameter optimization problem is formulated. The effects of optimal axle vibration absorbers on the DLC and the acceleration response are

derived to demonstrate their potential performance benefits. Furthermore, the results summarized in Table 3.3 suggest the existence of optimal damping, frequency and mass ratios for the effective realization of dynamic vibration absorber to enhance the road friendliness of a heavy vehicle.

Table 3.3 Comparison of DLC of tire forces of the vehicle with and with out the absorber.

Road Roughness	**Speed (km/h)**	**DLC (With Absorber)**		**DLC(With out Absorber)**		**% Reduction in DLC**	
		Front	***Rear***	***Front***	***Rear***	***Front***	***Rear***
Rough	80.0	0.217	0.218	0.914	0.193	10.6%	11.5%
	100.0	0.215	0.262	0.17	0.21	20.9%	19.8%
	120.0	0.257	0.281	0.22	0.23	14.4%	18.1%
Medium	80.0	0.164	0.147	0.158	0.141	4.0%	4.08%
	100.0	0.31	0.15	0.30	0.147	3.22%	2.0%
	120.0	0.242	0.280	0.216	0.262	10.7%	6.5%
Smooth	80.0	0.053	0.063	0.051	0.061	4.0%	9.17%
	100.0	0.06	0.054	0.058	0.052	3.33%	4.25%
	120.0	0.051	0.06	0.046	0.055	9.8%	8.33%

3.4.1 Optimization Problem

Since the axle vibration absorbers tuned to the wheel-hop frequencies do not affect the vehicle ride quality derived from the sprung mass acceleration response, a constrained objective function is formulated to minimize the DLC due to tire forces as a function of vehicle speed, V_K. A weighted objective function is developed to study the effectiveness of the absorber in a wide range of vehicle speeds:

$$\text{Minimize} \quad U(\overline{X}) = \sum_{k=1}^{3} \left[DLC_F(V_k) + DLC_R(V_k) \right] \qquad i = F, R$$

Subject to limit constraints $\xi_{Ai} \leq 1.0$; $0.8 \leq \Omega_i \leq 1.1$; and $0. < \mu_i \leq 0.1$ (3.7)

where $\overline{X}$ is the design vector, comprising the absorber frequency ratio (Ω_i), mass ratio (μ_i) and damping ratio(ξ_{Ai}). The optimization problem is solved for three different speeds (V_K=80, 100 and 120 km/h), using a nonlinear programming technique based upon the Quasi-Newton finite-difference gradient method [14]. It should be noted that the absorber mass ratio is limited to a maximum of 0.1 to achieve a lightweight absorber design. The equation of motion for the six-DOF vehicle model are solved under excitations arising from rough road, using direct integration techniques. The optimization problem, described in equation (3.7), is solved under excitations arising from a rough road at three selected speeds. The optimization was performed with different starting values in order to approach the true optimal parameters. The majority of the optimization runs converged to the absorber parameters: Ω_i= 0.856, ξ_{Ai}= 0.141, μ_i=0.1. The response characteristics of the vehicle model with optimal absorber are then evaluated for different road roughness and vehicle speeds.

3.4.2 Performance characteristics of the Optimal Axle Absorber

The vheicle model with optimal axle absorbers is solved under excitations arising from three different roads, while the vehicle speed is varied from 80 km/h to 120 km/h. The tire forces, expressed in terms of DLC, are compared with those derived for the vehicle model without the absorber, as a function of the road roughness and vehicle speeds, as shown in Table 3.3. The results show that optimal axle vibration absorbers reduce the DLC due to tire forces at front and rear axle tires, irrespective of the vehicle

speed and road roughness. The reduction in DLC ranges from 11.5%, to 20.93% for excitations arising from a rough road, and from 3.33% to 9.8% for the smooth road. Although the optimal absorber parameters are selected for excitations arising from rough roads, the results also demonstrate the effectiveness of the proposed absorber for the smooth roads.

Figure 3.13 and 3.14 illustrate a comparison of PSD of vertical and pitch accelerations derived at the driver seat coordinates and the unsprung mass vertical acceleration of the vehicle with and without axle absorbers. It is evident from the figure that the addition of axle absorbers does not affect the vehicle ride quality. The vertical and pitch acceleration response at the driver's seat location near the sprung mass resonance frequencies remain unaffected by the absorbers. The vehicle ride quality is mostly related to the acceleration response near the sprung mass resonance and in the 4-8 Hz frequency range. The influence of the axle vibration absorber on the ride quality is thus insignificant, while the vertical and pitch acceleration response in the vicinity of wheel-hop frequencies decrease considerably. The axle vibration absorbers affect the dynamic tire forces on the front and rear axles in a very similar manner, as shown in Figure 3.15. The peak dynamic tire forces due to front and rear axle tires in the vicinity of the unsprung mass resonant frequencies decrease considerably, when optimal absorbers are introduced. The tire forces in the vicinity of the side band frequency (6-9 Hz), however, increase. The tire forces near the sprung mass resonant frequencies remain unaffected by the axle absorber, as observed earlier from Figure 3.15.

The results presented in Figures 3.13, 3.14 and 3.15, and Table 3.3 illustrate that the dynamic tire loads in the vicinity of wheel hop frequencies can be reduced through

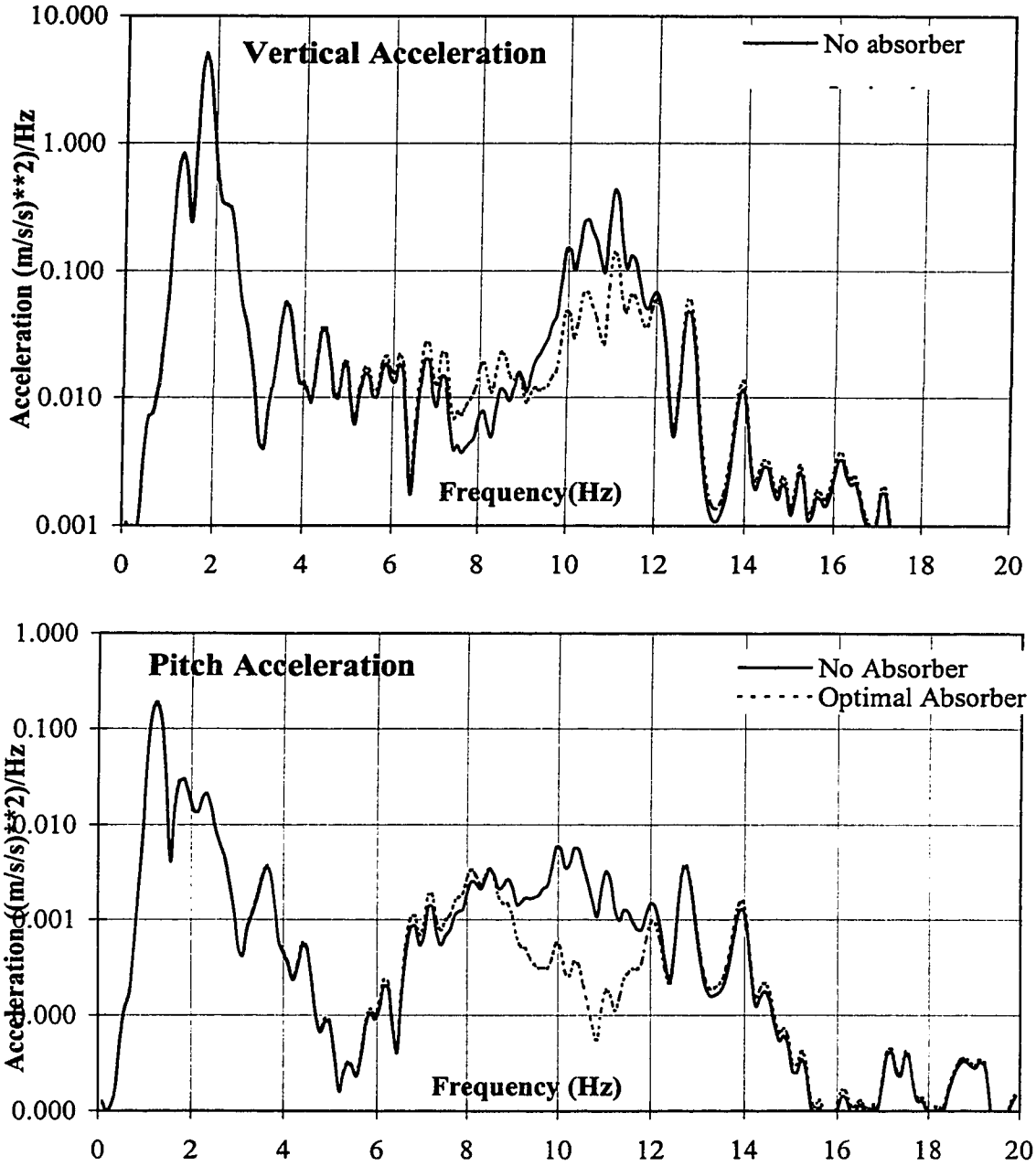

Figure 3.13 Vertical and pitch acceleration PSD response of the vehicle model with optimal axle absorber (Speed =120 km/h, Rough road)

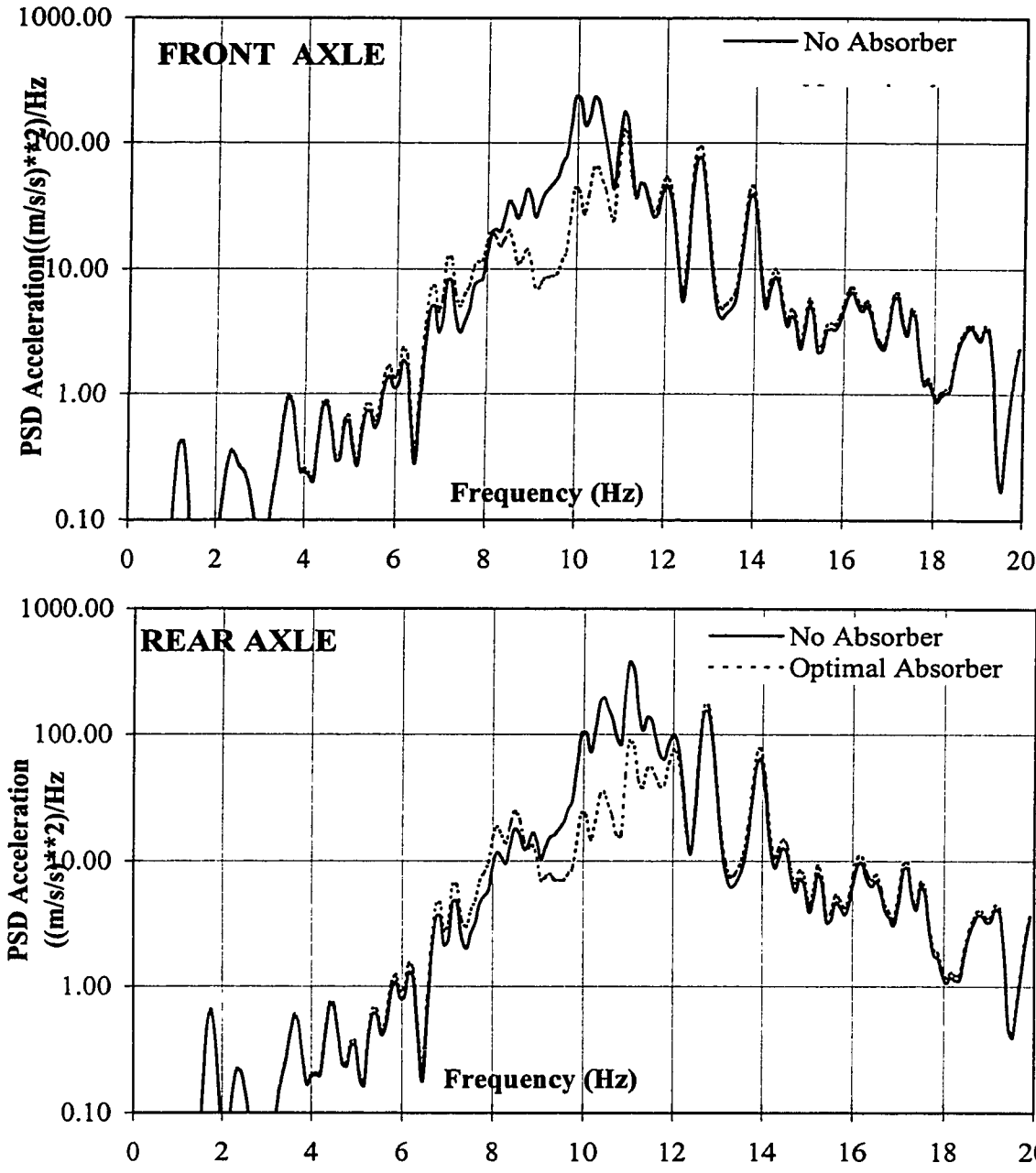

Figure 3.14 Vertical acceleration PSD response of unsprung mass with Optimal axle absorber (speed =120 km/h, Rough road).

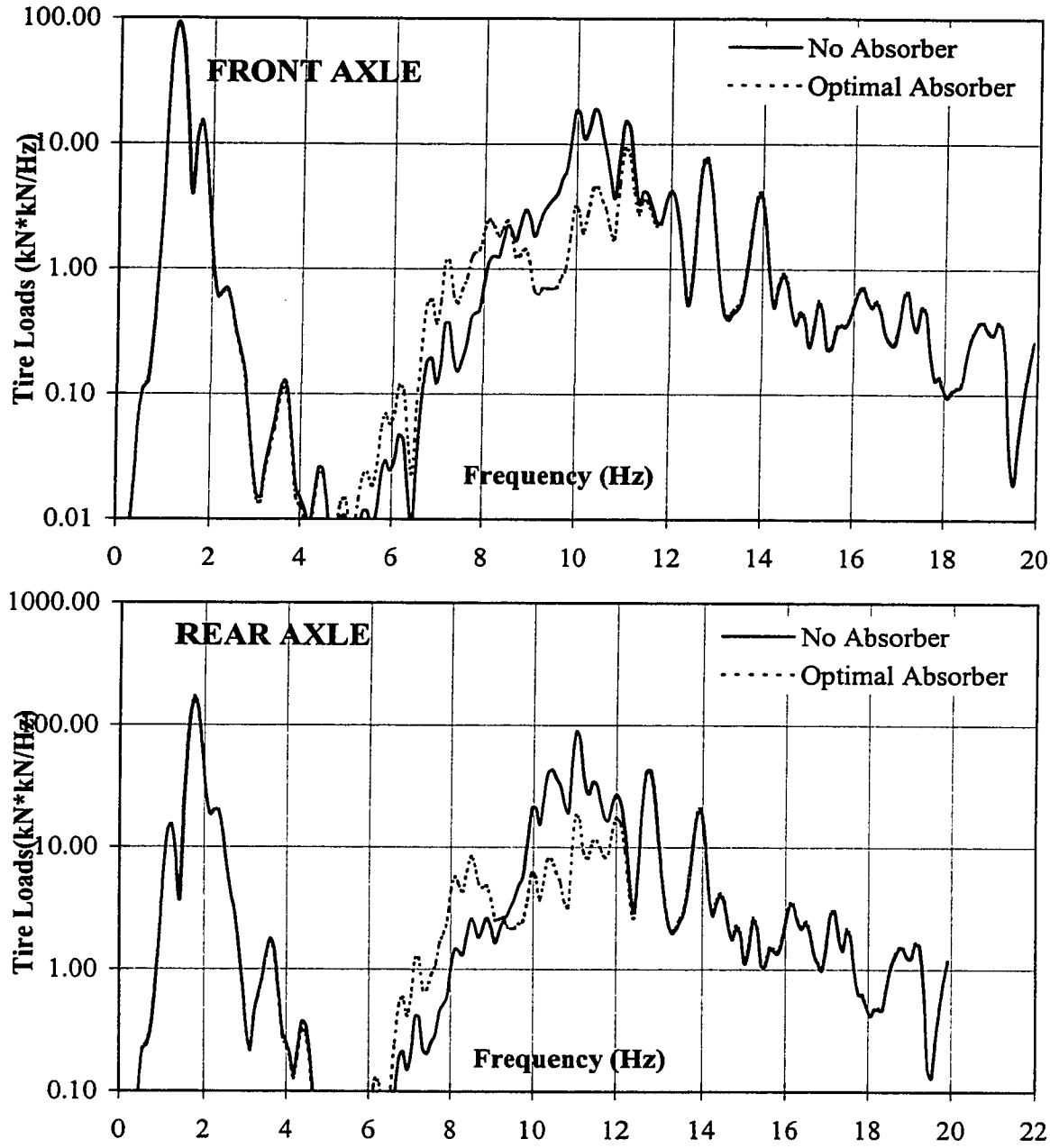

Figure 3.15 PSD of Tire load of the vehicle model with optimal axle absorbers (Speed =120 km/h, Rough road).

axle absorbers tuned near the unsprung mass resonant frequencies. The tuning of the absorber parameters is strongly dependent on the payload, tire and suspension properties, vehicle speed and road roughness. Variation in these operating and design variables may necessitate re-tuning of the absorber parameters. In the present analysis, the absorber tuning is attained for an operating speed range of 80-120 km/h and rough road. The effectiveness of the tuned absorber is further illustrated for vehicle operation on a smooth road.

3.5 SUMMARY

The enhancement of road friendliness of heavy vehicles is analytically investigated using the concept of a dynamic vibration absorber, tuned to the resonant frequencies of the unsprung mass of the vehicle model. The effectiveness of the dynamic vibration absorber, in reducing the dynamic loads, is strongly dependent upon its tuning parameters. A parametric study is performed to analyze the influence of the frequency ratio, damping ratio and mass ratio of the absorber on the tire loads and the acceleration response for deterministic and stochastic excitations at tire-road interface. A weighted multi parameter objective function is developed to study the effectiveness of the absorber in a wide range of vehicle speeds. The solution of the optimization problem has revealed that the damping ratio of 0.14, frequency ratio of 0.85 and mass ratio of 0.1 are desirable for the effective performance of the absorber. Further results of the study revealed that the optimal axle vibration absorber yields reduction in DLC in the range 11.5% to 20.93% for excitation arising from a rough road, while the reduction is 3.3% to 9.85% for the smooth road in the 80-120 km/h speed range. The combined effect of optimal axle

absorber and optimal suspension damping, in enhancing the road and driver friendliness, is illustrated in Chapter 5.

CHAPTER 4

ENHANCEMENT OF DRIVER AND ROAD FRIENDLINESS THROUGH OPTIMAL SUSPENSION DAMPING

4.1 INTRODUCTION

Variations in the dynamic tire forces of heavy vehicles are strongly related to vibration modes of the vehicle associated with vertical and pitch motions of the sprung and unsprung masses. The vibration modes and thus the dynamic wheel loads are dependent upon the vehicle and axle configurations, inertial and geometrical properties of the vehicle, and properties of the suspension and tire [10, 20 and 61]. The dynamic wheel loads in general, predominate in the low frequency range associated with the resonances of the sprung masses. The walking-beam suspensions, due to their light pitch mode damping, and air-suspensions, due to their reduced spring rate in rebound, also yield high dynamic loads in the higher frequency range in the vicinity of the wheel hop modes [17]. The control of vehicle vibration in these frequency bands through optimal suspension design can enhance both the road friendliness and ride quality of the vehicle. While soft suspension springs are highly desirable to enhance the ride quality and wheel load performance, the realization of adequate directional control and rattle space performance necessitates relatively hard suspension springs. The suspension springs are thus selected to achieve a compromise among these conflicting requirements, with relatively larger weighting placed on the rattle space and directional control performance requirements [60]. Since both the dynamic loads and the ride quality are related to vehicular vibration

modes, the suspension design with optimal damping offer significant potentials to enhance both the driver-and road-friendliness of the vehicle without affecting the rattle space and directional control requirements.

In this study, an analogy between the dynamic wheel loads and ride quality performance characteristics of heavy vehicles is initially, established through analysis of simple quarter-vehicle vehicle model. A weighted optimization function comprising the dynamic load coefficient (DLC) and the overall rms vertical acceleration at the driver's location, for linear and nonlinear suspensions, is formulated to determine the optimal design parameters of the damper. The results show that optimal asymmetric damping can enhance both the road-and driver-friendliness of the vehicle considerably. The dynamic wheel loads and ride performance characteristics of vehicle with optimal suspension damper and axle absorber are further analyzed and discussed.

4.2 ANALOGY BETWEEN THE RIDE QUALITY AND TIRE LOADS

While the influence of restoring properties of heavy vehicle suspension and axle configurations on the dynamic wheel loads has been reported in many analytical and experimental studies [49], the influence of dissipative properties of the suspension has been addressed only in limited number of studies [43, 60]. The influence of suspension damping on ride dynamics of vehicles, however, has been extensively investigated [12]. Since the vehicle ride quality and dynamic wheel loads are both related to vehicle vibration modes, the suspension damping considered adequate for improved ride quality can lead to enhanced road friendliness of the vehicle. An analogy between the dynamic wheel loads (DWL) and ride performance can be established through analysis of a linear

quarter-vehicle model. Since the ride quality of a vehicle relates to the exposure of the driver to the whole-body vehicular vibration measured in terms of vertical acceleration, is evaluated from the overall rms vertical acceleration of the sprung mass [98].

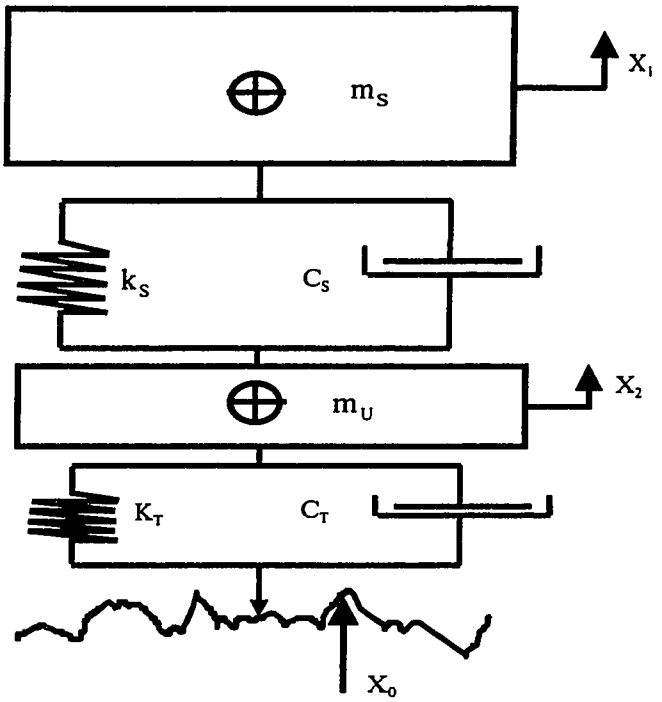

Figure 4.1 A two-DOF quarter-vehicle model.

Figure 4.1 illustrates a quarter-vehicle model comprising sprung and unsprung masses, m_s and m_u, constrained to move along the vertical axis, linear suspension spring K_S suspension damping C_S, and the linear tire parameters K_T and C_T. The equations of motion of the two-DOF vehicle model are formulated as:

$$m_S\ddot{x}_1 + F_S(z_1) + F_d(\dot{z}_1) = 0$$

$$m_U\ddot{x}_2 + F_T(z_2, \dot{z}_2) - F_S(z_1) - F_d(\dot{z}_1) = 0 \qquad (4.1)$$

where x_1 and x_2 are the deflection of the sprung and unsprung masses, respectively, and x_0 is the displacement excitation due to roads. $z_1 = x_1 - x_2$ and $z_2 = x_2 - x_0$. The vehicle model is

analyzed to determine the dynamic tire force F_T and the sprung mass acceleration $\ddot{x}_1$ arising from a randomly rough road. While the time history of F_T is analyzed to derive the DLC, the time history of $\ddot{x}_1$ is analyzed to yield the overall rms acceleration, $\hat{a}$:

$$DLC = \frac{\sqrt{\frac{1}{n}\sum_{i=1}^{n}(F_{Ti} - \overline{F}_T)^2}}{\overline{F}_T},$$

$$\hat{a} = \left[\frac{1}{T}\int_0^T \ddot{x}_1^{\,2}(t)dt\right]^{\frac{1}{2}}, \qquad (4.2)$$

where $\overline{F}_T$ is the mean tire force, T is the total simulation time. Equation (4.1) and (4.2) are solved for both linear viscous and nonlinear asymmetric damping to study the analogy between the DLC and the ride quality. Figure 4.2 illustrates the DLC and overall rms acceleration response of the vehicle model with linear viscous damping as a function of the uncoupled damping ratio, $\xi_S = \frac{C_S}{2\sqrt{k_S m_S}}$. The results clearly show that both the DLC and the overall rms acceleration decrease with an increase in suspension damping ratio. The results further indicate that the suspension damping influences the ride quality and tire loads in a similar manner. While an increase in suspension damping ratio beyond 0.15 yields only minimal further reduction in DLC, higher damping tends to deteriorate the ride quality at frequencies in the vicinity of the fundamental resonant frequencies of the seated occupant (near 5 Hz) [98].

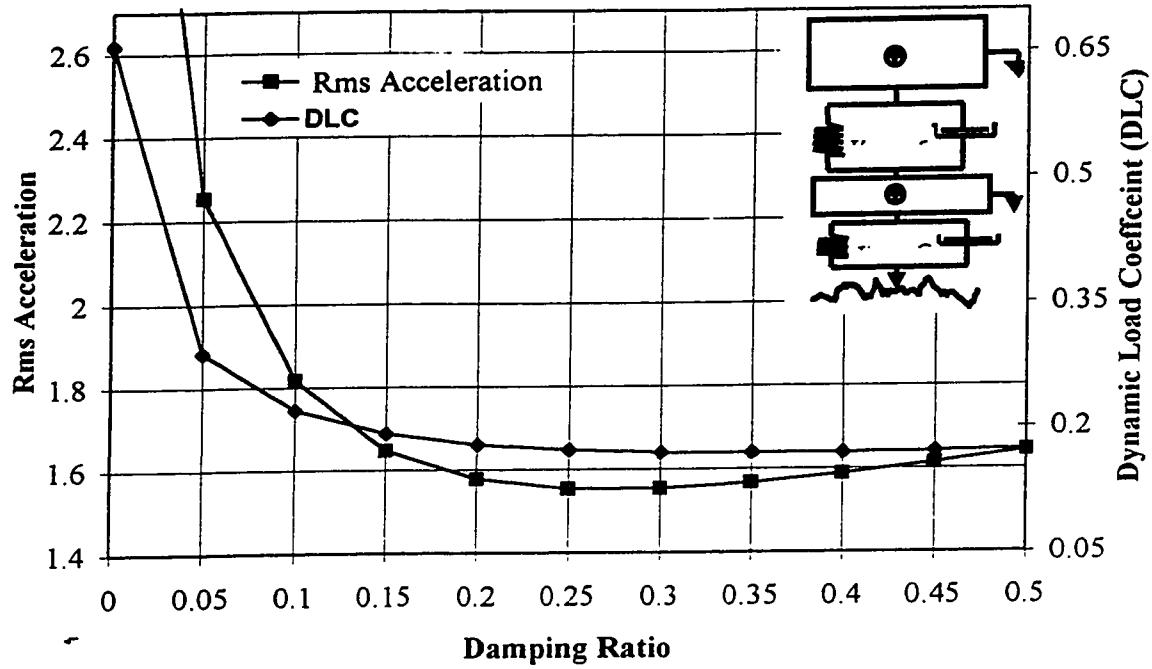

Fugure 4.2 Influence of suspension damping ratio on the DLC and overall rms acceleration.

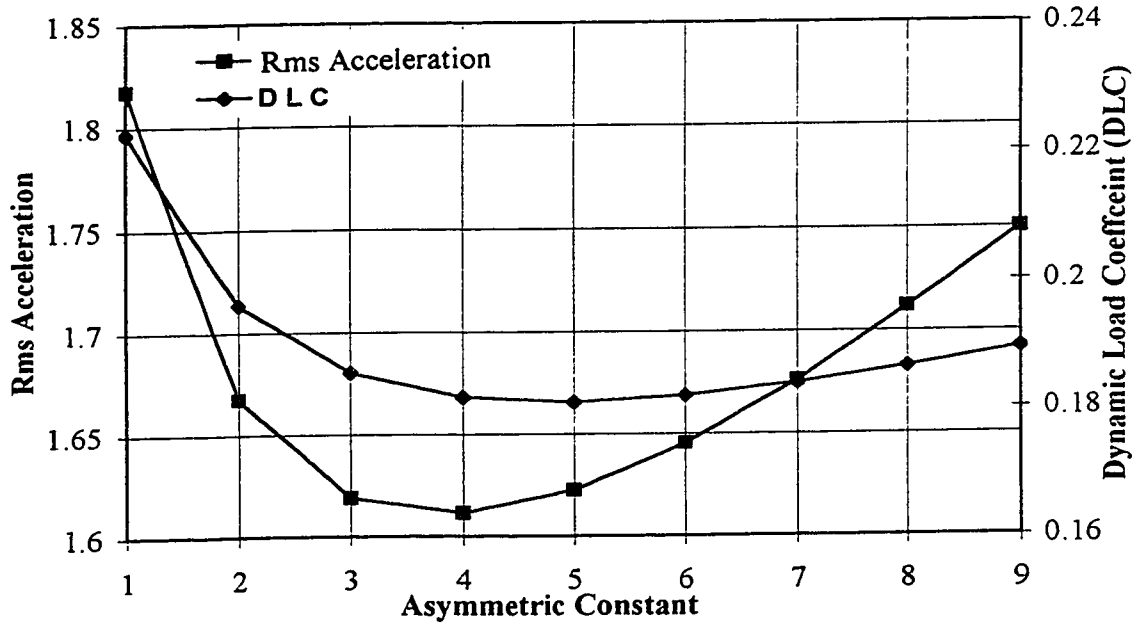

Figure 4.3 Influence of nonlinear asymmetric damping on DLC and overall rms acceleration.

Alternatively, suspension dampers with asymmetric damping properties in compression and rebound can effectively reduce the magnitude of tire forces while preserving the ride response [60]. Figure 4.3 illustrates the influence of asymmetry constant, the ratio of damping constant in rebound to that in compression, on the DLC and the overall rms acceleration response of the quarter vehicle model. The compression mode damping ratio in this example is selected as 0.10. It is evident from the figure that the damping affects both the overall rms acceleration and the DLC in a similar manner. The results presented in Figures 4.2 and 4.3 clearly illustrate an analogy between the road-and driver-friendliness characteristics of the vehicle. Thus the suspension damping considered adequate for improving the ride quality can lead to enhancement of road friendliness of the vehicle. The results presented in Figures 4.2 and 4.3 further reveal the existence of optimal compression damping ratio and asymmetry constant.

4.3 OPTIMAL SUSPENSION DAMPING FOR LINEAR SUSPENSION

From Figures 4.2 and 4.3 it is apparent that the suspension damping affects both the ride quality and dynamic wheel loads. A moderate increase in suspension damping yields considerable reduction in DLC and the overall rms acceleration response, a measure of the vehicle ride quality. While high suspension damping results in only slight reduction in the DLC, it tends to deteriorate the ride quality in the 3-8 Hz frequency range, which coincides with the whole-body resonance of human body [98]. In this study, optimal asymmetric suspension damping characteristics are derived to enhance the road friendliness of the vehicle with appropriate consideration of the ride quality. A multi parameter optimization problem is formulated and solved to determine the optimal

suspension damping. The optimal suspension damping parameters are strongly dependent upon the vehicle configuration, gross vehicle weight, axle loads, suspension type, road roughness and vehicle speed. The analytical model of the straight truck, presented in chapter 2, is considered for the optimization study, and the axle loads and gross vehicle weight are selected in accordance with the weights and dimensions regulations. The optimal damping properties are derived for linear, leaf and air suspension combinations, while the vehicle speed is varied in the 80-120 km/h range. Although the optimal suspension damping properties are identified for excitation arising from a rough road, the validity of the optimal solutions is also examined for the smooth and medium-rough road excitations.

4.3.1 Characterization of suspension damping

The four-DOF vehicle model with linear suspension is initially analyzed to study the influence of both linear and nonlinear asymmetric damping on the tire loads and the ride quality. The linear suspension damping is expressed in terms of uncoupled vertical mode damping ratios, ξ_F and ξ_R, given by

$$\xi_i = \frac{C_{qi}}{2\sqrt{K_{si}\varepsilon_i}};\ i=\ F, R\ (\text{Front \& Rear}) \tag{4.3}$$

where ε_i is the sprung mass supported by the suspension spring i and C_{1i} is the viscous damping coefficient. For asymmetric damping properties, described in Figure 2.13 C_{1i} represents the damping coefficient in the compression mode.

The low speed rebound damping is expressed by the asymmetry constant, $\beta_i = \frac{C_{2i}}{C_{1i}}$. The high velocity rebound damping, attributed to blow-off valves, is represented by reduction

factor, $\gamma_i = \frac{C_{3i}}{C_{2i}}$. The equations of motion for the four-DOF vehicle model, employing linear suspension springs, Equation (2.1), are then solved for excitations arising from two different measured road profiles, referred to as *rough* and *smooth* (Figure 2.15).

4.3.2 Problem Formulation and Optimization

From Figures 4.2 and 4.3, it is evident that the suspension damping affects both the ride quality and dynamic wheel loads. A weighted optimization function comprising the dynamic load coefficient (DLC) due to tire forces and the overall rms acceleration at the driver's location is thus formulated for a range of operating speeds:

$$U(\overline{X}) = \sum_{K=1}^{3} [\hat{a}(V_K) + DLC_F(V_K) + DLC_R(V_K)]; \tag{4.4}$$

The design vector $\overline{X}$ comprises the asymmetric damper parameters: compression mode damping ratio ξ_i; asymmetry constant, β_i; transition velocity, V_{SEi}; and damping reduction factor, γ_i. The design variables are subject to following limit constraints:

$0.0 < \xi_i \leq \xi_{iu}$ (0.05, 0.1, 0.15 and 0.20);

$1.0 \leq \beta_i \leq 20.0$;

$0.2 \leq \gamma_i \leq 0.9$;

$0.0 \geq V_{Se} \geq 0.2$ m/s. i =F, R (4.5)

The different values of upper limits on the compression mode damping ratio are selected to study its influence on the asymmetry factor. The $\hat{a}(V_K)$ is the overall rms acceleration computed at the driver's seat location corresponding to the vehicle speed V_K, given by:

$$\hat{a}(V_K) = \sqrt{\frac{1}{T}\int_0^T \ddot{Z}_S^2(V_K)dt}\ , \tag{4.6}$$

where, $\ddot{Z}_S$ is the vertical acceleration at the driver's location. It should be noted that the optimization function yields a weighted measure of DLC and the overall rms acceleration response over a range of vehicle speeds, V_K, ranging from 80 to 120 km/h. The optimization problem, described in equation (4.4), is solved for three different speeds using the method discussed in section (3.4.1).

4.3.3 Results and Discussions

The weighted optimization problem, described in the equation (4.4), is solved to determine optimal asymmetric damping parameters. The optimization is performed for excitations arising from a rough road over a speed range of 80-120 km/h. The influence of optimal damping properties on the DLC of tire forces and the overall rms acceleration, however, is evaluated for smooth as well as rough roads. The constrained optimization problem was solved in conjunction with the four-DOF vehicle model under different compression mode damping values. The optimal values of the asymmetry constant, transition velocity and reduction factor are established for compression damping ratio ranging from 0.05 to 0.2. The optimization was performed using an array of different starting values for each compression damping ratio. The minimization problem converged to near identical values of asymmetry constant, reduction factor and transition velocity, irrespective of the starting values $\hat{a}$.

Table 4.1, illustrates the optimal damper parameters corresponding to preselected values of compression mode damping ratio. The results show that the asymmetry constant decreases considerably with increase in the compression mode damping. A high uncoupled rebound damping ratio is required, when low compression damping is selected. The optimal values of the rebound damping ratio, however, remain near 0.8, for

Table 4.1 Optimal damping parameters for different compression mode damping ratios of linear spring suspension.

Compression Damping Ratio	Asymmetry Constant (β_i)	Rebound Damping Ratio ($\beta_i\xi_i$)	Transition Velocity (V_{se})	Reduction Factor (γ_i)	DLC (Front)	DLC (Rear)	â
0.05	16.34	0.82	*	1.0	0.129	0.152	0.9
0.1	8.0	0.8	0.166	0.34	0.129	0.152	0.9
0.15	4.56	0.7	0.181	0.364	0.129	0.152	0.9
0.2	3.01	0.6	0.193	0.366	0.129	0.152	0.9

ξ_i varying from 0.05 to 0.10. The rebound damping ratio decreases in a linear manner, when ξ_i is increased from 0.1 to 0.2. The results show that a high rebound damping is required to dissipate the high energy due to low compression mode damping. High compression mode damping, however, requires relatively lower rebound damping in order to preserve the ride quality of the vehicle. The results further show an interesting trend in the mean low velocity damping ($0.5*C_{1i}+ 0.5*C_{2i}$), which ranges from 0.4 to 0.45, for all values of ξ_i. The transition velocity, where blow-off damping occurs, tends to increase with increase in the compression damping ratio. The light compression mode damping ratio (0.05) tends to converge to very high value of transition velocity resulting in a single stage rebound damping ($\gamma_i = 1$). The transition velocity, however, varies only slightly from 0.166 to 0.193, when compression damping ratio varies from 0.10 to 0.20. Furthermore, the optimal reduction factors are observed to lie within a narrow range of, 0.34 to 0.366, irrespective of the compression mode damping. It should be emphasized that blow-off damping mostly relates to vibration isolation or ride quality. The results suggest reduction in rebound damping through blow-off flows by nearly 1/3. The DLC and rms acceleration response characteristics of the vehicle model are also investigated

using four sets of optimal damping parameters and presented in Table 4.1. The results reveal nearly similar values of DLC and overall rms acceleration, irrespective of the compression mode damping ratio. The light compression mode damping ($\xi_i = 0.05$), however, may yield significant resonant response under abrupt excitations.

Table 4.2 Comparison of DLC and rms acceleration of linear and optimal suspension damping.

Road	Speed	Linear Damper			Optimal Damper			%Reduction in DLC & Rms acceleration		
		DLC (Front)	DLC (Rear)	RMS	DLC (Front)	DLC (Rear)	RMS	DLC (Front)	DLC (Rear)	RMS
Rough	80	0.165	0.156	1.16	0.122	0.138	0.878	26.0%	11.5%	24.3%
	100	0.167	0.196	1.03	0.129	0.152	0.901	22.7%	22.5%	12.5%
	120	0.193	0.207	1.204	0.136	0.159	0.93	29.5%	23.1%	22.7%
Smooth	80	0.04	0.043	0.33	0.028	0.034	0.206	30.0%	20.9%	37.5%
	100	0.044	0.041	0.36	0.031	0.035	0.242	29.5%	14.2%	32.7%
	120	0.041	0.045	0.346	0.035	0.038	0.27	14.6%	15.5%	21.4%

The DLC and overall rms acceleration response of the vehicle model employing linear suspension springs and optimal asymmetric damper ($\xi_i = 0.1$) are compared with those of the vehicle model with constant damped damping suspension ($\xi_i = 0.1$, $\beta_i = 1.0$, and $\gamma_i = 1$), as shown in Table 4.2. The response characteristics of the linear and asymmetric suspension damping are compared for different road roughness and vehicle speeds. The results clearly show that the DLC due to front and rear tire forces reduce by 11.5% to 30%, when optimal asymmetric damping is introduced. The corresponding reduction in the rms acceleration ranges from 12.5% to 37.5% in the speed range considered in this study. The results suggest that asymmetric damping in highly desirable to enhance both the road-and driver-friendliness of the vehicle. Furthermore, the optimal asymmetric damping, derived under excitation from a rough road also yields

considerable reduction in DLC and rms acceleration under smooth road excitations. The optimal damping, however, yields most significant benefits near the high speed (120 km/h) under rough road excitations, and near low speed (80 km/h) under smooth road excitations.

The response characteristics of the vehicle model with linear spring and optimal asymmetric damping suspension, in terms of PSD of vertical and pitch acceleration, are compared to those of a linearly damped suspension as shown in Figure 4.4. The results are derived using the optimal suspension damping parameters: with $\xi_i = 0.1$, $\beta_i = 0.8$, and $\gamma_i = 0.34$, and V_{SEi}=0.166, while the linear damper parameter is selected as $\xi_i = 0.1$.

The linear damping yields high magnitude vertical and pitch acceleration peaks near the sprung and unsprung mass resonances, and considerably lower response at higher frequencies above 13 Hz. The asymmetric damping effectively suppresses the resonant peaks due to high rebound damping, and yields poor ride performance in the 2-8 Hz frequency range, and at higher frequencies. The PSD of front and rear tire forces, shown in Figure 4.5, also reveal similar influence. The results clearly show that the optimal suspension damping reduces both the acceleration responses at the driver's seat and the tire forces in the vicinity of the resonant frequencies. The vertical acceleration and tire force response characteristics of the optimally damped suspension, however, are slightly higher than those of the linearly damped suspension in the 2-8 Hz frequency range. Since the tire forces predominate in the vicinity of sprung and unsprung mass resonant frequencies, an asymmetric damping is considered to be highly desirable for enhancement of road-friendliness of the vehicle.

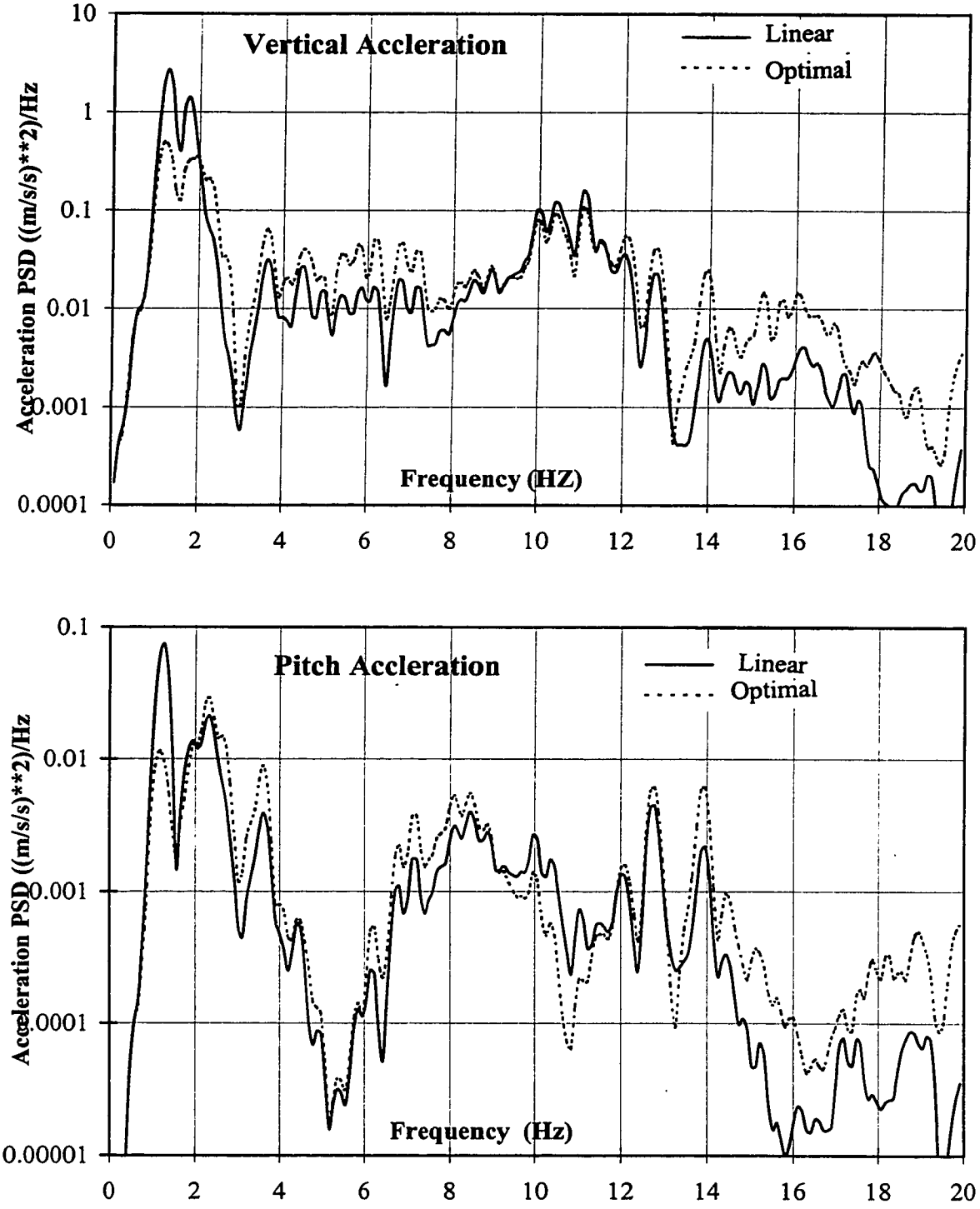

Figure 4.4 Comparison of Vertical and Pitch acceleration PSD response of linear spring vehicle model with linear and optimal asymmetric damping.

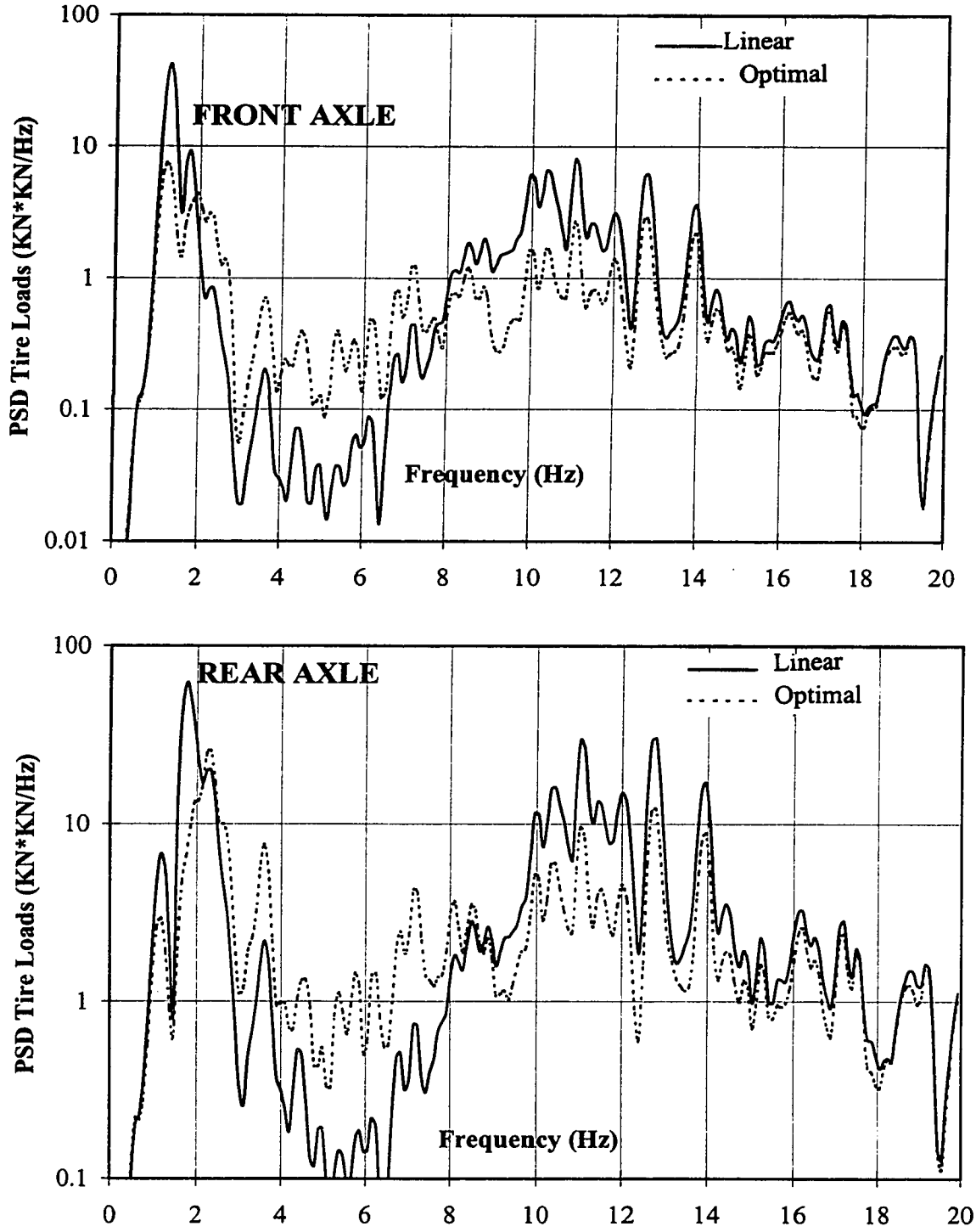

Figure 4.5 Comparison of PSD tire loads of the linear spring vehicle model with linear and optimal asymmetric damping.

4.4 OPTIMAL SUSPENSION DAMPING FOR NON LINEAR LEAF SUSPENSION

Leaf spring suspension is a complex force-producing mechanism which may exhibit varying levels of effective spring rate and hystersis, depending upon the loading of the spring and the amplitude of the oscillation. Although the inter-layer friction inherent within a leaf spring suspension yields considerable dissipaive properties, additional light optimal viscous damping can further reduce the dynamic loads and enhance the ride quality of the vehicle. The optimization problem, Equation (4.4), is thus formulated to investigate the influence of additional suspension damping on the DLC and rms acceleration of the vehicle model with front and rear leaf spring suspension.

$$\xi_i = \frac{C_{li}}{2\sqrt{K_{effi}\varepsilon_i}}; \quad i= \text{F, R (Front \&Rear).} \tag{4.7}$$

where K_{effi} (i= F, R) is the effective mean stiffens of the front and rear nonlinear leaf suspension, and ε_i is the sprung mass supported by the suspension spring i.

4.4.1 Problem formulation and Optimization

A weighted optimization function comprising the dynamic load coefficient (DLC) due to tire forces and the overall rms acceleration at the driver's location is formulated, as described in Equation (4.4). The design vector $\overline{X}$ comprises the asymmetric damper parameters: compression mode damping ratio, ξ_i; asymmetry constant, β_i; transition velocity, V_{SEi}; and damping reduction factor, γ_i, as described in section 4.3.1. The minimization problem is subject to limit constraints described is section 4.3.2.

4.4.2 Results and Discussions

The coupled differential equations of motion for the non-linear vehicle model, Equations (2.1), (2.6), (2.7) and (2.8), are solved for excitations arising from the rough road in conjunction with minimization problem of Equation (4.4). The minimization is performed for speeds ranging from 80-120 km/h and many different starting values. The solution revealed convergence to nearly identical damper parameters for each selected upper limit of the compression mode damping ratio.

Table 4.3 Optimal damping parameters for different compression mode damping ratios of leaf suspension.

Compression Damping Ratio	**Asymmetry Constant** (β_i)	**Rebound Damping Ratio** ($\beta_i\xi_i$)	**Transition Velocity** (V_{SE})	**Reduction Factor** (γ_i)
0.05	5.0	0.25	*	1.0
0.1	3.0	0.3	*	1.0
0.15	1.7	0.255	0.5	0.432
0.2	1.1	0.22	0.3	0.30

The resulting optimal parameters, summarized in Table 4.3, show that the asymmetry constant (β_i) decrease with increase in the compression damping ratio, as observed earlier for the linear spring suspension. The transition velocity tends to converge the upper limit for $\xi_i \leq 0.1$ which is considered as single stage rebound damping ($\gamma_i = 1$). While the reduction factor, γ_i, decreases to 0.432 and 0.3, for $\xi_i = 0.15$ and 0.2, respectively, the transition velocity (0.3-0.5 m/s) remains considerably higher than that obtained for linear spring suspension. The rebound damping corresponding to bleed flows approaches the to compression damping ($\beta_i \approx 1$) high compression damping ratio, $\xi_i = 0.2$. The optimization results thus reveal optimal values of asymmetric constant ($1.0 < \beta_i < 5.0$), reduction factor ($0.3 < \gamma_i \leq 1.0$), and transition velocities (V_{SEi}) as high as 0.5 m/s. The low values of asymmetry constant and the rebound damping can be

attributed to relatively high hysteretic damping of the multi-leaf spring suspension at low velocities. The hysteretic properties yield high damping at low velocities and very light damping at higher velocities. The leaf spring suspension thus requires relatively higher damping under higher magnitude relative velocities. The minimization problem thus converges to relatively higher values of the reduction factor, γ_i, and the transition velocity, V_{SEi}. The vehicle model with four sets of optimal parameters was analyzed for excitation arising from the rough roads. The results revealed nearly similar values of DLC and overall rms acceleration, irrespective of the compression mode damping ratio. The DLC and overall rms acceleration response of the vehicle model with optimal asymmetric damper ($\xi_i = 0.1$, $\beta_i = 3.0$, $\gamma_i = 1$) are compared with those of the vehicle model employing a typical hydraulic shock absorber, whose parameters were identified in the laboratory, as discussed in section 2.3.3. (Compression damping = 1941.0 Ns/m, $\beta_i = 8.0$ and $\gamma_i = 0.4$).

Table 4.4 Comparison of DLC and rms acceleration response of truck model with leaf spring suspension, and typical and optimal suspension damping.

Road	Speed	Typical Damper			Optimal Damper			%Reduction in DLC&Rms aceleration		
		DLC (Front)	DLC (Rear)	RMS	DLC (Front)	DLC (Rear)	RMS	DLC (Front)	DLC (Rear)	RMS
Rough	80	0.112	0.15	0.85	0.11	0.14	0.78	2%	6.7%	8.23%
	100	0.123	0.195	0.87	0.12	0.16	0.83	2.5%	17.9%	4.6%
	120	0.134	0.20	0.9	0.130	0.17	0.86	3.0%	17.5%	4.4%
Smooth	80	0.047	0.044	0.32	0.032	0.04	0.26	31.9%	9.0%	17.8%
	100	0.054	0.042	0.39	0.034	0.040	0.28	37.1%	4.8%	28%
	120	0.054	0.042	0.40	0.034	0.039	0.29	37.0%	7.2%	27.5%

The response characteristics of the linear and asymmetric suspension damping are compared for different road roughness and vehicle speeds. The results illustrated in Table

4.4 clearly show that the DLC due to front and rear tire forces reduce by 2% to 37.1%. The corresponding reduction in the rms acceleration ranges from 4.4% to 28% in the speed range considered in this study. The results further show that the DLC due to heavily loaded rear axle tires traversing a rough road reduces considerably with optimal asymmetric damping. The optimal damping, however, yields only small reduction in DLC front axle tire force due to relatively light load on the axle and high friction. The over all rms acceleration response of the sprung mass of the vehicle, traversing the rough road at high speeds, reduces only by 4.4 to 4.6%. The vehicle response under excitations arising from a smooth road reveals considerable reduction in the overall rms acceleration and DLC due to front axle tires. This reduction is most likely due to lower magnitudes of resonant response of the sprung and unsprung masses.

The PSD of vertical and pitch acceleration response of the sprung mass of the vehicle model with optimally damped leaf suspension are compared with those of the vehicle model employed a typical damper parameters, as shown in Figure [4.6]. The PSD of dynamic tire force response are also compared, as shown in Figure [4.7].

The results show that the optimal suspension damping reduces both the acceleration responses at the driver's seat and the tire forces in the vicinity of the resonant frequencies. The vertical acceleration and tire force response characteristics of the vehicle model with typical damper used in this study, however are slightly lower that those of the model with optimally damped suspension in the 2-8 Hz frequency range. The PSD of dynamic tire forces of the optimally damped suspension in the vicinity of un-sprung mass resonant frequencies are also lower than those obtained with the typical damper.

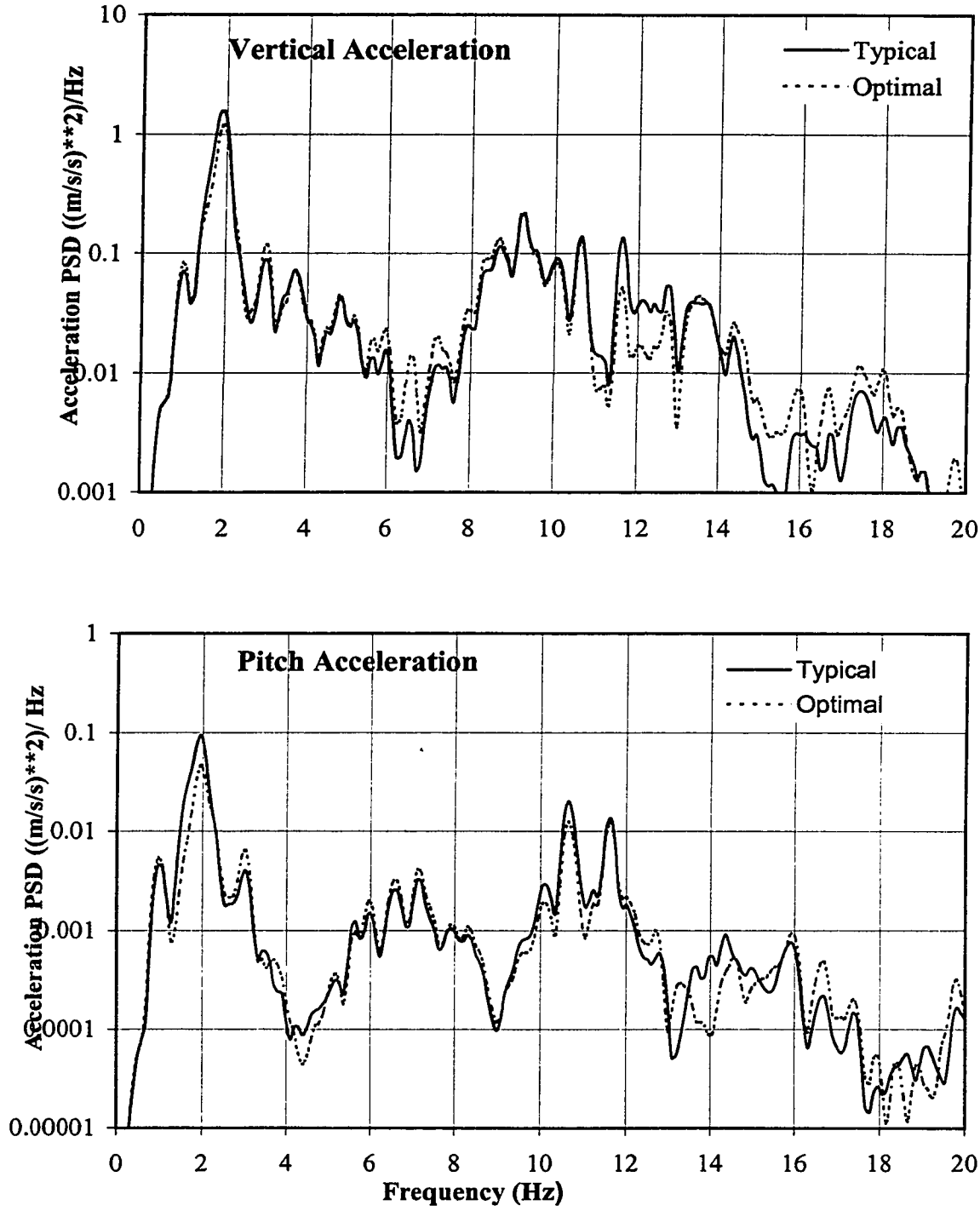

Figure 4.6 Comaprison of acceleation PSD response of leaf suspension vehicle model with typical and optiamal asymmetric suspension damping.

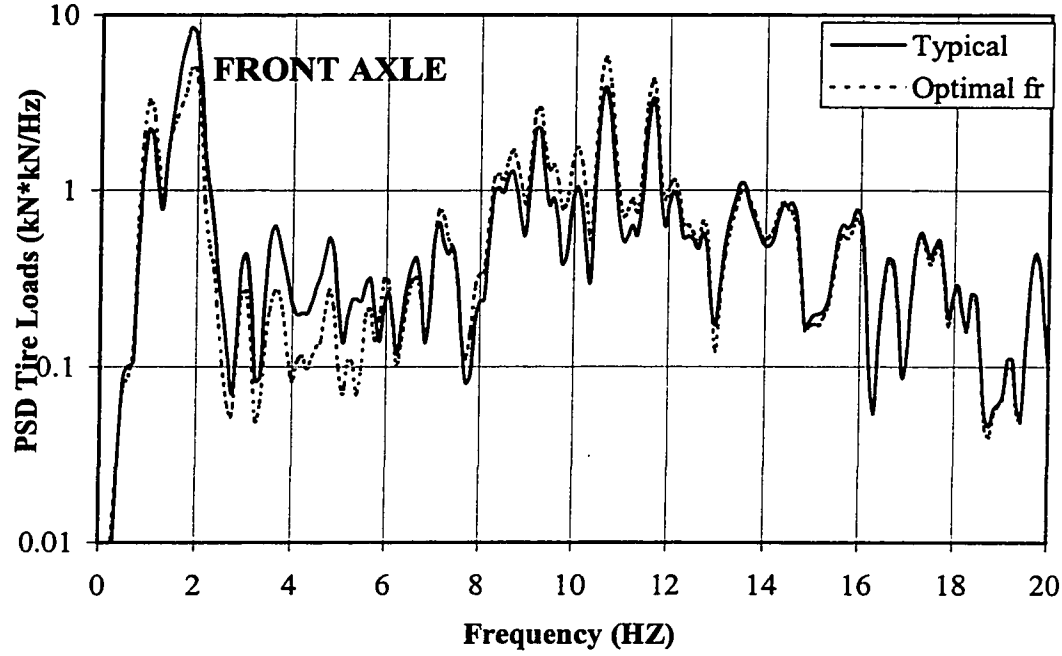

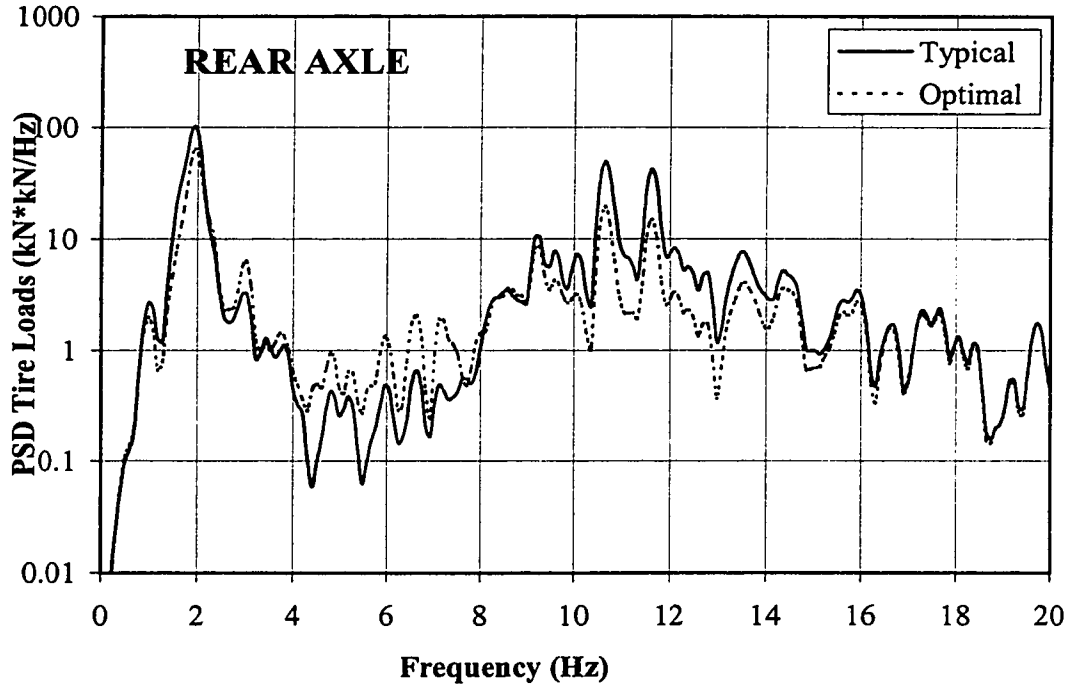

Figure 4.7 Comparison of PSD tire forces of leaf suspension vehicle model with typical and optimal asymmetric suspension damping

4.5 OPTIMAL DAMPING FOR NON-LINEAR AIR SUSPENSION

Although, air suspensions offer improved ride and tire road performance, their low inherent friction and relatively low natural frequencies operation requires adequate damping to control the excessive resonant vibration induced by the tire-road interactions. The four-DOF vehicle model incorporating non-linear force deflection the characteristics of front leaf-spring suspension and the rear air suspension are analyzed in conjunction with the optimization problem. of Equation (4.3). The minimization problem is solved for different values of damping ratio of the asymmetric damper, expressed in Equation (4.5), derive the optimal design vector $\overline{X} = \{ \beta_i, \gamma_i, V_{SEi} \}$, subject to following limit constraints:

$$0.0 < \xi_i \leq 0.05,\ 0.10,\ 0.15,\ 0.20;$$

$$1.0 \leq \beta_i \leq 20.0\,;$$

$$0.2 \leq \gamma_i \leq 0.9\,;$$

$$0.0 \geq V_{Sei} \leq 0.5 \ \text{m/s}, \tag{4.8}$$

where i =R. Optimization of the rear air suspension damper alone is performed, while optimal damping parameters, which were determined earlier, used for the front leaf suspension.

The upper limit of the asymmetry constant, β_i, in Equation (4.8), is relaxed to 20 in order to allow for the solution to converge towards relatively higher values.

4.5.3 Results and Discussions

The coupled differential equations of motion for the non-linear vehicle model are solved for excitations arising from the randomly rough road at speeds ranging from 80-120 km/h. The response characteristics are presented in terms of DLC of the tire forces and the overall rms acceleration response at the driver's location. The DLC and the acceleration response characteristics of the vehicle model with optimal damping are compared with those of model employing typical damper to demonstrate the potential benefit of the optimal suspension dampers. A total of four optimal solutions are obtained corresponding to different values of compression damping ratio, ranging from 0.05 to 0.20.

Table 4.5 Optimal damping parameters for different compression mode damping ratios of rear air suspension.

Compression Damping Ratio	**Asymmetry Constant** (β_i)	**Rebound Damping Ratio** ($\beta_i\xi_i$)	**Transition Velocity** (V_{SEi})	**Reduction Factor** (γ_i)
0.05	17.2	0.92	*	1.0
0.1	11.87	1.18	0.17	0.44
0.15	7.89	1.18	0.192	0.47
0.2	5.4	1.08	0.197	0.56

The optimal solution, summarized in Table 4.5, show that the asymmetry constant (β_i) decreases with increase in the compression damping ratio, as observed for the linear and leaf suspension vehicle models. The transition velocity, tends to converge to a very high value for light compression damping (ξ_i= 0.05), resulting in a single stage rebound damping (γ_i=1). The transition velocity, however, converge in the 0.17 to 0.197 m/s range for (ξ_i= 0.10). The optimal values of V_{Sei} similar to those obtained for the linear

spring suspension, and considerably lower than those for the leaf spring suspension. The DLC and rms acceleration response characteristics of the vehicle model were investigated using four sets of optimal damping parameters. The results revealed nearly similar values of DLC and overall rms acceleration, irrespective of the compression mode damping ratio. The DLC and rms acceleration response of the vehicle model with optimal asymmetric damper ($\xi_R = 0.1$, $\beta_R = 11.87$, $\gamma_R = 0.44$, $V_{SeR} = 0.17$) are compared with those of the vehicle model with the typical damping parameters. The response characteristics of the linear and asymmetric suspension damping are compared for different road roughness and vehicle speeds. The results show that the DLC due to rear tire forces reduce by 26% 41%. The corresponding reduction in the rms acceleration ranges from 27% to 46%.

Table 4.6 Comparison of DLC and rms acceleration of typical and optimal suspension damping.

Road	Speed	Typical Damper			Optimal Damper			% Reduction in DLC & Rms acceleration		
		DLC (Front)	DLC (Rear)	RMS	DLC (Front)	DLC (Rear)	RMS	DLC (Front)	DLC (Rear)	RMS
Rough	80	0.11	0.18	1.02	0.11	0.133	0.7	2%	26%	27%
	100	0.12	0.23	1.05	0.12	0.152	0.79	2.5%	34%	25%
	120	0.13	0.24	1.08	0.13	0.16	0.82	3.0%	33%	24%
Smooth	80	0.05	0.053	0.38	0.032	0.038	0.25	32%	28%	34%
	100	0.05	0.057	0.47	0.024	0.04	0.26	37%	29%	44%
	120	0.05	0.063	0.5	0.034	0.037	0.27	37%	41%	46%

The response characteristics, in terms of PSD of vertical and pitch acceleration of the vehicle model with optimal damped suspension are compared to with those of the vehicle model with the typical damper, as shown in Figure 4.8. The dynamic tire forces (Rear axle) of the vehicle with optimal and typical damping are also compared, as shown

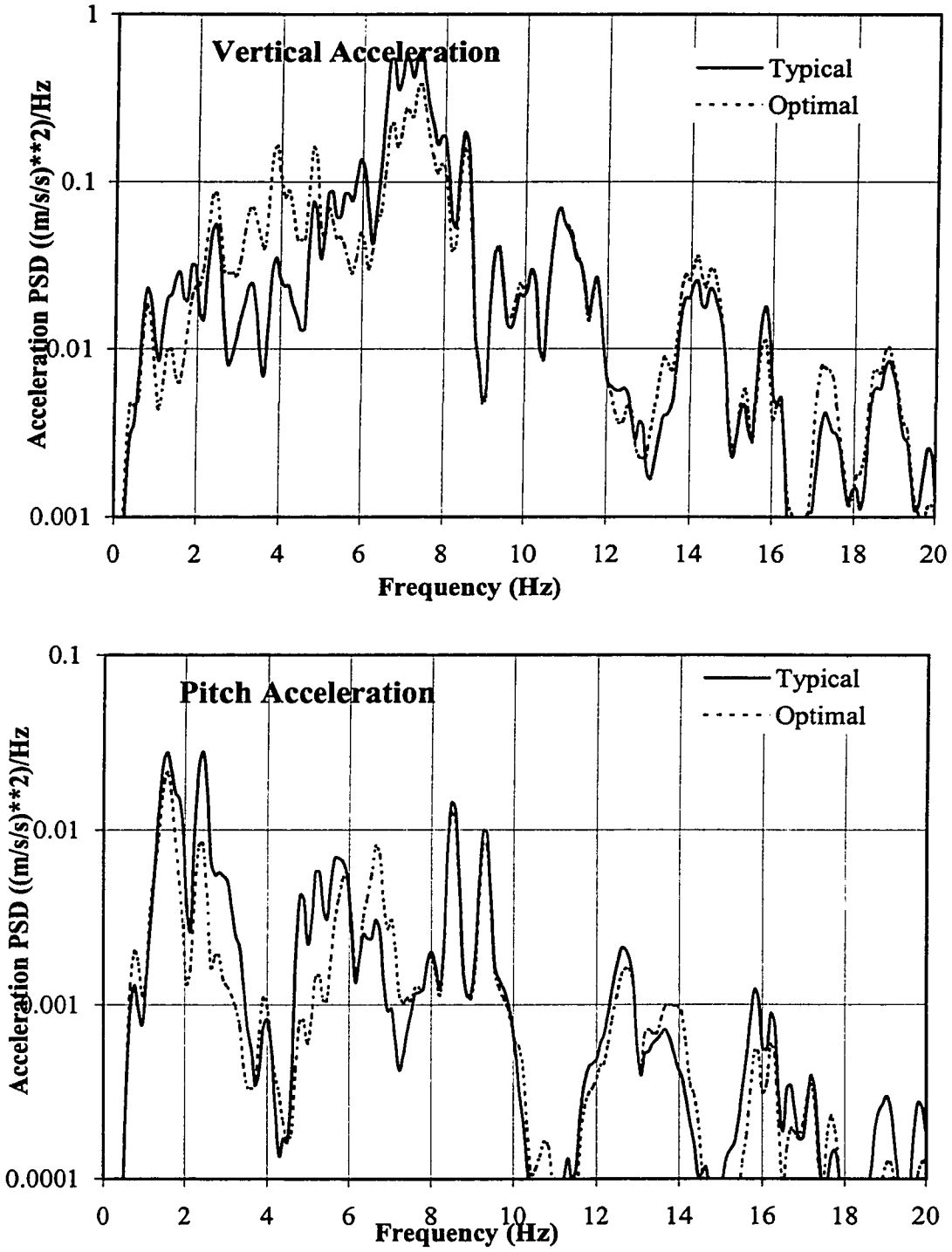

Figure 4.8 Comparison of Vertical and Pitch acceleration PSD response of rear air spring vehicl model with typical and optimal asymmetric damping.

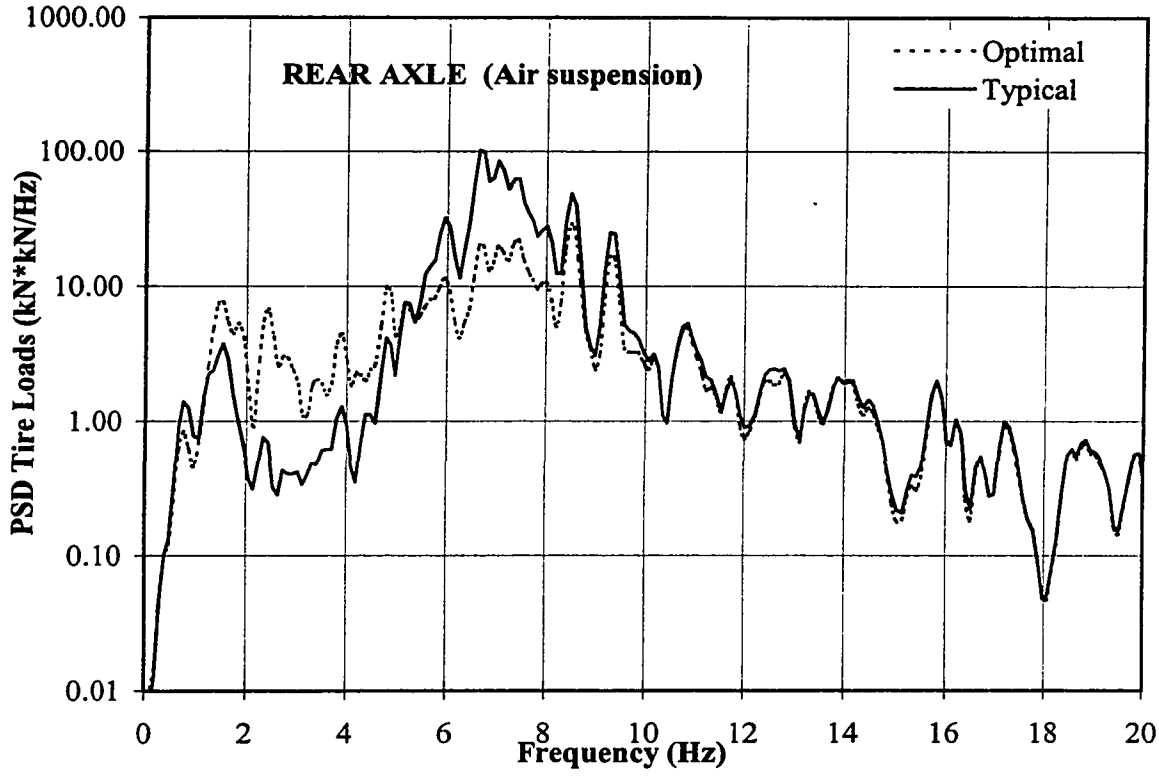

Figure 4.9 Comparison of PSD tire loads of the rear air spring vehicle model with typical and optimal asymmetric suspension damping.

in Figure 4.9. The results show that the optimal suspension damping reduces both the acceleration responses at the driver's seat and the tire forces in the vicinity of the sprung and unsprung mass resonant frequencies. The wheel hop frequency of rear unsprung mass is lower than those of linear and leaf suspensions due to lower stiffness of air suspension. The vertical acceleration and tire force response characteristics of the identified damped suspension parameters, however are slightly higher that those of the linearly damped suspension in the 2-8 Hz frequency range. The PSD of dynamic tire forces of the optimally damped suspension in the vicinity of unsprung mass resonant frequencies are also lower than those obtained from identified damped suspension parameters.

4.7 COMBINED EFFECT OF OPTIMAL DAMPING AND OPTIMAL ABSORBER

The influence of optimal damping and optimal absorber on the dynamic tire loads and ride is investigated for the linear, leaf-leaf (front and rear leaf suspension) and leaf-air (front leaf and rear suspension) suspension of the truck. Results show that optimal absorbers added to the optimal damping can further yield considerable reduction in dynamic loads in the wheel hop frequency ranges.

Table 4.7 Combined effect of optimal damping and optimal absorber on DLC and rms acceleration of linear truck suspension.

Road	Speed	Optimal Damping & Optimal Absorber			% Reduction relative to Optimal damping and no absorber		
		DLC (Front)	DLC (Rear)	RMS	DLC (Front)	DLC (Rear)	RMS
Rough	80	0.11	0.124	0.87	9.83%	10.0%	0.34%
	100	0.122	0.143	0.89	5.42%	5.9%	1.1%
	120	0.124	0.143	0.92	8.8%	10.0%	1.0%
Smooth	80	0.024	0.031	0.205	11.11%	5.8%	0.5%
	100	0.029	0.032	0.24	6.45%	8.5%	0.82%
	120	0.032	0.034	0.26	8.57%	10.5%	3.7%

Table 4.8 Combined effect of optimal damping and optimal absorber on DLC and rms acceleration of leaf-leaf truck suspension.

Road	Speed	Optimal Damping & Optimal Absorber			% Reduction relative to Optimal damping and no absorber		
		DLC (Front)	DLC (Rear)	RMS	DLC (Front)	DLC (Rear)	RMS
Rough	80	0.102	0.124	0.76	9.0%	11.42%	2.5%
	100	0.115	0.145	0.81	8.3%	9.4%	2.4%
	120	0.120	0.154	0.84	7.7%	6.6%	2.32%
Smooth	80	0.03	0.036	0.26	6.25%	10.0%	1.14%
	100	0.031	0.037	0.27	8.8%	7.5%	3.5%
	120	0.031	0.036	0.26	8.82%	7.6%	3.4%

Table 4.9 Combined effect of optimal damping and optimal absorber on DLC and rms acceleration of leaf-air truck suspension.

Road	Speed	Optimal Damping & Optimal Absorber			% Reduction relative to Optimal damping and no absorber		
		DLC (Front)	DLC (Front)	RMS	DLC (Front)	DLC (Rear)	RMS
Rough	80	0.10	0.124	0.74	9.0%	6.75%	0.13%
	100	0.11	0.14	0.78	8.3%	7.8%	1.26%
	120	0.120	0.13	0.82	7.6%	12.5%	0.0%
Smooth	80	0.031	0.037	0.24	6.25%	2.63%	4.0%
	100	0.022	0.036	0.25	8.3%	5.26%	3.6%
	120	0.032	0.036	0.261	8.82%	7.6%	3.4%

Tables 4.7, 4.8 and 4.9 show DLC and rms values of linear, leaf-leaf and leaf-air with optimal damping and optimal absorber respectively. Above tables also show comparison of percentage reduction in DLC and rms values when compared to optimal damping with no absorber. The results show that there is a considerable reduction in DLC in the range of 5.42% - 11.1% and a slight reduction in rms values for the linear suspension of truck compared to optimal damping with no absorber. Truck with the leaf-

leaf suspension a reduction in DLC due to combined effect found to be in the range of 6.25% to 11.42% compared to optimal suspension damping. Results also show a considerable enhancement of road friendliness and a decrease in DLC from 5.26 - 9.0% for leaf-air suspension of truck due to optimal damping and optimal absorber. Since the absorber can have influence only on wheel hop frequencies ranges, percentage reduction in rms values is not very significant with optimal absorber.

4.8 SUMMARY

An analogy between the DLC and vehicle ride quality related to overall rms acceleration is established through analysis of simplified vertical dynamic model of a vehicle. A weighted optimization function comprising DLC and overall rms acceleration at driver's location is formulated to derive optimal suspension damping for the linear and non linear suspension of a truck. The optimization problem is solved to derive optimal parameters of the asymmetric dampers. The effectiveness of the optimal damper is demonstrated by comparing its DLC and acceleration response with those of a typical damper. The additional benefits of an axle vibration absorber in improving the road-and driver-friendliness of the vehicle are further demonstrated.

CHAPTER 5

CONCLUSIONS AND RECOMMENDATIONS FOR FUTURE WORK

5.1 HIGHLIGHTS OF THE STUDY

Although most studies on dynamic tire loads have investigated the significant role of suspension springs in enhancing the tire loads, only few studies have investigated the role of suspension damping. The influence of suspension damping as the ride performance of vehicles, however, has been extensively investigated. The reported studies, however, are mostly limited to linear damping. In this thesis, the performance potentials of optimal asymmetric of suspension damping and dynamic axle vibration absorber to enhance the ride quality and reduce the tire induced road damage, are analytically investigated. An analogy between the dynamic wheel loads (road-friendliness) and ride quality (driver-friendliness) performance characteristics of heavy vehicles is established through analysis of a simplified vehicle model. In view of the direct analogy between the driver-and road-friendliness, it is proposed that both performance characteristics can be enhanced through optimal suspension damping and a tuned dynamic vibration absorber. The highlights of the investigation and findings are described below:

- ***Development of a representative vehicle model***

An in-plane model of a three axle truck is formulated to study its interactions with the road in terms of vertical tire loads transmitted to the road, and vertical acceleration transmitted to the driver station, assuming negligible contributions due to roll dynamics of the vehicle. Two closely spaced rear axles are grouped together and represented by a single composite axle. The vehicle body, chassis and cargo are characterized by a rigid sprung mass with two degrees of freedom: vertical and pitch. The front and composite rear wheel and axle assemblies are represented by rigid masses with only vertical degree-of freedom (DOF). Each unsprung mass is coupled to the sprung mass through the respective suspension components, modeled as parallel combinations of either linear of nonlinear energy restoring and dissipative elements. The tire terrain interactions are represented by the linear force-deflection properties of tires assuming point contact with undeformable road. The vehicle models employing different suspension is analyzed for stochastic excitation arising from rough and smooth roads.

- ***Identification of non linear suspension components***

  The force-deflection and force-velocity characteristics of suspension components are identified from the reported studies and laboratory measurements. Analytical models of nonlinear leaf and air springs, and dampers are derived and validated using the available data.

- ***Analogy between the dynamic wheel loads and ride quality***

  An analogy between the dynamic wheel loads and ride quality performance characteristics of heavy vehicles is established through analysis of linear quarter-

vehicle model. From the results it is proposed that the suspension damping considered adequate for improved ride quality can lead to enhanced road friendliness of the vehicle. The results further demonstrated the existence of optimal damping for both performance measures; tires loads and ride quality.

- ***Effectiveness of optimal dynamic axle vibration absorbers***

  Enhancement of road friendliness of heavy vehicles is analytical investigated using a concept of dynamic vibration absorber, tuned to the resonant frequencies of the unsprung masses of the vehicle model. A parametric study is performed to analyze the influence of frequency ratio, damping ratio and mass ratio of the absorber on the tire loads and the acceleration response for deterministic and stochastic excitations at tire-road interface.

- ***Optimal asymmetric damping to enhance ride and road friendliness***

  A performance criterion comprising dynamic load coefficient due to tires on different axles and overall rms acceleration transmitted to the driver station is formulated. The nonlinear vehicle models are solved in conjunction with the objective function for excitations arising from a rough road and different speeds, ranging from 80-120 km/h. The effect of optimal asymmetric damping parameters, derived from the solution of the optimization problem, on the DLC and the ride quality are evaluated through analysis of the vehicle model with linear and non linear suspension stiffness.

- ***Combined effect of optimal damping and absorber***

The combined effect of optimal suspension damping and axle vibration absorber on the dynamic loads and ride is investigated through analysis of the 6-DOF vehicle model employing linear, and nonlinear suspensions under varying operating condition. It is proposed that addition of optimal axle absorbers to the optimally damped suspension can further yield considerable reduction in dynamic loads in the wheel hop frequency range without effecting the ride quality associated with the whole-body vibration at frequencies in the vicinity of human body resonance.

5.2 CONCLUSIONS OF THE INVESTIGATION

The conclusions drawn from the investigation are summarized in the following sections.

5.2.1 Development of the vehicle model

- An in-plane vehicle model describing the vehicle-road interactions associated with vertical and pitch modes of vibration can yield significant insight into road-and driver-friendliness performance characteristics.
- Since the dynamic wheel loads and the ride quality are related to vehicle vibration modes, a vehicle model formulated to study the tire-road interactions can also be used to evaluate its ride dynamics.
- The ride and tire-load performance of the vehicle is strongly effected by the hysteresis of the leaf spring and dynamics of the trailing arm configuration of air springs. Nonlinear hysteretic models of the leaf suspensions and kinematic and dynamic

model of the air springs and linkages are thus extremely vital for development of an effective vehicle model.

- The force-deflection properties of a multi-leaf spring can be characterized by a linear envelope function and an exponential function, while those of an air bag can be approximated by an isothermal process.

5.2.2 Dynamic axle vibration absorber

The dynamic wheel loads tend to predominate in the vicinity of bounce mode resonant frequencies of the sprung and unsprung masses. A dynamic vibration absorber is most effective in a narrow frequency band around its uncoupled natural frequency. A lightweight dynamic vibration absorber tuned to the resonant frequency of the unsprung mass can be used to reduce the dynamic wheel loads. The effectiveness of the absorber, however, is dependent upon the tuning of the absorber parameters. Parametric study and design optimization is performed to derive parameters of an effective axle absorber. From the results, the following conclusions are drawn:

- The effectiveness of an axle absorber is strongly influenced by its non-dimensional tuning parameters (mass ratio, frequency ratio and damping ratio).
- A dynamic vibration absorber, tuned to the wheel hop frequency, does not affect the whole-body vehicle vibration transmitted to the driver in the important ride frequencies.
- While a dynamic vibration absorber, tuned to the low sprung mass bounce resonant frequency, may be considered impractical due to its large mass, an axle absorber can be conveniently implemented with minimal effect on the payload capacity.

- A dynamic axle vibration absorber with uncoupled damping ratio of 0.14, frequency ratio of 0.85, and mass ratio of 0.1 provides optimal performance in reducing the magnitudes of dynamic loads in the vicinity of wheel hop frequencies.
- An optimal axle dynamic vibration absorber can yield a reduction in DLC ranging from 11.5% to 20.93% for excitation arising from a rough road, while the reduction is 3.3% to 9.85% for the smooth road, in the 80-120 km/h speed range.

5.2.3 Analogy between the dynamic wheel loads and ride quality

An analogy between the dynamic wheel loads and ride quality performance characteristics of heavy vehicles is established through analysis of a linear quarter-vehicle model in order to illustrate the potential benefit of optimal damping in conjunction with different suspension springs used in heavy vehicles. The results of the study revealed the following:

- The suspension damping influences the ride quality and the tire loads in a similar manner;
- An increase in suspension damping ratio beyond 0.15 yields only minimal further reduction in DLC, and higher damping tends to deteriorate the ride quality at frequencies in the vicinity of the human body resonance;
- Suspension dampers with asymmetric damping properties in compression and rebound can effectively reduce the magnitude of tire forces while preserving the ride response;
- The optimal asymmetric damping can provide considerable reduction in both the overall rms acceleration and the DLC due to tire forces.

5.2.4 Optimal suspension damping

The constrained optimization problem, comprising DLC and overall rms acceleration at the driver's seat, was solved in conjunction with the four-DOF linear and nonlinear vehicle models to determine optimal asymmetric damping parameters. The optimization problem was solved for excitations arising from a rough road over a speed range of 80-120 km/h. From the results of the study, the following conclusions are drawn:

- The solution of the optimization problem for *linear suspension* revealed that the rebound mode damping ratio near 0.8 is desirable to achieve improved road friendliness and ride quality, when the compression damping ratio is selected in the 0.1 to 0.2 range. The transition velocity, ranging from 0.166 to 0.193 m/s, and the high-speed rebound damping reduction factor ranging from 0.34 to 0.366, are desirable to enhance the road-and driver-friendliness of the vehicle.
- The vehicle models employing optimally damped vehicle suspension resulted in 11.5% to 30% reduction in DLC, and 12.5% to 37.5% reduction in overall rms acceleration, depending upon the vehicle speed and the road roughness.

- The desirable rebound damping ratio for the *leaf suspension* is 0.3 for the compression mode damping ratio of 0.1. Results show that the existence of inherent Coulomb damping in the leaf suspension requires light compression mode damping. Damping ratios below 0.1 tend to converge to high values of transition velocity resulting in a single stage rebound damping. The results further show that an optimally damped Leaf spring suspension can lead to reduction in the tire forces,

ranging from 2% to 37.1%. The corresponding reduction in the overall rms acceleration range from 4.4% 28.0% in the speed range considered in this study.

- The solution of the optimization problem for air *suspension* revealed that the rebound mode damping ratio near 1.18 is desirable to achieve improved road friendliness and ride quality, when the compression damping ratio is selected in the 0.1 to 0.2 range. While the transition velocity and high-speed lies in a similar range (0.17 to 0.197 m/s), the rebound damping reduction factor is considerably lesser (0.44 to 0.56) than that obtained for the leaf spring. The optimally damped air suspension resulted in reduction in DLC in the 24.0% to 41% range, and in rms acceleration in the 24% to 46% range, depending upon the vehicle speed and road roughness.
- An optimal axle vibration absorber combined with an optimally damped linear spring suspension can yield further reduction, ranging from 5.42% - 10.5%, in DLC. The corresponding reductions for the leaf-leaf and leaf-air suspension are obtained as 6.6% to 11.42%, and 5.26 - 12.5%, respectively.

5.3 RECOMMENDATIONS FOR FUTURE WORK

The present research work yields significant insight into the effects of optimal suspension damping and dynamic vibration absorber on the dynamic tire loads and ride dynamics response characteristics of a heavy vehicle. Although the study clearly demonstrates the high potential benefits of the proposed concepts, following further systematic investigation need to be undertaken to fully realize the benefits.

- The articulated freight vehicles with excessive gross vehicle weight transmit considerably large dynamic loads to the pavements. It is thus recommended to

investigate the potential performance benefits of the axle vibration absorber and optimal asymmetric damper for such vehicles, using the methodology proposed in this dissertation.

- The potential performance benefits of the proposed concepts need to be explored through laboratory or field investigation. The analytical model, validated using the field data, can be employed to derive the optimal damper parameters. The design or selection of damper values then must be carried out to realize the optimal damping.
- Further studies may be undertaken to explore different vibration absorbers to suppress the axle vibrations over a wide frequency band. The concept in semi-active vibration absorbers may be further explored.
- It is further recommended to develop more comprehensive models of different configurations of air suspensions incorporating hysteresis due to the air bag, polytropic compression/ expansion of the air, and the elastic properties of the bushings.

1.5 REFERENCES

1. Gyenll, L., Mitchell, C.G.B. and Philips, S.D (1994) "Dynamic Pavement Loads and Tests Of Road Friendliness For Heavy Vehicle Suspensions", Heavy Vehicle Systems, Special series, Int J.of vehicle Design, Vol.,1. No.4, PP. 381-395.

2. Abbo, E, et al., "Analysis Of Moving Dynamic Loads On Rigid Pavements". ARRB/FORS Symposium of Heavy vehicle suspensions characteristics, Canberra, 1987.

3. Addis, RR, The effect of Wheel loads on road pavements IMechE conference on road wear: The interaction between vehicle suspension and the road, London, 1991.

4. Thrower, E.N., "Calculations of Stress, Strains and Displacements in a Layered Elastic Structure, Part II". Road Research Laboratory, RRL Rep. LR 373, 1971.

5. Rauchut, J.B., Roberts F.L., Kennedy T.W., "Response and Distress Models for Pavement Studies", TRR 641 pp 7-14 1979.

6. Pell, P.S., "Pavement Materials"., Proc. 6 th Int. Conf. on the Structural Design of Asphalt Pavements, Vol II pp 35-70, July 1987.

7. Gillespie, TD, et al., "Effects of Heavy Vehicle Characteristics on Pavement Response
and Performance". Transportation Research Board, NCHRP Report 1- 25 (1) 1992.

8. Anon, "AASHTO Guide for Design of Pavement Structures", American Association of State Highway and Transport Officials, Volume 1, 1986.

9. Peattic, KR, "Flexible Pavement Design. Ch 1". Developments in highway pavement engineering. Pell ps ed. Applied science publications Ltd, London 1978.

10. Mitchell, C.G.B and Gyenes, L. Dynamic Pavement Loads measured for a variety of tuck suspension 2nd international conference on Heavy Vehicle Weights and dimensions, Kelowns, British Columbia, 1989.

11. Monismith, C.L., Sousa, J. and Lysmer, J. Modern pavement design technology including dynamic load conditions. SAE conference on vehicle pavement interactions, SP 765, Indianapolis, 1989, SAE Trans 881845 (Society of Automotive Engineers).

12. Hahn, W.D. "Effects of Commercial Vehicle Designs on Road Stress-Vehicle Research results".

13. Cebon, D. An Investigation of the Dynamic Interaction between Wheeled Vehicles and Road Surfaces. Phd thesis, University of Cambridge, 1985.

14. Sweatman, P.F. A Study of Dynamic Wheel Forces in axle group Suspensions of Heavy vehicles. Special report, Australian Road Research Board, report number SR 27, 1983

15. Swetman, P.F. Effect of Heavy Vehicles Suspensions on Dynamic Road Loading, Australian Road Research Board Research Report ARR116, 1980.

16. Cebon, D. "Examination of Road Damage Caused by three Articulated Vehicles" Proc. ARRB/FORS symposium of Heavy vehicle suspension characteristics, Camerra,
March, 1987., pp 143-162

17. OECD, Dynamic Loading of Pavements. OECD Report, 1992.

18. Interaction Between Heavy Vehicles and Roads David Cebon. SAE sp-951 Cambridge University.

19. Mitchell, C.G.B. and Gyness L. "Dynamic Pavement Loads Measured for a Variety of Truck Suspension" 2nd int. conf. on Heavy vehicle weights and dimensions kelowna, British Columbia, 1989.

20. Baker R, I and Alpab, "The Speed Effect in Pavement Deflection", Acta Technics, 85 (1-2) pp 11-28, 1977.

21. Chan, Gp. et al., "Laboratory Measured Tire Pavement Contact Pressures". FHWA Load Equivalencies Workshop, Washington D.C. FHWA, 1988.

22. Heas, R.C.G and Papaginnaks, A.T., "Understanding Pavement Rutting". Special Workshop on rutting in asphalt pavements, Toronto, Roads and Transport Association of Canada., 1986.

23. Tilking,. J.T "Wide Base Radian Truck tires: Properties and Performance," Heavy vehicle systems, special series, Int. J. of Vehciel Design, Vol, 2, Nos. 3/4, pp. (1985) 187-207.

24. Huhatala, M., "Field Test to Compare Tires". FHWA Load Equivalence workshop, Washington D.C, 1988.

25. Marshek, K.M., et al., "Experimental Investigation of Truck Tire Inflation Pressure on Pavement of Truck Tire Inflation Pressure on Pavement-tire Contact Area and Pressure Distribution". University of Texas Center for Transportation Research. Report No. 386-1, 1985.

26. Eisenmann, J., Birman D and Hilmes A., "Effects of Commercial Vehicle Design on Road Stress-Research Results Relating to the Roads". 'Stressund Autobahn, (Translated by TRRl as WP/V&ED/97/29), 37(6) pp 238-244, 1987.

27. Haas, RCG and Papgiannakis AT, "Understanding Pavement Rutting". Special workshop on rutting in ashphalt pavements, Toronto, Road and Transport Association of Canada 1996.

28. Bonaquist, R., An assessment of the increased damage potentials of wide based single tires '7 th Int. Conf. on Asphalt pavements, Ed. Brown Sf and Hicks RG 4 Vols. Nottingham, UK, International Society for Asphalt pavements, 1992.

29. Gillespie, T.D., et al., "Effects of Heavy Vehicle Characteristics on Pavement Response and Performance". Transportation Research Board, NCHRP Report 1-25 (1), 1992.

30. Robust, J.B., Roberts, F.L and Kennedy, T.W. Response and distress models for pavement studies, Transport Research Record 715 TRB, 1979, pp 7-14.

31. PAGE, J.A review dynamic loading caused by vehicle suspensions, TRRL supplementary report 82uc, crowthrone, 1974.

32. Dickerson, RS and Mace DGW (Dynamic pavement force measurements, with a two axle heavy goods vehicle. TRRL, Supplementary Report SR 688, 1981.

33. Hazh, WD, "Measurements of Road Loading by HGV Suspensions survey of the Germen research Program". 'IMechE Conference on Road Wear. The interaction between vehicle suspension and the road, London, 1991.

34. Ervin, Rd. et al., "Influence of Truck Size and Weight Variables on the Stability and Control on the Stability and Control Properties of Heavy Trucks". University of Michigan Transportation Research Institute, UMTRL 83-10/2, 1983.

35. Gillespie, T.D., "Modeling Truck Dynamic Loads". FHWA load equivalence workshop, Washington D.C., FHWA 1988.

36. Tec, Potter "Road-Damaging Potential of Measured Dynamic Tire Forces in fixed Traffic", Department of Mechanical Engineering, University of Cambridge [1994].

37. Alpab, I and Baker R, "The Speed Effect in Pavement Deflection", Acta Technics, 85 (1-2) pp 11-28, 1977.

38. Annon, "The AASHO Road Test, Report 5, Pavement Research," Highway Research Board, special report 61 E, 1962.

39. Ferrari, P., "Calculation of the Deformations Caused by Vehicles to Flexible Pavements". 3 rd Int conf. Structural Design of Asphalt pavements, University of Michigan, Anna Arbor 1972.

40. Hardy, M.S and Cebon D, "The Response of Flexible Pavements to Moving Dynamic loads. 'Proc. Inst Acoustics, 10(2), pp 485- 492, 1988.

41. Cole, D.J., and Cebon D, "Assessing the Road-Damaging Potential of Heavy Vehicles." Proc. I.Mech.e., Part D. 205 pp 223-233, 1991.

42. Gillespie, TD, "Heavy Truck Ride". SAE. SP 607, 1985.

43. Heath, A and Good MC, "Heavy Vehicle Design Parameters and Dynamic Pavement Loading". Australian Road Research, 15(4) pp 249-263, 1985.

44. Sayers, M and Gillespie TD, "Dynamic Pavement/Wheel Loading for Trucks with Tandem Suspensions" Proc 8 th IAVSD symposium on the dynamics of vehicles on roads and an Railway trucks, Cambridge, MA, Swets and Zetilingers, 1983.

45. Hu, G, "Use of Road Simulators for Measuring Dynamic Wheel loads". SAE Interaction, SAE 881194, SP 765 Indianapolis, SAE, 1988.

46. Smith A.R., "Frame Bending, Fifth wheel locations-special body moving and Loading problem." SAE special report SR 260, 1965.

47. Ribarits, J.Aurell andE. Andersers, "Ride Comfort Aspects of Heavy Truck design." SAE Tran., 781064 p.p 4046-4069, 1975.

48. P,.Michelberger and D.Szole, "Speed Dependent Vertical Vibrations of Elastic Vehicle Bogies," Int.J.Vehicle Design, 8(1) pp. 8-95, 1985.

49. Whittemore, Alan P., al., "Dynamic Pavement Loads of Heavy highway Vehicles", National cooperative Highway Research Program Report No. 105 (1970).

50. Hodric, K., et al (1985) "Determination of Road Stress factor for Busses," US DOT Report

51. Heath, A.N., and M.C. Good (1985) "Heavy Vehicles Design Parameters and Dynamic Pavement Loading", Australian Road Research, Vol, 15, No.4.

52. Heath, A.N., "Heavy Vehicle Design Affecting Dynamic Pavement Loading." ARRB Smp. on Heavy Vehicle suspension characteristics, March 1987.

53. Karadayi, R, and Masada G.Y., A Nonlinear Shock Absorber Mode, Proc. of the 1988 ASME Winter Ann Meeting (1988).

54. Rakheja, S. et al. (1989) "Ride Vibration of Articulated Vehicles and Significance of Secondary Suspension", SAE 1989 Noise and Vib. conf., SAE Publ. No p-222, May 16-18, pp 139 147.

55. Sweatman, P.F.(1983) "A Study of Dynamic Wheel Forces in Axle Group Suspensions of Heavy Vehicles". ARRB special Report No. 127.

56. Rakheja, S. et. al, (1988) "Ride Vibration Levels at the Driver-Seat Interface", Interim Report, Transport Development Centre, Transport Canada.

57. Cebon, D (1986), Simulation of the Response of Leaf Springs to Broad Band Random Excitations VSD, 15(6), 1986.

58. Fancher, Ps et al., (1980), Measuremtn and representation of the Mechanical properties of truck leaf spring. SAE 800905.

59. Cole, D.J., Cebon, D (1994), Modification of a heavy vehicle suspension to reduce road damage (1994). University Engineering Department Cambridge.

60. Rakheja, S Woodroofe, JHF; (1994), Role of suspension damping in enhancement of road friendliness of heavy vehicles. Engineering Foundation Conf. Noordwijkerhout.

61. Cebon, David (1989) "Vehicle Generated Road Damage; A Review", Vehicle system dynamics, Vol. 18, pp 107-150.

62. Anon, (1982) council Directive 92/7/EEC Council of the European community.

63. Jacklin, D.J., (1993), Parametric testing of heavy goods vehicle suspension system. TRL Research Project 120C/VE.

64. Woodroffe, John "Heavy Truck Suspension Dynamics; Methods for Evaluating Suspension Road Friendliness and Ride Quality" SAE 962152 (1996).

65. Orr L.W., "Truck Pavement Factors- The Truck Manufacturers View Poin"; SAE Special Publication sp 765, Paper number 881842, Nov, 1988.

66. Woodroffe J.H.F., P.A. Leblanc and A.T. Papgiannakis, "Suspension Dynamics Experimental Findings and Regulatory Implications", SAE paper no. 881847, 1988.

67. Throwes E.N., "A parametric Study of Fatigue Prediction Model for Bituminious Road Pavements." TRRRL Report LR 892, 1979.

68. Peattie, K.R., "Flexible of Pavement Design ch.I. Development in Highway Pavement Engineering", applied science publications Ltd., London 1978.

69. Ulliditz, P., and Bush C., "Mathematical Models for Predicting Pavement Performance." Transpr. Res. Rec 949. TRB, 1983, pp 32-44.

70. Cebon, D, "Vehicle Generated Road Damage; A review", Vehicle system dynamics Vol 18, 1989, pp 107-150

71. Papagiannakis A.T, and J.H.F. Woodroofe, ''Suitability of Alternative Pavement Roughness Statistics to Describe Dynamic Axle Loads of Heavy Vehicles"., Proceedings of the 2nd International symposium of heavy vehicle weights and dimensions, June 18-22, 1989, Kelowna B.C.,

72. Heath, A.N. (1987) "Heavy Vehicle Design Affecting Dynamic Pavement Loading", ARRB Symp on Heavy Vehicle Suspension characteristics, March 1987.

73. Missio, G.K., and R.M. Carson, "Corrugation of unmetalled roads, Part I: Vehicle Dynamics," Proceedings of the Imeche Vol 203, pp 205-214.

74. Hedrick, J.K., K.Yi, "The effect of alternative heavy truck suspension on flexible pavement response". Presented at the second international symposium heavy vehicle weights and dimensions Vol 1. June 8-22, 1989, Kelowna British Columbus, Canada.

75. Cole, D. J, Cebon, D., "Simulation and measurement of dynamic tire forces" presented at the second international symposium of heavy vehicle weights and dimensions Vol 2, June 18-22, 1989, Kelore.

76. N, Sakuma et al., "Heavy Duty Truck Ride Comfort Analysis by Computer Simulation", SAE paper No. 871557, 987.

77. Van Deussen D.B, "Trcuk Suspension System Optimization," SAE Trans., 1971, paper No. 710222.

78. Lay M.G., and Kinder, D.F., "Review of the fourth power law", ARRb, Internal report AIR000-248, 1988.

79. Kitis, L., Wang, B.P and Pilkey, W.D., Vibration reduction over a frequency range. J.of Sound and vibration, 1983, 89(41, 559-569)

80. Ebrahimi, Nader, D., On optimum design of vibration absorbers, Trans ASME J. of Vib., Aco., Stress and reliability in design, 1987, 109, 214-215.

81. Captain, K.M., Boghani, A.B., and wormely, D.M., "Analytical tire models for dynamic vehicle simulations", Vehicle system dynamics, Vol 8, pp-1-329 1979.

82. Creighton, D.C, Revised vehicle dynamic module. User's guide for program VEHDYN II 'Research note No. SL- 86-9, US, Army Engineer waterway experimental statistics, Vicksburg, Miss, May 1986.

83. Anon, "A guide to the structural design of pavements for new roads", Road research laboratory, Road Note 29, 1970.

84. Baladi, G., Fatigue life and permanent deformation characteristics of asphalt concrete mixes. 'Tramp. Res. Rec. TRB, 1227 pp 75-87, 1989.

85. Donald, G., et al., "Pavement design: A guide to the structural design of road pavements", NAASRA, 1987.

86. Vinson, T.s., Jackson NM and Jung D, "Thermal cracking resistance of asphalt concrete; and experimental approach." 7 th Int., Conf. on Asphalt pavements, Ed Brown SF and Hicks RG. 4 Vols Nottinghanm UK, International Society for Ashphalt pavements, 1992.

87. Peattie, K.R., "Flexible pavement design ch.1. Developments in Highway pavement engineering." 1 Pell Ps ed. Applied science publications Ltd., London. 1978.

88. Scrivner, F.H., and Duzan H.c., "Application of AASHO road test equations to mixed traffic." Proceedings of a conference on the AASHO Road test, st, Lous, MO, National Academy of science-National Research council, Special Report 73, 1962.

89. Addis, R.R., and Whitmarsh RA., "Relative damaging power of wheel loads in mixed traffic." Transport and road research laboratory, Laboratory report LR 979, 1981.

90. Kinder, D.F., and Lay M.G., "Review of the fourth power law", ARRb, Internal report AIR000-248, 1988.

91. Thrower, EN, "A parametric study of fatigue prediction model for bituminous road pavements" TRRL, Laboratory Report LR 892, 1979.

92. Annon, "Impacts of heavy freight vehicles" OECD, Paris, 1982.

93. Christison, JT, Anderson Ko and Schields BP, In situ measurements of Strains and deflections in a full-depth asphaltic concrete pavements.' Proc. Assoc, Asphalt paving Technology, 47, pp 398-430, 1978.

94. Annon, "Heavy trucks, climate and pavement damage", OECD Road transport research, Paris, 175 p 1988.

95. Stiharu. I and Rakheja. S, CONCAVE 03-95; Laboratory testing and characterization of an airide spring' prepared for Forestry Engineering Research Institute of Canada.

96. Pche. A., Juras. D., D.Rathwell and S.Rakheja, CONCAVE 02-95 "Laboratory testing characterization of a neway shock absorber". Prepared for Forestry Engineering Research Institute of Canada.

97. Damien, T.M. et al. (1982) "Pavement profiling various pavements: Ottawa/Smith Falls', John Emery Geotechnical Engineering Report.

98. ISO (1987) "Measurement and evaluation of human exposure to whole body mechanical vibration and repeated shocks", International Standards ISO- 2631.

99. Sweatman. P.F., Addis. R.R., Road Transport Technology-4, '"Proceedings of the fourth international symposium on heavy vehicles and dimensions".

100. Bank T.A., et.al (1980) "Some ABC's of Air Spring Suspensions for Commerical Road Vehicles". SAE Technical Paper Series 800482. Congress and Exposition Cobo Hall Detroit.

INFORMATION TO USERS

This manuscript has been reproduced from the microfilm master. UMI films the text directly from the original or copy submitted. Thus, some thesis and dissertation copies are in typewriter face, while others may be from any type of computer printer.

The quality of this reproduction is dependent upon the quality of the copy submitted. Broken or indistinct print, colored or poor quality illustrations and photographs, print bleedthrough, substandard margins, and improper alignment can adversely affect reproduction.

In the unlikely event that the author did not send UMI a complete manuscript and there are missing pages, these will be noted. Also, if unauthorized copyright material had to be removed, a note will indicate the deletion.

Oversize materials (e.g., maps, drawings, charts) are reproduced by sectioning the original, beginning at the upper left-hand corner and continuing from left to right in equal sections with small overlaps. Each original is also photographed in one exposure and is included in reduced form at the back of the book.

Photographs included in the original manuscript have been reproduced xerographically in this copy. Higher quality 6" x 9" black and white photographic prints are available for any photographs or illustrations appearing in this copy for an additional charge. Contact UMI directly to order.

UMI®

Bell & Howell Information and Learning
300 North Zeeb Road, Ann Arbor, MI 48106-1346 USA
800-521-0600